

**Reconstruction of the Holocene Indian monsoon climate
variability based on biogeochemical analyses of lake sediments**

Dissertation

with the aim of achieving a doctoral degree

at the Faculty of Mathematics, Informatics, and Natural Sciences,

Department of Earth Sciences

of the Universität Hamburg

submitted by

Philip Menzel

from

Hamburg

Hamburg

2014

Day of oral defense: 4th June 2014

The following evaluators recommended the admission of the dissertation

Prof. Dr. Kay-Christian Emeis

and

Dr. Birgit Gaye

Hamburg, 16th June 2014

Prof. Dr. Christian Betzler

(Head of the Department of Earth Sciences)

Zusammenfassung

Ziel dieser Arbeit war eine Rekonstruktion des holozänen Monsunklimas Indiens mithilfe biogeochemischer Analysen von Seesedimenten. In einem ersten Schritt werden auf Aminosäureanalysen basierende Abbau- und Quellindikatoren, die ursprünglich aus marinen Proben entwickelt wurden, auf ihre allgemeine Anwendbarkeit in Seen überprüft (Kapitel 3). Zusätzlich werden die heutigen hydrologischen und biogeochemischen Eigenschaften des zentralindischen Lonar Sees, der für die Paläoklimarekonstruktion ausgewählt wurde, untersucht (Kapitel 4). Schließlich werden die daraus ermittelten Klimaproxies für eine Paläoklimarekonstruktion an einem ca. 10 m langen Sedimentkern aus dem Lonar See genutzt (Kapitel 4).

In Kapitel 3 erläutere ich die Ergebnisse der Aminosäure- und Hexosaminanalysen von Sediment-, Boden-, Gefäßpflanzen-, und Schwebstoffproben von vier indischen Seen aus unterschiedlichen Klimaregionen. Schwerpunkt liegt auf der Identifizierung von aminosäurebasierten Abbau- und Quellindikatoren, die universelle Anwendbarkeit in lakustrinen Ökosystemen zeigen. Anhand einer Hauptkomponentenanalyse wurde ein Seesediment-Abbauindikator berechnet, der für den Vergleich des Abbaugrades organischer Substanzen von Studienorten mit unterschiedlichen Umwelt- und Klimaeigenschaften geeignet sein sollte.

Kapitel 4 fasst die Untersuchung der heutigen Umweltbedingungen des abflusslosen Lonar Sees im zentralindischen Staat Maharashtra zusammen. Der See ist eutroph, brackig, alkalisch und in Wassertiefen > 4 m permanent anoxisch. Aufgrund der hohen pH-Werte und anoxischen Bedingungen dominieren Denitrifikation und Ammoniak Verflüchtigung den gelösten anorganischen Stickstoffkreislauf und verursachen sehr hohe $\delta^{15}\text{N}$ -Werte der in dem See wachsenden Organismen. Unterschiedliche Redoxbedingungen in den flachen ufernahen Sedimenten und den tiefen distalen Sedimenten führen zu unterschiedlichen

Abbaumechanismen und Aminosäurezusammensetzungen sowie $\delta^{15}\text{N}$ -Werten des organischen Materials. Basierend auf den Aminosäurezusammensetzungen des organischen Materials, welches unter oxischen beziehungsweise anoxischen Bedingungen abgebaut wurde, wird ein Redox-Index berechnet, der während der Paläoumwelt- und Paläoklimarekonstruktion in Kapitel 5 Anwendung findet.

Die Ergebnisse der biogeochemischen und mineralogischen Analysen des Sedimentkerns aus dem Lonar See, der die holozäne Sedimentationsgeschichte des Sees wiedergibt, werden in Kapitel 5 vorgestellt. Die Ergebnisse der C/N-Verhältnisse, der stabilen Kohlenstoff- und Stickstoffisotopie, der Korngrößenverteilung, sowie der aminosäurebasierten Abbauintizes werden mit klimasensitiven Messgrößen anderer Datensätze aus Südasien und der Nordatlantikregion verglichen. Neben einem langfristigen Klimaübergang von feuchten Bedingungen im frühen Holozän zu trockeneren Bedingungen während des späten Holozäns in der Region des Lonar Sees, der mit der Veränderung der Sonneneinstrahlung auf der Nordhalbkugel korreliert, können mehrere Klimaveränderungen im Hundertjahresrhythmus identifiziert werden. Diese kleinerskaligen Klimaveränderungen korrelieren mit in der Literatur beschriebenen Klimaschwankungen in der Nordatlantikregion. Synchrone Veränderungen zu trockenerem Klima in Indien und kälterem Klima in der Nordatlantikregion implizieren eine Verbindung zwischen den beiden Klimasystemen oder gemeinsame Reaktionen auf identische Impulse. Korrelationen zwischen den Klimaveränderungen in beiden Regionen und der ^{14}C -Nukleidproduktionsrate, einem Solarleistungsindikator, deuten darauf hin, dass Änderungen in der Solarleistung für die Verbindung zwischen den beiden Systemen verantwortlich sein könnten. Bezüglich der archäologischen Geschichte Indiens lässt sich vermuten, dass verringerte Niederschläge, die anhand der Untersuchungen der Seesedimente des Lonar Sees für 4,6 bis 3,9 cal ka BP rekonstruiert wurden, zum Niedergang der Induskultur etwa 3,9 ka BP beitrugen.

Abstract

The studies presented in this thesis focus on the reconstruction of the Holocene Indian monsoon climate based on biogeochemical analyses on lake sediments. In a first step, amino acid-based organic matter degradation and source proxies are tested for their general applicability in different lacustrine environments in India (chapter 3). Additionally, the modern hydrological and biogeochemical properties of the central Indian Lonar Lake that was selected for the palaeo-climate reconstruction are investigated (chapter 4). Finally, the gathered information is integrated into the palaeo-climate reconstruction conducted on a ca. 10 m long sediment core (chapter 4).

In chapter 3, I report the results of amino acid and hexosamine analyses of sediment, soil, vascular plant, and suspended matter samples of four Indian lakes from different climate regimes. Focus is on the identification of amino acid-based degradation and organic matter source proxies that show universal applicability in lacustrine environments. Based on a principal component analysis, a lake sediment degradation proxy is calculated that should be suitable for comparison of the state of organic matter degradation between study sites with different environmental and climatic properties.

Chapter 4 summarises the investigation of the present day conditions of endorheic Lonar Lake in Maharashtra, central India. The lake is eutrophic, brackish, alkaline, and permanently anoxic at water depths > 4 m. Due to high pH and anoxic conditions, denitrification and ammonia volatilisation dominate the dissolved inorganic nitrogen cycle and cause very high $\delta^{15}\text{N}$ values of organisms that grow within the lake. Different redox condition in the sediments of the shallow, nearshore and the deep, distal sediments result in differing organic matter degradation mechanisms and related amino acid assemblages as well as $\delta^{15}\text{N}$ values. Based on the different amino acid assemblages in organic matter degraded under oxic and organic matter degraded under sub- to anoxic conditions, a redox proxy is calculated that is

also applied to the Lonar Lake sediment core during the palaeo-environmental and palaeo-climate reconstruction (chapter 5).

The results of the biogeochemical and mineralogical analyses on the Lonar Lake sediment core that covers the Holocene sedimentation history of the lake are presented in chapter 5. The results of C/N ratios, stable carbon and nitrogen isotopes, grain-size, as well as amino acid derived degradation proxies are compared with climatically sensitive proxies of other records from South Asia and the North Atlantic region. In addition to a long term climate transition from humid conditions during the early Holocene to more arid conditions during the late Holocene at Lonar Lake, delineating the northern hemisphere insolation, several centennial scale climate shifts can be identified. These centennial scale climate shifts correlate with climate variations in the North Atlantic region that were reported in the literature. Contemporaneity of shifts to drier climate in India and colder climate in the North Atlantic region indicate connection between the two climate systems or reaction to identical forcings. A correlation of the climate shifts in both regions with the ^{14}C production rate, a solar output proxy, suggest this forcing to be responsible for the connection between the two systems. Regarding the archaeological history of India, the strong dry phase during 4.6 – 3.9 cal ka BP as reconstructed from Lonar Lake sediments corroborates the hypothesis that severe climate deterioration contributed to the decline of the Indus Civilisation about 3.9 ka BP.

Contents

Zusammenfassung _____	i
Abstract _____	iii
Contents _____	v
1. Introduction _____	1
2. The use of amino acid analyses in (palaeo-) limnological investigations:	
A comparative study of four Indian lakes in different climate regimes _____	16
3. Influence of bottom water anoxia on nitrogen isotopic ratios and amino acid	
contribution of recent sediments from small eutrophic Lonar Lake, central India ____	50
4. Linking Holocene drying trends from Lonar Lake in monsoonal central	
India to North Atlantic cooling events _____	83
5. Conclusions and outlook _____	122
Acknowledgements _____	126
Figure captions _____	127
Table captions _____	131
List of abbreviations _____	134
References _____	137
Curriculum vitae _____	155
List of publications _____	156

1. Introduction

1.1. Indian Monsoon

The Indian climate is dominantly driven by the Indian monsoon but also influenced by the mid-latitude westerlies in the north. The interaction between Indian monsoon and mid-latitude westerlies changes regionally, seasonally, as well as historically and to some extent controls the amount of precipitation and the occurrence of extreme events (Demske et al. 2009). The meteorological mechanism inducing the Indian monsoon is the seasonal shift of the Intertropical Convergence Zone (ITCZ). The ITCZ is a near-surface low pressure belt, which is characterised by ascending masses of warm air causing advection of the trade winds, usually associated with strong winds and precipitation in the regions that are located between the ITCZ and an adjoined ocean (Bookhagen et al. 2005a). The ITCZ shifts annually approximately between the tropic of Cancer and the tropic of Capricorn (Gupta et al. 2003) (Figure 1.1), due to changes in regional insolation driven by the declination of the sun (Bookhagen et al. 2005a). During boreal summer, the ITCZ is located above the Tibetan Plateau, causing the transport of warm and wet air masses from the Arabian Sea and the Bay of Bengal over the Indian subcontinent towards the Himalayan mountains. The Himalaya range, being an orographic barrier, induces heavy rainfall at its southern boundary during the summer or southwest monsoon and prevents significant moisture transport further north. This causes the arid to semi-arid climate conditions north of the mountain range (Wulf et al. 2010). During boreal winter, the ITCZ is located south of India on the southern hemisphere, thus the wind direction is inverted blowing from the high pressure cell over the Tibetan Plateau in the northeast towards the Indian Ocean. Hence, the winter or northeast monsoon is characterised by cool and dry weather over most of India (Clift and Plumb 2008). In northwest India, the

mid-latitude westerlies also contribute to the wind-regime and the related precipitation. The westerlies mostly bring in winter precipitation in the form of snow.

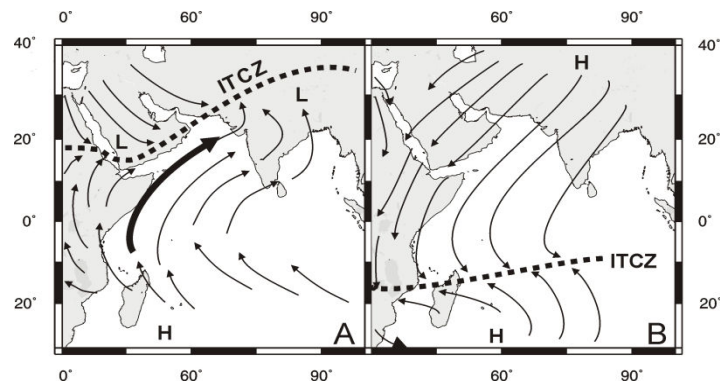


Figure 1.1: Approximate location of the ITCZ and dominant wind directions during boreal summer (A) and boreal winter (B) (Fleitmann et al. 2007).

1.2. Palaeo-monsoon and climate reconstructions

Climate reconstruction becomes more and more important in unravelling the forcings and driving mechanisms of climate changes. This is especially important to understand and predict present and future climate changes in a global warming scenario. Palaeo-reconstruction in monsoon-influenced regions is most promising, since the monsoon is an annually occurring, relatively steady phenomenon. Thus, it shows periodic imprint on different environmental archives, and changes in its influence can comparatively reliably be identified. Hence, several studies have focussed on the variability of the monsoon climate since the last glacial maximum (*see* Clift and Plumb 2008).

Driven by periodic variations in Earth's orbital parameters, changes in solar energy are largely responsible for the long term, global climate changes as for example the intensity of Northern Hemisphere Glaciation (Shackleton and Opdyke 1977). Regional climate patterns, such as monsoon systems, are also strongly influenced by variations in the energy budget, and thus vary according to the glacial-interglacial cycles (Sirocko et al. 1993). It is suggested that

the large (millennial) scale monsoon variability is mostly driven by changes in northern hemisphere insolation and glacial boundary conditions (Prell and Kutzbach 1987). These linkages affect the temperature gradients between ocean and continent which account for the monsoon strength. Weaker temperature gradients not only reduce the wind speed and the amount of moisture transported from the ocean to the continent, but they also determine the pole-ward extension of the ITCZ, and thus of the monsoon precipitation (Fleitmann et al. 2007). Large scale changes in monsoon strength and extend had severe influence on the natural environment and therefore on the livelihood of human beings and might have affected the development, prosperity, and decline of ancient cultures (Madella and Fuller 2006). The millennial scale monsoon development during the Holocene, as well as centennial monsoon strength variations, their potential causes and tele-connections, and the possible influence of monsoon strength variability on ancient civilisations are topic of the discussion of chapter 4.

1.3. Lake sediments

Compared to the oceans, lakes are relatively small, isolated ecosystems. This feature makes them prime candidates for the study of biogeochemical cycles and related researches. Important differences between lakes and oceans with respect to biogeochemical analyses are the usually larger contribution of material of terrestrial origin to lake sediments, the shallower depth of lakes compared to the open ocean, and the typically higher sedimentation rate in lakes. The two latter aspects account for the often enhanced incorporation of organic matter into lake sediments and its reduced state of degradation (Meyers and Ishiwatari 1993; Meyers 1997).

Lake sediments are suitable for palaeo-climate reconstructions due to their incorporation of both aquatic and terrestrial material. Thus, lake sediments contain information on changes of the hydrology and biology of the lake itself as also on changes in land plant vegetation and

erosion and transport of terrestrial sediment. Therefore, several more or less independent proxies can be obtained from lake sediment based analyses. Additionally, lakes can build up continuous, seasonally laminated sediments, which can help to construct reliable high-resolution age models for the laminated parts of lake sediment records.

1.4. Biogeochemical proxies

1.4.1. Ratio between organic carbon and total nitrogen (C/N)

The ratio between organic carbon and total nitrogen (C/N) in environmental studies is commonly used to determine the dominant source of organic matter. This is due to the characteristic compositions of terrestrial and aquatic organic matter. Vascular plants, significantly contributing to terrestrial organic matter, are enriched in carbon-rich and nitrogen-poor cellulose and lignin, whereas the mostly nonvascular aquatic organic matter contains relatively large amounts of carbon- and nitrogen-rich proteins and lacks lignin and cellulose (Meyers and Ishiwatari 1993). Thus, aquatic OM is typically characterised by atomic C/N ratios of 4 to 10, whereas terrestrial OM usually shows atomic C/N ratios > 20 (Meyers and Teranes 2002). And since degradation only has minor effects on the C/N ratio of OM (Meyers 1997), it is a good source proxy in sediments with varying contribution of terrestrial and aquatic OM. However, the most important limitation of C/N ratio as proxy of OM origin is associated with the contribution of inorganic nitrogen to the measured total nitrogen. Hence, in sediments showing low OM, and thus low organic carbon (ca. $< 0.3\%$) and nitrogen contents, the percentage of inorganic nitrogen, such as ammonium sorbed by clay minerals (Müller 1977), can contribute significant percentages to the total nitrogen portion, thereby considerably lowering the C/N ratio (Meyers and Teranes 2002).

1.4.2. Stable isotopes

Stable isotope chemistry is used in environmental science as source and sink as well as process proxy (Peterson and Fry 1987). That is due to the fact that different isotopes of the same element show different physical characteristics, which can also slightly affect some of their chemical properties (Hoefs 2009). Isotopic fractionation occurs due to equilibrium or kinetic processes, with equilibrium processes not being accompanied by chemical reactions but by the exchange of different isotopes of an element between individual chemical compounds, different phases, or between molecules (Hoefs 2009). Kinetic effects drive different isotopic composition between products and educts of unidirectional or incomplete processes (Hoefs 2009). During chemical reactions, the compounds including light isotopes generally react more easily than those including heavy isotopes, due to the fact that light isotopes form weaker bonds than heavy isotopes (Hoefs 2009). Both equilibrium and kinetic processes affect the isotopic composition of several chemical compounds and complex materials that are commonly analysed during environmental investigations, and the isotopic composition of these materials can be determined and used to reconstruct the fractionating processes, which potentially allows for revelation or reconstruction of specific environmental patterns.

The magnitude of isotope fractionation associated with an individual process is calculated in form of a fractionation factor (α). α is defined as the ratio of the ratios of two isotopes (R) of an element, for example ^{13}C and ^{12}C , in two different chemical compounds (X, Y):

$$\alpha_{x-y} = \frac{R_x}{R_y} \tag{1.1}$$

$$R = \frac{^{13}\text{C}}{^{12}\text{C}} \tag{1.2}$$

α is often dependent on external conditions, such as temperature.

The isotopic composition of a chemical compound is commonly expressed as delta value (δ), which gives the ratio between the isotopic composition of the analysed compound and the isotopic composition of a reference standard in per mill:

$$\delta (\text{‰}) = [(R_{\text{sample}} / R_{\text{standard}}) - 1] \times 1000 \quad (1.3)$$

During this study, the stable carbon and nitrogen isotopic composition of organic matter from different environmental samples was determined and interpreted. The most important processes driving isotopic differences of the two elements in organic matter are listed in the following paragraphs.

1.4.2.1. Stable carbon isotopes

Carbon plays a major role in natural biogeochemical cycles, since all organisms dominantly consist of water and different carbonic compounds. In terrestrial aqueous environments, carbon is mostly present in the form of dissolved inorganic carbon (DIC), dissolved organic carbon (DOC), and particulate organic carbon (POC). Usually, DIC is higher concentrated in natural terrestrial water (10 mmol/l) compared to DOC (1 – 2 mmol/l) (Darling et al. 2006). The distribution of the different DIC forms in water is pH-dependent, with dissolved CO₂ (CO₂(aq)) dominating in acidic water (pH < 4.3), bicarbonate (HCO₃⁻) being the dominant form at pH values between 4.3 and 8.3, and carbonate (CO₃²⁻) being the dominating form in alkaline water (pH > 8.3) (Schlesinger 1997).

Carbon exhibits two stable isotopes, ¹²C and ¹³C, which show natural abundances of 98.93 % and 1.07 %, respectively (Berglund and Wieser 2011). The standard for carbon isotopic analyses is Vienna Pee Dee Belemnite (VPDB).

The $\delta^{13}\text{C}$ values of DIC in surface waters are determined by several mechanisms, such as the exchange with atmospheric CO_2 , pH values that determine the dominant form of DIC, respiration of organic carbon, dilution of inorganic carbonate rocks, CO_2 uptake during photosynthesis, redox conditions that influence the mechanisms and inorganic products of organic matter decomposition, and the development and stability of stratification. A brief overview of important sources and transformation processes that affect $\delta^{13}\text{C}$ of DIC and OM in lakes is shown in Figure 1.2. In closed lakes, the $\delta^{13}\text{C}$ values of DIC are very sensitive to factors like the precipitation/evaporation ratio and the geology and vegetation of the catchment area (Lei et al. 2012). A detailed description of the effects of these factors on the isotopic contribution of DIC is given in chapter 4.3.4.4.

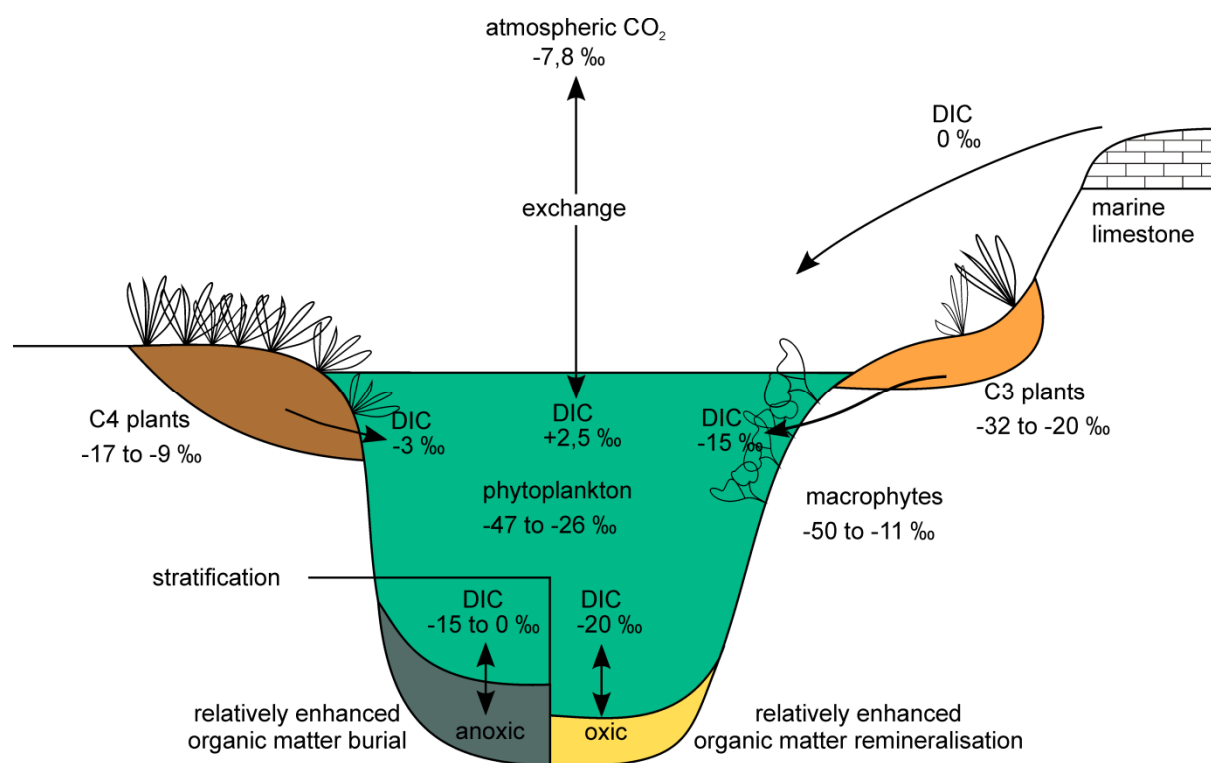


Figure 1.2: Overview of $\delta^{13}\text{C}$ values of major carbon sources to lakes and resulting $\delta^{13}\text{C}$ values of DIC (modified after Martens (submitted) and Leng et al. (2006)).

Terrestrial plants show characteristic $\delta^{13}\text{C}$ values of -38 to -8 ‰ . The CO_2 fixation in plants is associated with two fractionating steps; the uptake and intracellular diffusion of CO_2 and the enzymatic fixation or biosynthesis of organic carbon (Hoefs 2009). According to different

CO₂ uptake and fixation mechanisms, three types of plants can be discerned: C₃ plants using the Calvin Cycle for carbon fixation usually show $\delta^{13}\text{C}$ values between -38 and -22 ‰, C₄ plants using the Hatch-Slack-Cycle for carbon fixation typically have $\delta^{13}\text{C}$ values of -15 to -8 ‰, and CAM plants using the Crassulacean Acid Metabolism cycle of carbon fixation show $\delta^{13}\text{C}$ values of -30 to -13 ‰ (Darling et al. 2006). With respect to climate variability, the growth of C₃ plants is favoured during relatively wet conditions, whereas C₄ and CAM plants usually dominate during relatively dry conditions. C₄ plants dominantly comprise grasses and macrophytes growing in tropical environments, especially in savannas (Mariotti and Peterschmitt 1994). Concerning the environment, C₄ plants are almost absent at elevations > 3000 m above sea level (Tieszen et al. 1979).

$\delta^{13}\text{C}$ values of phytoplankton is more diverse compared to terrestrial plants, even though most phytoplankton species use the Calvin Cycle pathway of CO₂ fixation. However, the concentration of CO₂, and thus the fractionation during photosynthesis, is much more variable in aquatic compared to subaerial environments. The same holds true for the $\delta^{13}\text{C}$ values of the photosynthetic educt, which is transmitted into the photosynthetic product. Air CO₂ shows almost universally $\delta^{13}\text{C}$ values of about -7.8 ‰, whereas the $\delta^{13}\text{C}$ values of DIC are much more variable, depending on various factors as mentioned above.

1.4.2.2. Stable nitrogen isotopes

Nitrogen is a crucial nutrient for the production of organic matter and alike silica and phosphorus occasionally growth limiting. Nitrogen is often the growth-limiting nutrient in eutrophic lakes, whereas phosphorus often is limiting in oligotrophic lakes (Chapin III et al. 2011). The most important dissolved nitrogenous nutrient forms in aqueous systems are ammonium (NH₄⁺), ammonia (NH₃), nitrate (NO₃⁻), and nitrite (NO₂⁻) (Talbot 2001). The

abundance of the different forms is closely linked to a couple of transformation processes, which are shown in Figure 1.3 and described below:

- Nitrogen fixation: During this process, microorganisms transform the inert nitrogen molecule (N_2) into bio-available nitrogenous nutrients (Hoefs 2009). Especially photoautotroph cyanobacteria are capable of fixing N_2 in aqueous systems.
- Nitrification: Nitrification describes microbially mediated oxidation that transforms ammonium via multiple intermediates into nitrite and nitrate, occurring under aerobic conditions (Wetzel 2001).
- Denitrification: Under an- and suboxic conditions, microbes use oxidised nitrogen nutrient forms as oxygen source and reduce them to molecular nitrogen (N_2) (Wetzel 2001).
- Ammonium and nitrogen assimilation: These are the uptake processes that convert the inorganic nitrogen nutrients into nitrogenous organic matter. In high productive lakes, these processes are capable to totally deplete nitrogenous nutrients in the photic zone. The uptake of ammonium is energetically more beneficial than the uptake of nitrate, and thus preferred (Talbot 2001).
- Ammonification: Under anaerobic conditions, this microbially mediated process remineralises organic-bound nitrogen. The organic nitrogen is converted to ammonium and ammonia (Talbot 2001).
- Ammonia volatilization: This inorganic transformation process occurs to significant extent in waters showing pH values > 8.5 and elevated ammonium concentrations, the latter often linked to sub- or anoxic waters. Under these conditions, the equilibrium between ammonium and ammonia is shifted towards ammonia, which can escape the water column in gaseous state (Casciotti et al. 2011).

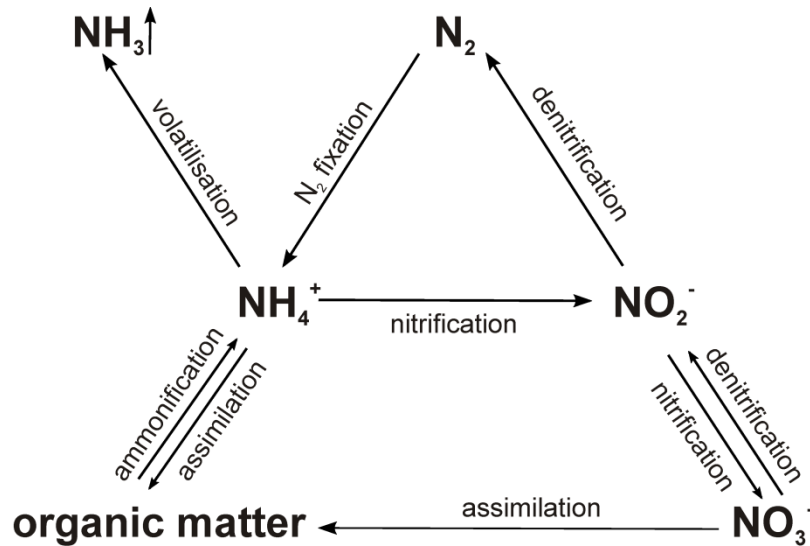


Figure 1.3: Schematic nitrogen cycle (modified after Hensen et al. (2000)).

The natural abundance of the two stable nitrogen isotopes ^{14}N and ^{15}N is 99.64 % and 0.36 %, respectively (Berglund and Wieser 2011). The standard of nitrogen isotope investigation is air N_2 .

Due to the high complexity of chemical and biological processes involved in the nitrogen cycling in natural environments, the interpretation of nitrogen isotopic ratios is more difficult compared to carbon isotopic ratios. The fractionation factors associated with the different transformation processes are shown in Table 1.1. $\delta^{15}\text{N}$ values might be altered during degradation. The degree of alteration depends on the redox conditions during degradation, with stronger enrichment of the heavy isotope under aerobic conditions (Lehmann et al. 2002). Even though terrestrial plants show a wide range of $\delta^{15}\text{N}$ values (Maksymowska et al. 2000), lake sediments with high contribution of terrestrial organic matter are usually depleted in ^{15}N compared to sediments with high aquatic organic matter contribution (Meyers 1997). Thus, $\delta^{15}\text{N}$ of organic matter in lake sediments can give some source information, which, however, should be confirmed by other source sensible proxies. A brief overview of important sources and transformation processes that affect $\delta^{15}\text{N}$ of DIN and OM in lakes is shown in Figure 1.4.

Table 1.1: Fractionation factors (α) of different nitrogen transformation processes.

Process	Fractionation factor α	Reference
Inorganic processes		
N ₂ dissolution in water, $N_{2(g)} \rightarrow N_{2(aq)}$	1.00085	Collister and Hayes 1991
Ammonia volatilisation, $NH_4^+_{(aq)} \rightarrow NH_{3(g)}$	1.020 – 1.035	Casciotti et al. 2011
Biochemical processes		
Nitrogen fixation, $N_2 \rightarrow N_{org}$	0.998 – 1.002	Casciotti 2009
Nitrate assimilation, $NO_3^- \rightarrow N_{org}$	1.006 – 1.020	Granger et al. 2004
Ammonium assimilation, $NH_4^+ \rightarrow N_{org}$	1.011 – 1.014	Hoch et al. 1992; Voss et al. 1997
Ammonification, $N_{org} \rightarrow NH_4^+$	1.001	Collister and Hayes 1991
Nitrification (Ammonia oxidation), $NH_3 \rightarrow NO_2^-$	0.996 – 1.0194	Casciotti et al. 2003
Nitrification (Nitrite oxidation), $NO_2^- \rightarrow NO_3^-$	0.9872	Casciotti 2009
Denitrification, $NO_3^- \rightarrow N_2$	1.022 – 1.030	Brandes et al. 1998

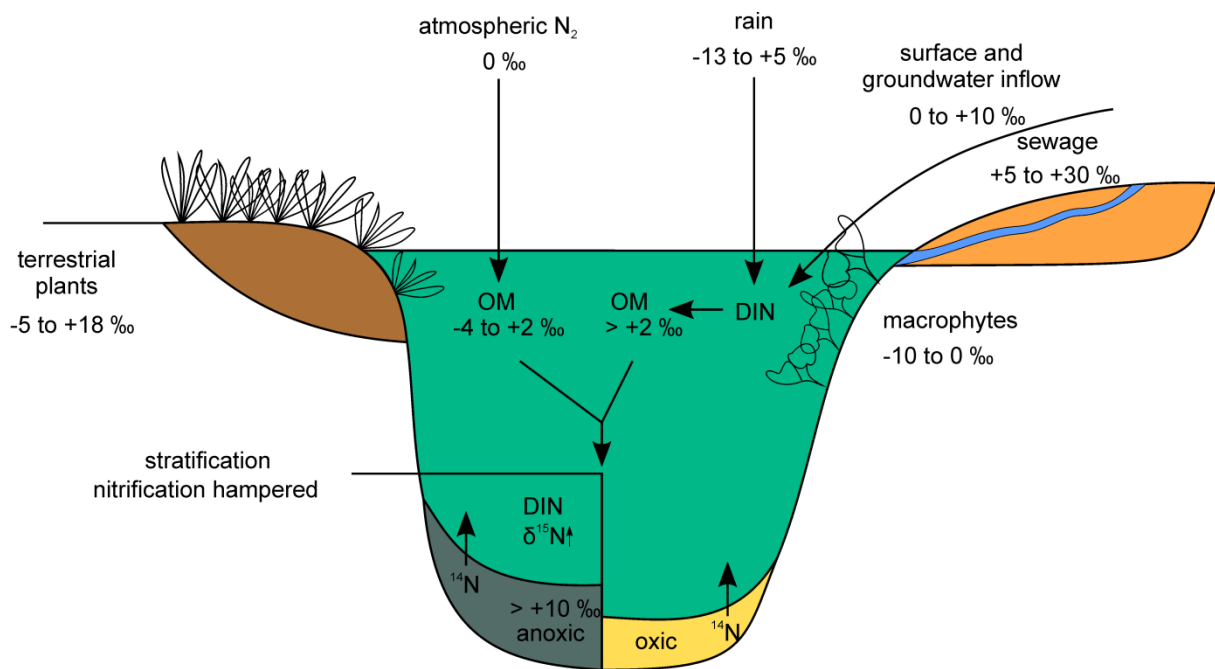


Figure 1.4: Overview of $\delta^{15}\text{N}$ values of major nitrogen sources to lakes (modified after Martens (submitted) and Leng et al. (2006); values after Maksymowska et al. (2000) and Talbot (2001)).

1.4.3. Amino acids

The majority of nitrogen in organic matter is usually present in the form of amino acids (Wakeham et al. 1997), which are the building blocks of proteins. The individual amino acids are classified due to their reactive side chains (Figure 1.5).

	DI	RI	LDI	Indicative properties
Asp	■		■	associated with carbonate shells (Carter & Mitterer, 1978)
Glu	■		■	associated with carbonate shells (Carter & Mitterer, 1978) labile, associated with cell plasma (Hecky et al., 1973)
Thr	■		■	associated with siliceous organisms (Hecky et al., 1973)
Ser	■		■	
Gly	■		■	
Ala	■		■	
Val	■		■	labile (Cowie & Hedges, 1992)
Ile	■		■	
Leu	■		■	
Tyr	■	■	■	labile, associated with cell plasma (Hecky et al., 1973)
Phe	■	■	■	
Trp				
His	■		■	sorption to mineral surfaces (Hedges & Hare, 1987)
Lys			■	
Arg	■		■	
Orn			■	
β-Ala		■	■	degradation product of Asp (Cowie & Hedges, 1994)
γ-Aba		■	■	degradation product of Glu (Cowie & Hedges, 1994)
Cya				no amino acid by chemical definition
Met	■		■	
Mso				
Tau				
Glum				associated with chitin (zooplankton) (Benner & Kaiser, 2003)
Galam				associated with bacteria (Kandler, 1979)

Figure 1.5: Overview of analysed amino acids (modified after Martens (submitted)).

During degradation, amino acids are, in general, preferentially decomposed (Lee 1988). Thereby, not only the general amino acid concentration declines but also the composition of the amino acid assemblage alters (Lee 1988). Hence, the state of degradation can be identified from the amino acid assemblage of organic matter, and different amino acid-based degradation indices were invented. The most common are the degradation index (DI) (Dauwe and Middelburg 1998; Dauwe et al. 1999) and the reactivity index (RI) (Jennerjahn and Ittekkot 1997). A comprehensive investigation of amino acid-based organic matter degradation and source indices, with special focus on the applicability of such indices to lacustrine environments, is given in chapter 2.

1.5. Thesis outline and project

The studies presented in this PhD thesis were conducted within the framework of the DFG-funded HIMPAC (Himalaya: Modern and Past Climate) project. HIMPAC is an international project, with participation of primarily German and Indian research institutes. The scope of the HIMPAC research is to identify the Holocene climate variability over the Indian subcontinent by means of multi-proxy and multi-archive investigations. Additionally, extreme events, such as droughts and floods, and variations in the interaction between the Indian monsoon and large-scale climate phenomena, such as El Niño Southern Oscillation or North Atlantic Oscillation are subject of investigation. Therefore, several climate archives, as for example, lake sediments, speleothems, peat profiles, tree-rings, and the geomorphology were examined. The palaeo-climate reconstructions should help to identify the most prominent factors controlling the climate variability over the Indian subcontinent and further help to decipher future changes in climate and their influence on the natural and socio-economic environment against the background of prevailing global warming.

Subject of my research were lake sediments with focus on biogeochemical proxies, especially amino acids and stable carbon and nitrogen isotopes, which were used to identify modern lake processes and mechanisms controlling and influencing the biogeochemical cycles within the lakes. Based on these investigations, the applicability of individual biogeochemical proxies in reconstructing the palaeo-environment and palaeo-climate was assessed (chapters 2 and 3). Finally, by using the most promising biogeochemical proxies, a reconstruction of the Holocene palaeo-climate based on a continuous sediment record from the central Indian Lonar Lake was performed and compared with other regional and global palaeo-climate reconstructions whereupon possible mechanisms that could have controlled the identified changes were discussed and appraised (chapter 4).

The three main chapters base on publications in international journals; these publications, in addition to others, are listed on page 156.

2. The use of amino acid analyses in (palaeo-) limnological investigations: A comparative study of four Indian lakes in different climate regimes

Abstract

In the present study, we report the results of comprehensive amino acid (AA) and hexosamine (HA) analyses of four Indian lakes from different climate regimes. We focus on the investigation of sediment cores retrieved from the lakes but data of modern sediment as well as vascular plant, soil, and suspended particulate matter samples from individual lakes are also presented. Commonly used degradation and organic matter source indices are tested for their applicability to the lake sediments, and we discuss potential reasons for possible limitations. A principal component analysis including the monomeric AA assemblages of all analysed samples indicates that differences in organic matter sources and the environmental properties of the individual lakes are responsible for the major variability in monomeric AA distribution of the different samples. However, the PCA also gives a factor that most probably separates the samples according to their state of organic matter degradation. Using the factor loadings of the individual AA monomers, we calculate a lake degradation index (LDI) that might be applicable to other palaeo-lake investigations.

2.1. Introduction

Amino acid (AA) and hexosamine (HA) analyses yield reliable information about the state of organic matter degradation in modern as well as in palaeo-sediments especially from the marine environment (Lee 1988; Cowie and Hedges 1994; Wakeham et al. 1997; Dauwe et al. 1999; Keil et al. 2000) but also from limnological and fluvial systems (Kemp and Mudrochova 1973; Gupta et al. 1997; Meckler et al. 2004; Unger et al. 2005; Das et al. 2010). The accumulation of individual AA monomers can be due to their production during specific degradation processes or to their relative accumulation due to their resistance to degradation processes (Lee and Cronin 1984; Lee 1988). They may, furthermore, be protected from degradation by incorporation into shell material or by sorption to mineral surfaces (Hecky et al. 1973; King 1977; Müller and Suess 1977; Carter and Mitterer 1978; Hedges and Hare 1987; Henrichs and Sugai 1993).

AA composition in marine samples is very similar in different regions and variations depend mostly on the degradation state of organic matter. In contrast, the variations in AA composition are much larger in terrestrial influenced systems where sources of organic matter have a stronger imprint on AA spectra potentially complicating their interpretation (Meckler et al. 2004; Gaye et al. 2007; Unger et al. 2013).

Many attempts were made to summarise the degradation or source information that can be obtained by AA and HA analyses in terms of individual indices that have universal applicability. Early information about the state of organic matter degradation gathered from AA analyses was based on the diminished concentration of AA in marine sediments with progressing sediment depth and the reduced percentage of nitrogen associated with AA (Emery et al. 1964; Kemp and Mudrochova 1973; Rosenfeld 1979). Later, the enrichment and depletion of individual AA monomers was found to be related to progressing degradation (Whelan 1977; Lee and Cronin 1982). According to these findings, ratios between

proteinogenic AA monomers and their respective degradation products or intermediates were used to assess the state of organic matter degradation (Henrichs et al. 1984; Ittekkot et al. 1984b). Also, the sensitivity of AA-based proxies to different stages of organic matter decomposition (Cowie and Hedges 1994; Unger et al. 2005; Davis et al. 2009) and to different environmental conditions (Cowie et al. 1995; Nguyen and Harvey 1997; Keil et al. 2000) was investigated. Based on the previous works, more complex degradation indices were invented as for example ratios of the sums of different protein and non-protein AAs (Jennerjahn and Ittekkot 1997; Gupta and Kawahata 2007) or the combination of the differences in molar percentage of individual AAs between samples and a reference data set, weighted on the basis of a principal component analysis (Dauwe and Middelburg 1998; Dauwe et al. 1999). In a next step, AA- and HA-based indices were also applied to terrestrial systems (Das 2002; Verma and Subramanian 2002; Jennerjahn et al. 2004), and the adopted indices were tested and adapted to the different environments (Meckler et al. 2004; Ingalls et al. 2006; Menzel et al. 2013).

Early source information gathered from AA and HA analyses was based on the preferential association of individual AAs and HAs with specific organisms, as for example bacteria (Schleifer and Kandler 1972; Lee and Bada 1977; Kandler 1979), or biologically produced substances, such as chitinous (Degens and Mopper 1975; Müller et al. 1986), calcareous (King 1977; Müller and Suess 1977; Carter and Mitterer 1978; Ittekkot et al. 1984a), and siliceous (Hecky et al. 1973; King 1977) matter. Additionally, characteristic AA assemblages of terrestrial and aquatic organic matter were investigated (Degens and Mopper 1975; Cowie and Hedges 1992), and ratios and sums of individual AAs and HAs were invented to characterise the dominant origin of organic matter in sinking particles and sediments (Ittekkot et al. 1984b; Müller et al. 1986; Lomstein et al. 2006).

In this study, we analysed the AA assemblages of sediment cores of four lakes from different climate regimes as well as samples from the vicinities of two of the investigated

lakes and tested the different AA-based degradation and organic matter source indices. The aim was to identify degradation and organic matter source indices that show universal applicability and to detect factors that potentially bias the use of individual indices in lake systems.

2.2. Study sites

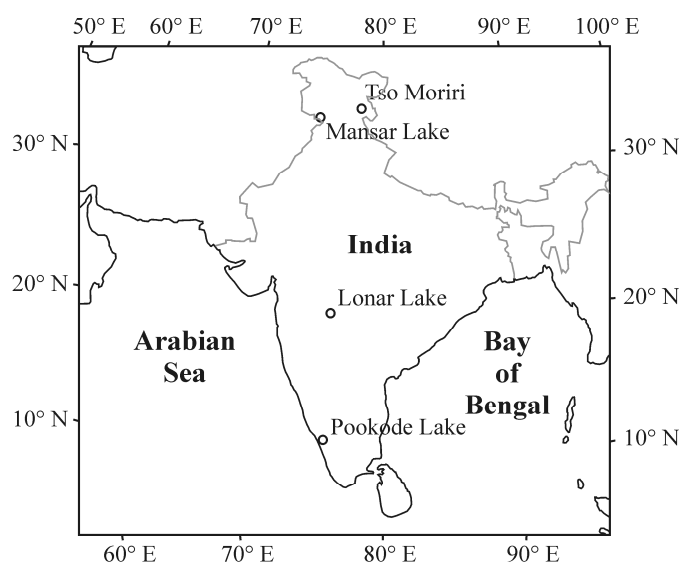


Figure 2.1: Map showing the locations of the four investigated lakes.

Four Indian lakes were investigated during this study: The Tso Moriri in Leh district of Jammu and Kashmir state in northern India, the Mansar Lake in Udhampur district of Jammu and Kashmir state in northern India, the Lonar Lake in Buldhana district of Maharashtra state in central India, and the Pookode Lake in Wayanad district of Kerala state in south India (Figure 2.1). Table 2.1 summarises some general and environmental properties of the four lakes.

Table 2.1: Locations as well as hydrological and meteorological properties of the four lakes, Tso Moriri, Mansar Lake, Lonar Lake, and Pookode Lake.

	Tso Moriri	Mansar Lake	Lonar Lake	Pookode Lake
Latitude	32° 55' N	32° 42' N	19° 59' N	11° 33' N
Longitude	78° 19' E	75° 09' E	76° 30' E	76° 02' E
Elevation (m a.s.l.)	4500	650	480	770
N-S Extension (km)	27 ^a	1.2 (NW-SE) ^d	1.2 ^g	0.3 ^k
E-W Extension (km)	5 – 7 ^a	0.6 (NE-SW) ^d	1.2 ^g	0.2 ^k
Surface area (km ²)	150 ^a	0.6 ^d	1 ^h	< 0.1 ^k
Max. depth (m)	105 ^a	38 ^d	7 ⁱ	7 ^k
pH	9 – 9.5 ^a	8 – 8.5 ^e	9 – 10.5 ⁱ	6 – 7 ^l
Dissolved oxygen (mg/l)	5.4 – 6.6 ^a	7.1 – 9.8 ^e	0.1 – 16.4 ⁱ	6.3 – 7.4 ^l
Conductivity (mS/cm)	1.6 ^a	0.19 – 0.20 ^e	13 – 21 ⁱ	0.03 – 0.05 ^l
Annual Precipitation (mm)	100 – 300 ^b	1500 ^d	700 ^j	4400 ^l
Min. annual air Temp. (°C)	-40 ^c	+1 ^f	+11 ^j	+7 ^k
Max. annual air Temp. (°C)	+30 ^c	+42 ^f	+42 ^j	+35 ^k

a: Mishra et al. (unpubl.); b: Bookhagen and Burbank (2010); c: Mishra and Humbert-Droz (1998); d: Das et al. (2010); e: Al-Mikhlaifi et al. (2003); f: Trivedi and Chauhan (2009); g: Prasad et al. (2014); h: Menzel et al. (2013); i: Basavaiah et al. (2014); j: http://indiawaterportal.org/met_data/; k: Veena et al. (2014); l: Nirmala et al. (1991)

2.2.1. Tso Moriri

The modern Tso Moriri is a closed, alpine lake. The lake is ice covered between ca. mid October and early March. It is fed by two perennial streams and several ephemeral melt water inflows. The lake water is oxidic, alkaline, slightly brackish, and oligotrophic (Hutchinson 1937; Chandan et al. 2008). Tso Moriri is located in the orographic rain shadow of the North Western Himalaya in a cold arid to semi-arid region. Ca. 70% of the annual precipitation falls during summer and is associated with the Indian summer monsoon, whereas 30% falls during winter in the form of snow and is brought in by the mid latitude westerlies (New et al. 2002; Bookhagen and Burbank 2010). The geological setting of the surrounding area is characterised by granitic intrusions and metamorphic rocks, such as gneisses, schists, marbles, quartzites, eclogites, and metasediments (Fuchs and Linner 1996; Rao and Rai 2002; Eparad

and Steck 2008). The catchment of the lake is sparsely vegetated, with domination of steppe and desert-steppe vegetation (Leipe et al. in press).

2.2.2. Mansar Lake

Mansar Lake is a subtropical, tectonic, fresh-water lake situated in the Lesser Himalayas. The lake is fed by precipitation, runoff, and underground springs; no perennial stream enters the lake whereas one outlet exists in the northeast (Das et al. 2010). The annual precipitation is dominantly provided by the Indian summer monsoon. The lake is oxic and slightly alkaline with pH values varying seasonally with highest values during spring prior to the monsoon onset and lowest values during and shortly after the summer monsoon (Al-Mikhlaifi et al. 2003). Phosphate concentrations of > 0.03 mg/l indicate the eutrophic nature of the lake. The lake is eutrophic as indicated by phosphate concentrations > 0.03 mg/l (Kumar 2005). The surrounding area comprises of sedimentary rocks mainly sand-, silt-, and mud-stones (Das et al. 2010). The vegetation of the vicinity of Mansar Lake is characterised by forested slopes with *Pinus roxburghii* dominated forest on the slope crests and *Quercus incana* dominated forests around the lake (Trivedi and Chauhan 2009).

2.2.3. Lonar Lake

Lonar Lake is an almost circular, closed, tropical lake situated in a meteorite crater that formed on the ca. 65 Ma old Deccan Plateau basalts during the Pleistocene. The lake is fed by three perennial streams and by ephemeral runoff during the monsoon season (Anoop et al. 2013b). The local climate is semi-arid with a long dry period between October and May (Riedel et al. submitted). Lonar Lake is situated in the so called 'core monsoon zone' (Gadgil 2003), and thus receives its annual rainfall almost exclusively during the summer monsoon

period between June and September (Basavaiah et al. 2014). The modern lake water is hyposaline, alkaline, eutrophic (phosphate concentration = 4.4 – 6.7 mg/l), and exhibits sub-to anoxic bottom water (Basavaiah et al. 2014). Due to lake water eutrophication, Lonar Lake experiences annual phases of strong algal growth. The algal assemblage is strongly dominated by cyanophyta, which are growing under saline and alkaline conditions and which are capable of using HCO_3^- as inorganic carbon source. The vicinity of the lake is vegetated with different forest types. The alluvial plain surrounding the lake hosts semi-evergreen forest with dominant invasive *Prosopis juliflora* forest near shore. The crater slopes are characterised by dry deciduous *Tectona grandis* forest, whereas the crater rim and the surrounding plains are dominated by thorn shrub vegetation like *Acacia nilotica* (Riedel et al. submitted). An alluvial fan formed in the northeast of the lake where two of the three perennial streams enter the lake. Today, the fan is under agricultural use and crops, such as banana (*Musa x paradisiaca*), millet (*Setaria italica*, *Sorghum bicolor*), corn (*Zea mays*), custard-apple (*Annona reticulata*), and papaya (*Carica papaya*) are cultivated (Menzel et al. 2013).

2.2.4. Pookode Lake

Pookode Lake is a tropical, closed basin freshwater lake situated in the Western Ghat region. The lake has no tributary and is fed by monsoon rain and surface runoff. Most of the annual precipitation falls during the summer monsoon between June and September (Nirmala et al. 1991). The lake water is oxic, meso – eutrophic (phosphate concentration = 0.02 – 0.08 mg/l) with neutral to slightly acidic pH (Nirmala et al. 1991). The surrounding rocks belong to the Wayanad Group and consist of charnockite and hornblende-biotite gneiss (Veena et al. 2014) covered by ferruginous loamy soils (Sandeep et al. 2011). The phytoplankton assemblage comprises Chlorophyceae, Cyanophyceae, and Bacillariophyceae. The most abundant species is the Chlorophyceae *Ulothrix sp.* (Nirmala et al. 1991). The zooplankton

community is represented by *Protozoa*, *Rotifera*, *Arthropoda*, and *Plathyhelminthes*; Pookode Lake also hosts fishes, snakes, turtles, and water birds (Nirmala et al. 1991). Macrophytes like *Nymphaea nouchali* grow within the lake, whereas its vicinity is characterised by densely forested hills (Sabu and Ambat 2007), with key dicotyledonous species of the Western Ghats, such as *Syzygium caryophyllatum*, *Symplocos cochinchinensis*, *Meliosma simplicifolia*, *Litsea lavigata*, *Cinnamomum malabathrum*, *Leea indica*, *Aporosa lindleyana*, *Cyanotis* sp., a monocotyledonous species of *Pandanus* and a pteridophyte species of *Asplenium* in addition to several species of grasses, sedges, and other herbs.

2.3. Methods and material

2.3.1. Sampling

Surface sediments, soil, and terrestrial plant samples were collected in January 2007, May 2008, and February 2011 from Lonar Lake and in July 2011 from Tso Moriri. Additionally, suspended particulate matter was filtered from Lonar Lake in February 2011 and sediment trap samples were collected for the intervals February to May 2011, and May to October 2011 at Lonar Lake. Using a UWITEC piston corer, sediment cores were retrieved in December 1998 from Mansar Lake, in May 2008 from Lonar Lake, in July 2011 from Tso Moriri, and in May 2012 from Pookode Lake. The sediment cores were opened and sub-sampled in the laboratory. All samples were freeze-dried and afterwards ground manually in an agate mortar.

2.3.2. Analytical methods

Total carbon (TC) and total nitrogen (TN) contents of the samples were determined on a Carlo Erba NC2500 element analyser. A fraction of grounded sample material was weighted

and wrapped into pre-combusted tin capsules and analysed via flash combustion in the element analyser. The total organic carbon (TOC) content of samples was determined following the same procedure after decalcification of sample fractions with 20% HCl in pre-combusted silver capsules. Calibration standard for these measurements was acetanilide. Precision of this method is 0.05% for carbon and 0.005% for nitrogen.

AA and HA analyses were carried out on a Biochrom 30 Amino Acid Analyser according to the method by Roth and Hampař (1973). Before analysis, samples were hydrolysed for 22 hours with 6 mol/l HCl under a pure argon atmosphere at 110°C. Un-reacted HCl was removed from the hydrolysate by evaporation using a vacuum rotating evaporator (Büchi). The residue was resolved into an acidic buffer (pH 2.2) and injected into the analyser. Using this method, we quantified the 18 AA monomers aspartic acid (Asp), threonine (Thr), serine (Ser), glutamic acid (Glu), glycine (Gly), alanine (Ala), valine (Val), methionine (Met), isoleucine (Ile), leucine (Leu), tyrosine (Tyr), phenylalanine (Phe), β -alanine (β -Ala), γ -aminobutyric acid (γ -Aba), histidine (His), ornithine (Orn), lysine (Lys), and arginine (Arg) as well as the 2 HAs glucosamine (Gluam) and galactosamine (Galam). Asp and Glu potentially include the respective contributions from asparagine and glutamine after hydrolysis with HCl. All AA and HA molar concentrations were calculated against a standard (SIGMA AA-S-18 with addition of Orn, β -Ala, γ -Aba, Gluam and Galam), which was analysed prior to the measurements. Duplicate measurement of the standard solution resulted in a relative error of 0.1 to 1.3 % for the concentrations of individual AA monomers. Duplicate measurement of a single sediment sample revealed a relative error of < 1 % for AA and HA concentrations, < 10 % for low concentrated (< 1 mol%) AA monomers, and < 2.5 % for higher concentrated (> 1 mol%) AA monomers.

2.3.3. Approach

AAs and HAs are commonly used to determine the state of OM degradation in sediments. Additionally, they can give information about the dominant organisms contributing to the deposited OM. The total AA and HA contributions to the samples are source and degradation indices. But, since the total amounts of AA in sediment and OM samples are highly dependent on the TOC and TN contents of the samples, we normalized the AA concentrations to TOC and TN content of the samples. These values are given in percent TOC and TN incorporated into AAs and are named AA-C and AA-N. And, whereas AA-C of sediment samples is influenced by the state of degradation but much more dependent on the ratio between TOC rich but AA poor terrestrial plant material and TOC and AA rich aquatic OM, AA-N is less source dependent but much more influenced by the state of organic mater degradation (Cowie and Hedges 1994).

To assess the state of OM degradation, we also calculated ratios and indices based on the monomeric distribution of the AAs, the reactivity index (RI), which was invented by Jennerjahn and Ittekkot (1997), and the degradation index (DI), developed by Dauwe and Middelburg (1998) and Dauwe et al. (1999).

Briefly, the RI is the ratio between the sum of the two aromatic AA Tyr and Phe and the sum of the two non-protein AA β -Ala and γ -Aba:

$$RI = \frac{\text{Tyr} + \text{Phe}}{\beta\text{-Ala} + \gamma\text{-Aba}} \quad (2.1)$$

Since the aromatic AA are relatively enriched in cell plasma, they are preferentially lost during decay processes (Hecky et al. 1973). The abundance of non-protein AA in fresh OM is minimal but increases during degradation due to the fact that the non-protein AA are metabolic products of microbial proteinogenic AA decay (Cowie and Hedges 1992). Hence, high RI values indicate fresh OM while low values characterise degraded OM.

The DI is calculated on the basis of the molar percentages of the 14 protein AA Asp, Thr, Ser, Glu, Gly, Ala, Val, Met, Ile, Leu, Tyr, Phe, His, and Arg. It compares the monomeric distribution of the AAs of a sample with the data set of Dauwe et al. (1999) according to the formula:

$$DI = \sum_i \left[\frac{\text{var}_i - \text{AVGvar}_i}{\text{STDvar}_i} \right] \times \text{fac.coef.}_i \quad (2.2)$$

where var_i is the original mole percentage of each AA in the sample, AVGvar_i and STDvar_i are the arithmetic average and the standard deviation, and fac.coef._i the factor coefficient of the first axis of a principle component analysis (PCA) of the individual AAs in the data set of Dauwe et al. (1999). Positive values indicate less degraded and negative values more degraded state of the OM compared with the average of the data set of Dauwe et al. (1999).

In addition to the above mentioned AA-based indices, we performed principal component analyses of the 18 individual AA monomers for every investigated lake and for the combined data set to calculate a new, lake-specific AA index on the basis of the DI calculation (Dauwe and Middelburg 1998; Dauwe et al. 1999).

In addition, we calculated other AA- and HA-based degradation indices, such as ratios between proteinogenic AAs and their non-protein degradation products (Henrichs et al. 1984; Ittekkot et al. 1984b), the Ox/Anox ratio, which distinguishes between aerobic and anaerobic degradation (Menzel et al. 2013), and the percentage of Gly of the sum of Gly, Ser, and Thr (Lomstein et al. 2006). Furthermore, organic matter source indices, such as the ratio between AAs and HAs (Ittekkot et al. 1984a; Müller et al. 1986), the ratio between the two measured HAs Gluam and Galam (Kandler 1979; Haake et al. 1992), the Asp/Gly ratio (Ittekkot et al. 1984a; Ittekkot et al. 1984b), and the sum of Gly, Ser, and Thr (Lomstein et al. 2006), were calculated and their applicability examined.

2.4. Results

The results of the AA analyses of the four lakes are summarised in Table 2.2.

Table 2.2: Average TOC, C/N, AA, AA-C, and AA-N values of specific groups of samples of the four lakes.

	TOC (%)	C/N (atomic)	THAA (mg/g)	AA-C (%)	AA-N (%)
Tso Moriri					
Vascular plants	46.2	31.6	92.1	9.3	52.7
Soils	0.7	11.5	1.6	9.7	30.3
Surface sediments	1.7	10.3	5.5	13.2	37.6
Sediment core	0.8	10.2	1.7	7.9	21.3
<i>Section 0 m – 3.9 m</i>	1.2	9.0	2.9	10.6	26.5
<i>Section 3.9 m – 7.3 m</i>	0.4	11.2	0.5	5.6	16.8
Mansar Lake					
Sediment core	3.6	12.0	5.8	7.4	23.7
<i>Section 0 m – 16.8 m</i>	1.7	9.6	4.0	8.9	24.8
<i>Section 17 m – 24.3 m</i>	6.4	15.2	8.2	5.5	22.2
Lonar Lake					
SPM	31.9	6.5	283.9	40.0	77.6
Vascular plants	43.1	39.6	85.6	8.7	51.2
Soils	0.5	15.8	3.0	13.4	38.0
Sediment trap material	24.1	6.9	196.4	35.9	64.5
Sediment core	3.5	22.6	2.2	3.8	19.0
<i>Section 0 m – 3.1 m</i>	1.6	14.0	3.7	9.2	33.9
<i>Section 3.1 m – 6.1 m</i>	1.4	22.9	1.0	2.6	17.1
<i>Section 6.1 m – 9.1 m</i>	4.7	26.6	2.4	2.1	14.8
<i>Section 9.1 m – 9.8 m</i>	1.3	15.5	0.2	0.7	3.3
<i>Section 9.8 m – 9.9 m</i>	0.4	13.1	0.2	1.7	6.8
Pookode Lake					
Sediment core	16.7	13.6	45.2	11.8	44.1
<i>Section 0 cm – 42.5 cm</i>	15.1	13.7	40.7	11.7	44.6
<i>Section 44 cm – 48.5 cm</i>	28.3	12.4	76.9	12.0	40.8

Highest AA concentrations are present in suspended particulate matter (SPM) samples, which were available only from Lonar Lake, followed by sediment trap samples, also collected from Lonar Lake (Table 2.2). The vascular plants, which were sampled at Tso

Moriri and Lonar Lake, show AA content of about one third of that of SPM. The AA-C values of the sediment core samples from Tso Moriri, Mansar Lake, and Pookode Lake are in the same range, whereas the Lonar Lake core sediments show lower AA-C values. On the other hand, similar average AA-N values are present in Tso Moriri, Mansar Lake, and Lonar Lake core sediments, whereas the Pookode Lake samples show higher values. The AA-C values of vascular plant samples are much lower compared to SPM and sediment trap samples, whereas AA-N values of vascular plants are less depleted with respect to SPM and sediment trap samples (Table 2.2).

As shown in Figure 2.2 A, the monomers Gly, Asp, Ala, and Glu contribute most (> 9 mol%) to the AA assemblages of the different lake core sediment samples. The Lonar Lake sediments are an exception; here, Leu, Ala, Val, and Gly are the most abundant (> 9 mol%) monomers. The vascular plant samples from Tso Moriri and Lonar Lake are characterised by high AA monomer contributions of Glu, Asp, Gly, Ala, and Leu (8.6 mol% – 13 mol%), whereas the soils of the vicinity of the two lakes show AA spectra dominated by Asp, Gly, Glu, and Ala (10.6 mol% – 16.7 mol%). Suspended particulate matter filtered from Lonar Lake is highly enriched in Glu (17.6 mol%), followed by Ala, Asp, and Gly (9 mol% – 11.5 mol%).

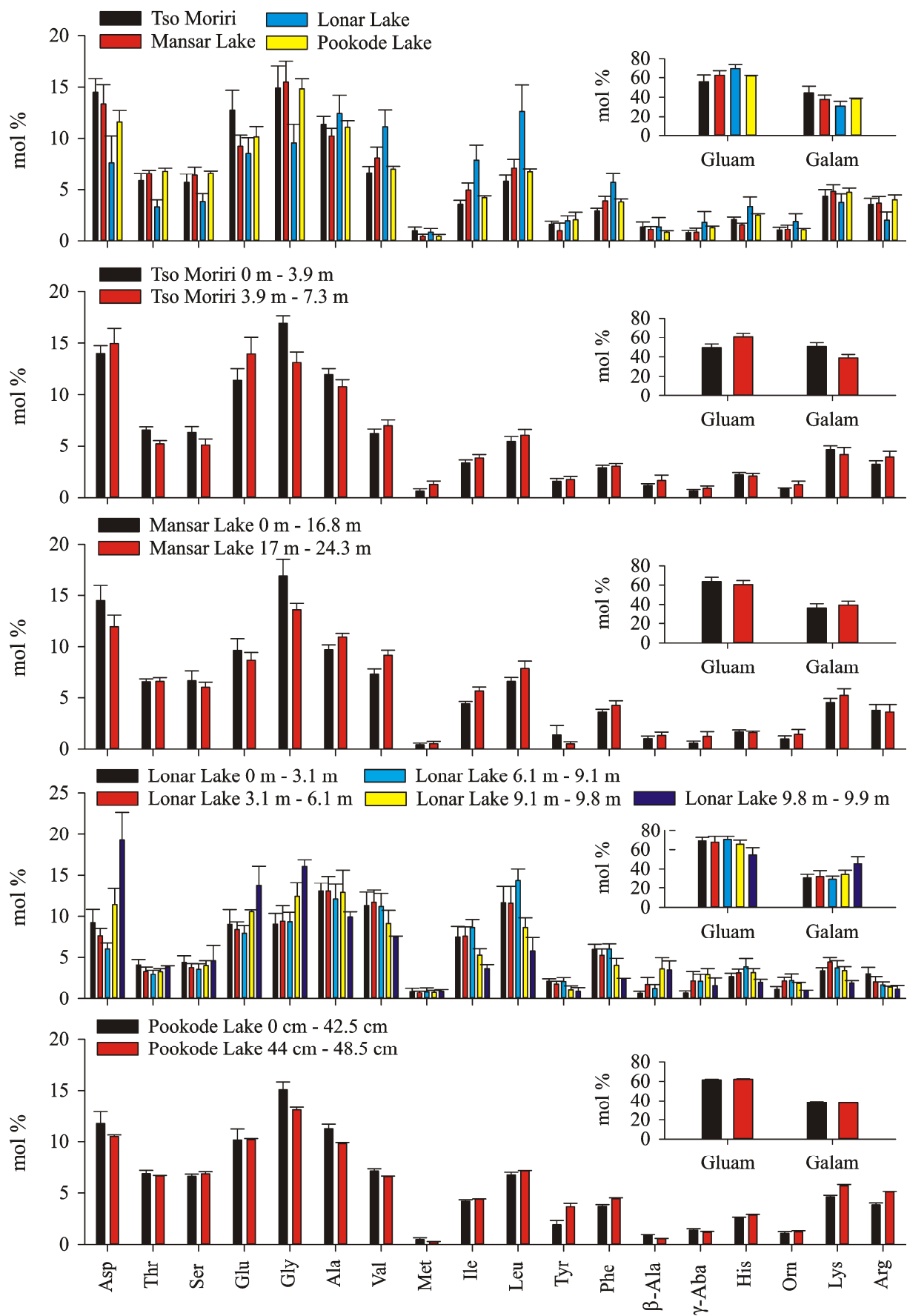


Figure 2.2: Monomeric AA and HA assemblages of the sediment core samples of the four lakes.

2.4.1. AA variability within the Tso Moriri sediment core

The most pronounced differences concerning the AA results within the Tso Moriri core can be seen between the upper ca. 3.9 m of the sediment sequence and the underlying ca. 3.4 m.

The AA content of the upper part of the core shows a mean value of 2.9 mg/g dry sediment, whereas the lower part only contains 0.5 mg/g. The mean AA-C and AA-N percentages of the upper part of the core are 10.6 % and 26.5 %, respectively. The lower part of the core shows mean AA-C and AA-N values of 5.6 % and 16.8 %, respectively.

The monomeric AA assemblage of the upper part of the core is relatively enriched in Gly, Thr, Ser, Lys, and Ala and depleted in Met, Orn, β -Ala, γ -Aba, Glu, Arg, Ile, Val, Tyr, and Leu compared to the lower part (Figure 2.2 B). Furthermore, the ratio between the two HAs Gluam and Galam is lower in the upper part compared to the lower part of the Tso Moriri core (Figure 2.2 B).

2.4.2. AA variability within the Mansar Lake sediment core

The results of the AA analyses of the Masar Lake sediment core have been published by Das et al. (2010) and interpreted with respect to palaeo-climate variability. Broadly, the core can be divided into an upper part from 0 m – 16.8 m and a lower part from 17 m – 24.3 m.

The mean AA content of the upper part of the core is 4.0 mg/g and generally decreases downcore. The lower part of the core shows a mean AA content of 8.2 mg/g with no marked internal trend. Average AA-C and AA-N percentages in the upper part are 8.9 % and 24.8 %, respectively. Similarly to the AA content, both AA-C and AA-N show a decreasing trend with increasing depth. The lower part of the core is characterised by mean AA-C and AA-N values of 5.5 % and 22.2 %, respectively.

The monomeric AA assemblage of the two parts of the core differs with Tyr, Gly, Asp, Glu, and Ser being relatively enriched in the upper part and γ -Aba, Orn, β -Ala, Ile, Val, Leu, Phe, Met, Lys, and Ala being enriched in the lower part (Figure 2.2 C). The ratio between the two HAs indicates slightly elevated contribution of Gluam to the upper part compared to the lower part of the core (Figure 2.2 C).

2.4.3. AA variability within the Lonar Lake sediment core

The Lonar Lake sediment core has been analysed for different proxies and interpreted with respect to palaeo-climate (Anoop et al. 2013b; Prasad et al. 2014; Menzel et al. submitted). According to the AA analyses and supported by the findings of the afore-mentioned authors, the Lonar Lake sediment core can roughly be divided into five subunits: the first subunit comprising the upper part of the core between 0 m – 3.1 m, the second subunit between 3.1 m – 6.1 m, the third subunit from 6.1 m to 9.1 m, the fourth subunit between 9.1 m – 9.8 m, and finally, the fifth subunit at the bottom of the core (9.8 m – 9.9 m) comprising a palaeosol and underlying hard clay.

The mean AA content, AA-C, and AA-N values of the single subunits are given in Table 2.2. The average monomeric AA assemblages of the individual subunits are shown in Figure 2.2 D and reveal some major differences. Compared to the mean AA assemblage of the Lonar Lake sediment core, the first subunit is enriched in Arg, Thr, Asp, Ser, and Tyr and depleted in γ -Aba, β -Ala, Orn, His, and Lys. The second subunit is relatively enriched in Lys, β -Ala, γ -Aba, and Orn and depleted in Met and Tyr. The third subunit shows relatively elevated percentages of Leu, Ile, His, Orn, and γ -Aba and diminished percentages of Asp, Thr, Arg, and β -Ala. The fourth subunit is enriched in β -Ala, γ -Aba, Asp, Gly, and Glu and depleted in Tyr, Ile, Leu, Arg, Phe, Val, and Lys, whereas the fifth subunit shows enrichment of Asp, β -Ala, Gly, Glu, Ser, and Thr and depletion of Phe, Leu, Ile, Tyr, Lys, Orn, Arg, His, Val, Ala,

and γ -Aba. The Gluam/Galam ratio shows highest values in the third and lowest values in the fifth subunit (Figure 2.2 D).

2.4.4. AA variability within the Pookode Lake sediment core

According to the AA data, the Pookode Lake short core can be divided into a top part from 0 cm to 42.5 cm and a bottom part from 44 cm to 48.5 cm.

The mean AA content of the top part of the sediment core is 41 mg/g dry sediment, whereas the mean AA content of the bottom part of the core is 77 mg/g dry sediment. The AA-C and AA-N percentages of the two parts of the core are quite identical, being 11.7 % and 44.6 % in the top part and 12.0 % and 40.8 % in the bottom part, respectively.

In comparison, the monomeric AA assemblage of the top part of the core is relatively enriched in Gly, Ala, Asp, β -Ala, Met, and γ -Aba, whereas the bottom part is relatively enriched in Tyr, Arg, Lys, Phe, His, and Orn (Figure 2.2 E).

2.5. Discussion

Several AA- and HA-based indices have been used in environmental science to decipher the state of OM degradation of and the OM source to different types of samples. Some of these indices are based on the overall AA and HA contribution to samples and ratios between AAs, HAs, or AA- and HA-bound compounds and other chemical constituents, whereas others are based on the contributions, amounts, and ratios of different AA and HA monomers. Most of these indices were first invented for marine samples, which often show negligible contribution of terrestrial OM, such as vascular plants, fungi, or soil OM, and thus are more uniform with respect to their OM sources and the related AA contribution and monomeric assemblages. Here, we test the different indices for their applicability to samples from different lacustrine environments.

2.5.1. AA-C and AA-N

The organic carbon and total nitrogen normalised AA contents of samples are occasionally used as degradation proxies (Cowie and Hedges 1994; Colombo et al. 1998; Lomstein et al. 2006; Carstens and Schubert 2012). However, AA-C can only serve as a degradation proxy in environments that show comparable OM sources, since AA-C values of vascular plants and marine organisms are explicitly different (Haake et al. 1992; Verma and Subramanian 2002; Meckler et al. 2004; Menzel et al. 2013; Unger et al. 2013). AA-C values of suspended particulate material from Lonar Lake are in the range of 33 % – 49 %, whereas vascular plant samples from Lonar Lake (Menzel et al. 2013) and Tso Moriri show AA-C values of 2 % – 18 % (Table 2.2). Thus, AA-C is less suitable as a degradation proxy in lake sediments, but can be used as source indicator, with low values relative to AA-N indicating higher amounts of vascular plants.

AA-N, on the other hand, shows less variation between aquatic and terrestrial OM than AA-C (Cowie and Hedges 1992; Cowie and Hedges 1994; Menzel et al. 2013), making it a better degradation proxy for bulk OM investigations. However, aquatic OM usually yields higher AA-N values than terrestrial OM; especially woody vascular plant samples show AA-N values as low as 23 % (Cowie and Hedges 1992), apparently indicating that AA-N in samples that are dominated by woody OM might be biased. But, since woody OM usually account for negligible amounts of the overall AA and TN contribution of a sediment sample, due to the very low AA and TN concentration in wood compared to other OM (Cowie and Hedges 1992), AA-N can be used as a reliable organic reactivity index even in samples that are dominated by woody OM. This is corroborated by our data, which show comparable AA-N values for the sediment cores from Tso Moriri (22.1 %), Mansar Lake (23.7 %), and Lonar Lake (19.0 %). Other indices indicate similar states of OM degradation within these three cores, as suggested by the AA-N values, whereas AA-C values are much higher in Tso Moriri (8.1 %) and Mansar Lake (7.4 %) compared to Lonar Lake (3.8 %) that shows the highest mean C/N ratio of the three lakes, indicating higher contribution of terrestrial OM. A cross-plot of AA-C and AA-N shows that both values seem to be sensitive to degradation as they decrease linearly (Figure 2.3). Sediment samples from core sections that probably have comparable OM sources plot on a line through the origin, but the gradient of the line is depending on the amount of terrestrial vs. aquatic OM contributing to the sediments. For example, the samples from Lonar Lake core section > 3.1 m, which show a mean C/N ratio of 25.3 lie on a much steeper line than those from the Lonar Lake core section 0 m to 3.1 m (Figure 2.3), which is characterised by less degradation and a lower mean C/N ratio (14.0) due to eutrophication induced phytoplankton growth (Anoop et al. 2013b). Thus, AA-N shows great potential in comparing the state of degradation between different samples and different sites, whereas AA-C can only be used as degradation proxy when the OM sources are almost constant.

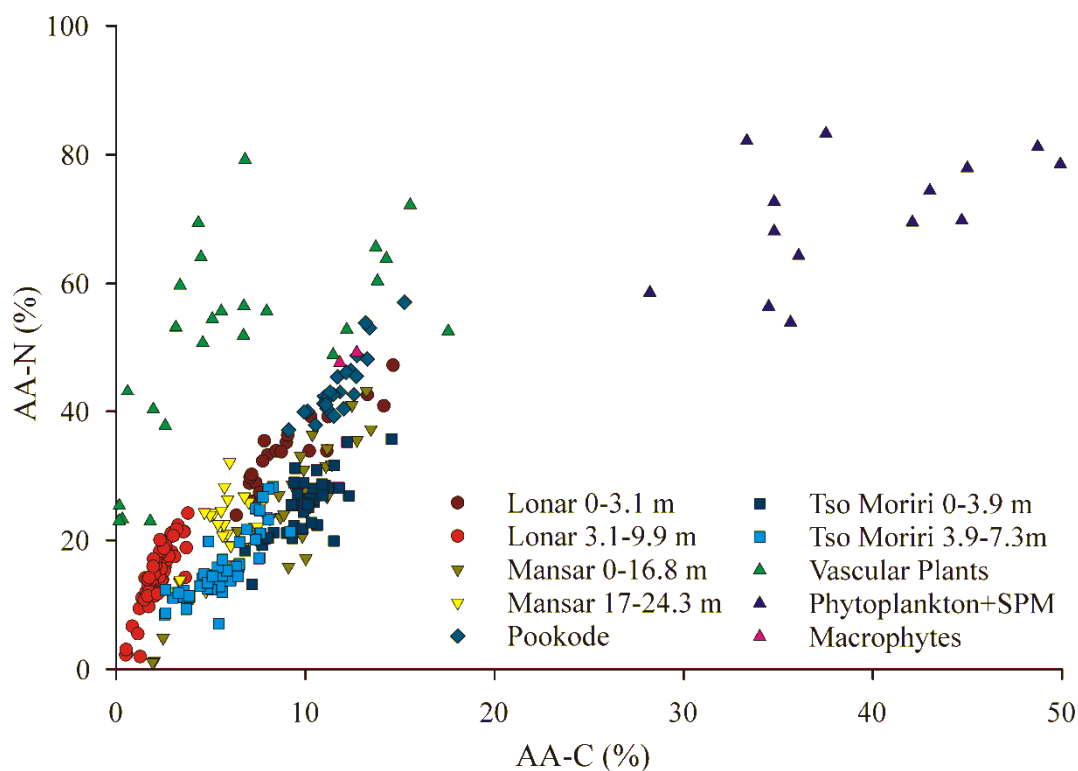


Figure 2.3: Cross-plot of AA-N and AA-C-values of sediment core, vascular plant, plankton, suspended particulate matter, and macrophyte samples. Macrophyte, 6 plankton, and 11 vascular plant paired values reported by or calculated from Cowie and Hedges (1992).

2.5.2. Degradation indices: DI, RI, new Lake degradation index (LDI)

The degradation index (DI) (Dauwe and Middelburg 1998; Dauwe et al. 1999) and reactivity index (RI) are often applied to environmental AA analyses to assess and compare the state of OM degradation (Unger et al. 2005; Gaye et al. 2007; Gupta and Kawahata 2007; Lahajnar et al. 2007; Möbius et al. 2011; Carstens and Schubert 2012). However, some studies on AA contribution to marine, fluvial, and lacustrine sediments have shown that the DI and RI cannot universally be used to compare the state of OM degradation from different environments (Unger et al. 2005; Gupta and Kawahata 2007; Davis et al. 2009; Möbius et al. 2011; Carstens and Schubert 2012). Only for the Pookode Lake we find a significant positive correlation between the two indices (Figure 2.4), and Lonar Lake sediments have highest DI values.

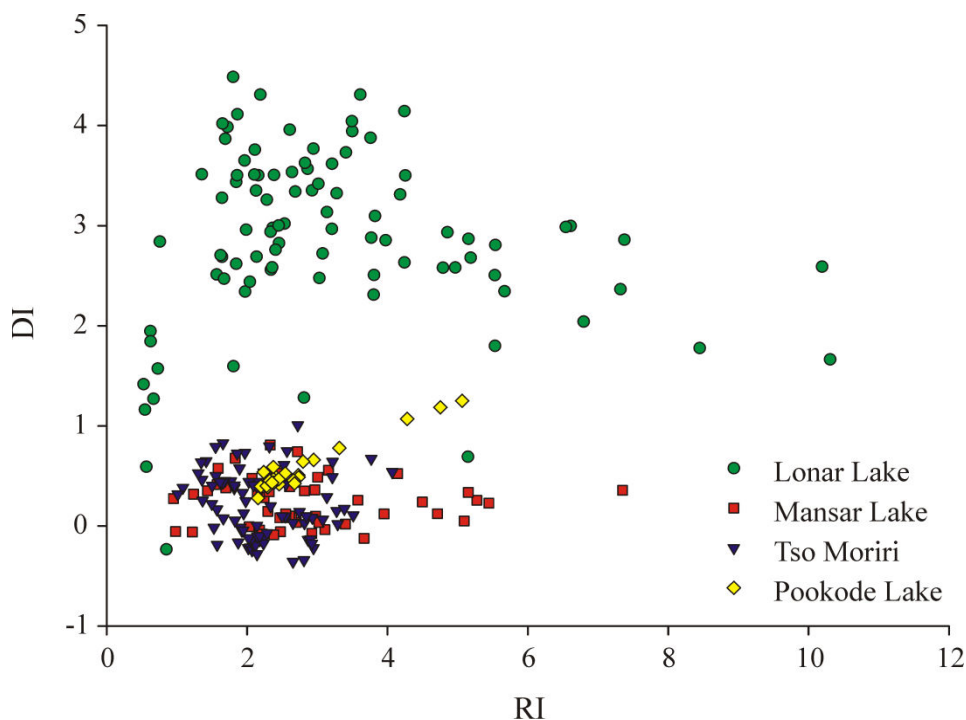


Figure 2.4: Cross-plot of DI and RI values of the sediment core samples of the four lakes.

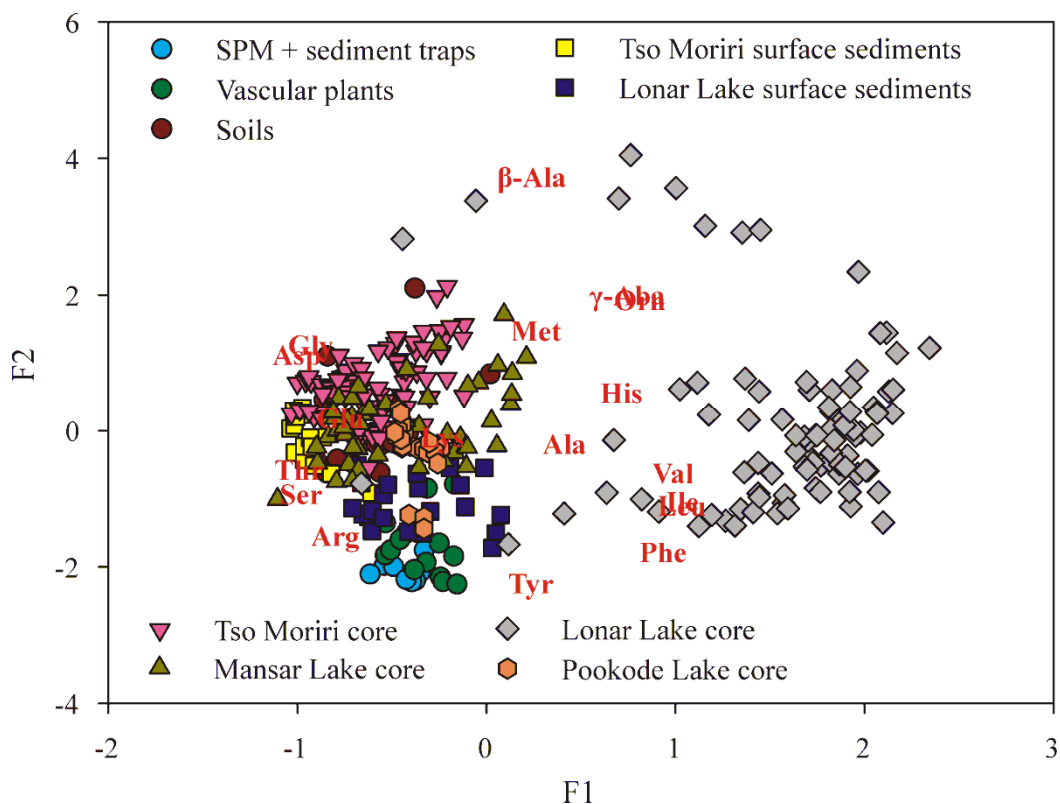


Figure 2.5: Cross-plot of first and second PCA axis factors of the PCA of the monomeric AA contribution of the combined data set.

To decipher if the RI or the DI are suitable to assess the degradation rate, we performed PCAs of the AA assemblages of the four lakes separately as well as for the combined lake samples (Figure 2.5) and compared them to the original data set used for the DI calculation (Dauwe et al. 1999) (Table 2.3). Lonar Lake core sediments with unusually high DI values are enriched in Leu, Val, Ile, His, and Phe and depleted in Gly, Asp, Arg, Thr, Ser, and Glu compared to the DI data set of Dauwe et al. (1999). The fact that this deviation is most pronounced in core sections that show highest C/N ratios, indicating strongest contribution of terrestrial OM, suggests that the DI might in general not be suitable to decipher the degradation status of sediments from environments that show high contribution of terrestrial OM. The interpretation of the monomeric AA assemblages of the different sediment cores indicates that specific monomers show different behaviour during degradation in our data compared to their factor loadings for the DI calculation (Dauwe et al. 1999). Repeatedly, the negative loading, and thus the enrichment during degradation of the AA monomers Arg and Val as well as Thr could not be confirmed in our data set (Table 2.3). The enrichment of Arg during degradation in the DI data set might be related to the adsorption of basic AAs to clay minerals, which prevents them from degradation especially in fine grained deep sea sediments (Hedges and Hare 1987; Keil et al. 2000). This is a process not relevant in the investigated relatively coarser grained lake sediments. The negative DI factor loading of Thr is presumably related to the abundance of Thr in diatom cell walls (Hecky et al. 1973; King 1977). As most investigated lake sediments have low diatom content Thr is not significantly enriched. The different behaviour of Glu during degradation in some of our samples with much lower F1 coefficients than in the DI (Table 2.3) might be linked to different redox conditions during degradation. Whereas Glu is often enriched in fresh planktonic material and preferentially lost during early degradation (Cowie and Hedges 1992; Keil et al. 2000; Menzel et al. 2013), it can be enriched during degradation under aerobic conditions (Cowie et al. 1995) especially in

gram-positive bacteria (Keil et al. 2000). Particularly in lake samples deposited under low oxygen concentrations, Glu is relatively depleted.

Table 2.3: AA monomer DI coefficients (Dauwe et al. 1999) and first PCA axis loadings of individual PCAs of the four lake sediment cores.

	DI coefficient	Tso Moriri F1 coefficient	Mansar Lake F1 coefficient	Lonar Lake F1 coefficient	Pookode Lake F1 coefficient
Asp	-0.102	0.051	-0.094	-0.141	-0.092
Thr	-0.129	-0.111	0.005	-0.088	0.032
Ser	0.015	-0.098	-0.069	-0.072	0.090
Glu	0.065	0.046	-0.069	-0.132	-0.051
Gly	-0.099	-0.117	-0.114	-0.133	-0.079
Ala	-0.043	-0.091	0.115	0.048	-0.048
Val	-0.044	0.101	0.131	0.103	-0.034
Met	0.134	0.094	0.029	0.006	-0.046
Ile	0.139	0.103	0.132	0.141	0.099
Leu	0.169	0.084	0.108	0.143	0.103
Tyr	0.178	0.060	-0.078	0.068	0.108
Phe	0.134	0.049	0.102	0.131	0.123
β-Ala		0.089	0.071	-0.095	-0.100
γ-Aba		0.086	0.099	-0.026	-0.012
His	0.158	-0.009	-0.028	0.039	0.110
Orn		0.102	0.079	0.036	0.024
Lys		-0.048	0.082	0.028	0.120
Arg	-0.115	0.079	-0.015	-0.043	0.114

These deviations from the DI show that it is highly recommended to calculate an individual PCA of AA results from a specific study site, since the grouping of individual AA monomers could be used to identify specific causes for the AA monomer variability within the data set. As for example the grouping of relatively labile AA monomers opposing a group of relatively stable AA monomers indicates sensitivity to degradation state (Dauwe and Middelburg 1998; Dauwe et al. 1999), whereas grouping of AA monomers most abundant in specific OM compounds, such as siliceous, calcareous, microbial, or terrestrial plant OM, most probably indicates sensitivity to OM source variation (Ingalls et al. 2006; Gaye et al. 2007). The incorporation of other data into such a PCA might further enhance its interpretability, as for example incorporation of the C/N ratio can be used to identify the sensitivity of the AA

monomeric assemblage of a data set with respect to variability in aquatic and terrestrial OM contribution. Hence, degradation indices that are calculated on the basis of an individual AA monomer-based PCA should be limited to the PCA axis that shows highest sensitivity to the state of degradation, and thus separates most labile AA monomers and most stable AA monomers.

Table 2.4: Average molar percentages (Avg.), standard deviations (SD), and factor coefficients (fac. coeff.) of each AA monomer used for LDI calculation.

	Avg (mol%)	SD (mol%)	fac. coeff.
Tyr	1.78	0.76	-0.223
Phe	4.08	1.21	-0.177
Arg	3.31	1.02	-0.153
Leu	8.18	3.12	-0.109
Ile	5.10	1.96	-0.103
Ser	5.63	1.36	-0.092
Val	8.06	2.21	-0.061
Thr	5.46	1.50	-0.056
Ala	11.43	1.44	-0.018
Lys	4.14	0.81	-0.008
Glu	11.01	2.50	0.020
His	2.42	0.92	0.058
Asp	11.97	3.30	0.114
Gly	13.16	3.05	0.128
Met	0.70	0.41	0.149
Orn	1.16	0.70	0.194
γ -Aba	1.02	0.79	0.203
β -Ala	1.13	0.65	0.376

The results of a PCA comprising the AA analyses of the whole data set, including the four lake sediment cores and the surface sediment, soil, vascular plant, SPM, and sediment trap samples, indicates that the first axis, explaining 49.3 % of the variability of the data, seems to be sensitive to redox conditions and the contribution of degraded terrestrial, especially woody, OM to the samples, whereas the second axis of this PCA seems to be most sensitive to the

state of OM degradation. Therefore, we calculated a lake degradation index (LDI) based on the factor loadings of the second axis of the PCA of our whole data set. The arithmetic mean, standard deviation, and second PCA-axis factor loading of the individual AA monomers are listed in Table 2.4. This index characterises the state of OM degradation of the samples from the four investigated lakes and might be applicable to other terrestrial aquatic environments, especially other lake sediments, too. The LDI produces positive values for relatively degraded and negative values for relatively fresh samples. The LDI, therefore, correlates negatively with indicators of organic matter freshness such as the AA-N, RI, and, with some limitations (as discussed above) with the AA-C as well as with ratios between proteinogenic AAs and their degradation products (Table 2.5). It correlates positively with the %Gly/(Gly+Ser+Thr) and the Ox/Anox indicator, which both rise with increasing degradation (*see* below). Additionally, the LDI is independent of terrestrial and aquatic source indicators such as C/N and Gly+Ser+Thr (Table 2.5).

Table 2.5: Correlation between different AA- and HA-based OM source and degradation indices as well as C/N ratio of the combined data set.

	C/N	AA-C	AA-N	AA/HA	Asp/ β-Ala	Glu/ γ-Aba	Arg/ Orn	Gluam/ Galam	Thr+Ser+ Gly	%Gly (T+S+G)	Ox/ Anox	RI	DI
LDI	-.059	-.515**	-.658**	-.377**	-.545**	-.327**	-.421**	-.387**	.048	.686**	.491**	-.531**	-.198**
C/N	1	-.486**	-.162*	.067	-.205**	-.221**	.043	.505**	-.535**	-.020	-.576**	-.120	.688**
AA-C		1	.819**	.239**	.770**	.657**	.375**	-.017	.351**	-.446**	.160*	.724**	-.342**
AA-N			1	.432**	.650**	.476**	.475**	.275**	.273**	-.606**	-.018	.578**	-.198**
AA/HA				1	.493**	.192**	.514**	.685**	-.057	-.434**	-.027	.284**	.040
Asp/ β-Ala					1	.753**	.646**	.333**	.063	-.516**	-.004	.900**	-.083
Glu/ γ-Aba						1	.465**	.101	.079	-.357**	.067	.896**	-.123
Arg/ Orn							1	.603**	.002	-.442**	-.018	.554**	-.005
Gluam/ Galam								1	-.227**	-.454**	-.255**	.216**	.306**
Thr+Ser+ Gly									1	-.134	.598**	-.057	-.878**
%Gly (T+S+G)										1	.133	-.458**	.123
Ox/ Anox											1	-.137	-.834**
RI												1	.050

The results of the PCA of the combines lake samples indicate that the RI is suitable to decipher the state of degradation of OM in lakes as the aromatic AAs are the most labile (most negative LDI factor loadings), whereas the non-protein AAs are the most stable AAs (most positive LDI factor loadings). This is due to the fact that the aromatic AAs are enriched in cell plasma, which is easily degradable, and the non-protein AAs β-Ala and γ-Aba become

enriched during degradation as they are decomposition products of Asp and Glu, respectively (Ittekkot et al. 1984b). However, OM of terrestrial origin can be enriched in γ -Aba compared to OM of aquatic origin (*see* chapter 5.4), especially when vascular plants undergo environmental stress, as for example extreme temperature, drought, highly alkaline or saline soils (Kinnersley and Turano 2000). At Tso Moriri, the vascular plant samples show higher contribution of γ -Aba than all other samples, including soil and sediment core samples. Nevertheless, this effect is to some extent countered by elevated aromatic AA content, especially Phe (*see* chapter 4.5.4), in undegraded terrestrial OM (Cowie and Hedges 1992), making RI a reliable proxy to evaluate the state of OM degradation in environments with different OM sources. However, it should be noted here that if non-protein AAs are considered individually, only β -Ala content should be taken as an indicator of organic matter degradation.

2.5.3. Specific organic matter source indices

The most important difference in OM origin in lacustrine environments certainly is the ratio between aquatic and terrestrial OM contribution to the sediments. Several studies have deciphered the differences in AA assemblages of various aquatic and terrestrial organisms (Hecky et al. 1973; King 1977; Ittekkot et al. 1984a; Ittekkot et al. 1984b; Cowie and Hedges 1992), suggesting that these differences are transferred into the sediments. However, to estimate the percentage of aquatic versus terrestrial OM contribution to sediments, the calculation of the simple ratio between organic carbon and total nitrogen usually shows universal applicability (Meyers 1994). C/N ratios of all samples correlate positively with Leu, Ile, Val, Phe, His, γ -Aba, and Orn and negatively with Asp, Gly, Arg, Thr, Glu, and Ser, suggesting that the former are enriched in land plants and soils whereas the latter are enriched in aquatic material. In Lonar lake that shows highest C/N ratios, and thus highest terrestrial

contribution, the correlation is positive between C/N and Orn, Leu, His, γ -Aba, and Ile and negative between C/N and Asp, Thr, Ser, Arg, and Glu. The missing correlation between C/N and Val, Phe, and Gly in Lonar Lake sediments is probably due to the exceptional plankton assemblage in Lonar Lake, comprising mostly of cyanophyceae, which are relatively enriched in Val and Phe and depleted in Gly (Becker 2007) compared with most other phytoplankton (Lee 1988), especially those including substantial contribution of diatoms (Cowie and Hedges 1992).

We also tested other AA-based OM source indices used to identify high contribution of specific organisms to environmental samples. Dominance of Asp over Gly in suspended and sinking material was interpreted as being evidence of high calcareous OM contribution, whereas dominance of Gly over Asp was interpreted as being evidence of high siliceous OM contribution (Ittekkot et al. 1984a; Ittekkot et al. 1984b; Müller et al. 1986). This is based on findings that show high contribution of Gly to siliceous organisms (Hecky et al. 1973; King 1977; Cowie and Hedges 1992) and high contribution of Asp to calcareous organisms (Degens 1976; King 1977; Carter and Mitterer 1978). However, these indices of siliceous and calcareous OM sources can only be applied to relatively undegraded OM. Gly can be highly enriched during degradation, due to its significant contribution to microbial produced OM (Keil et al. 2000) and its relatively reduced decomposability compared to most other AAs (Sigleo and Shultz 1993), whereas Asp might be preferentially enriched during aerobic degradation (Cowie et al. 1995). To assess the contribution of specific OM sources to sediments, other indices are needed. The relative contribution of siliceous OM to even more degraded sediments can be reconstructed from the molar percentage of Gly, Ser, and Thr of the total AA assemblage in combination with the percentage of Gly of the afore mentioned three AA monomers [$\%Gly/(Gly+Ser+Thr)$] (Lomstein et al. 2006). Since siliceous OM is enriched in Gly, Ser, and Thr (Hecky et al. 1973; King 1977), sediments with high contribution of siliceous OM show contributions of the sum of Gly, Ser, and Thr of ca. >27

mol%, as for example in the Pookode Lake sediment core and the upper parts of the Tso Moriri and Mansar Lake sediment cores. To assure that the high values of this sum are not driven by strong contribution of microbial-originated or degradation-related enrichment of Gly, %Gly/(Gly+Ser+Thr) needs to be calculated. Percentages of ca. > 60% might indicate Gly enrichment due to enhanced degradation, which should be confirmed by relatively low AA/Galam ratios (*see* below) or high β -Ala content of the respective samples.

Since none of the four lakes investigated during this study shows high contribution or evidences of former dominance of calcareous organisms, related AA-based indices could not be tested.

2.5.4. HA-based indices

Aminosugars showed the potential to be used as indices of microbial degradation and microbial contribution to the OM of different environmental samples (Benner and Kaiser 2003; Niggemann and Schubert 2006; Carstens et al. 2012). The ratio between the HAs Gluam and Galam can, however, also be an indicator of chitinaceous or microbial OM source. Gluam/Galam ratios > 4 usually indicate high contribution of chitinaceous OM to sinking particulate matter (Haake et al. 1992; Haake et al. 1993; Lahajnar et al. 2007), since chitin is a polymer of Gluam (Benner and Kaiser 2003). On the other hand, Gluam/Galam ratios of < 3 usually indicate relatively high contribution of microbial OM (Benner and Kaiser 2003). However, chitin in aqueous systems is prone to microbial recycling (Davis et al. 2009) so that Gluam/Galam ratios of surface sediments usually fall to 1.2 – 1.9 (Liebezeit 1993; Benner and Kaiser 2003) even at locations that show Gluam/Galam ratios > 4 of sinking particles (Lahajnar et al. 2007). To avoid this bias induced by microbial reworking, Müller et al. (1986) used the AA/Gluam ratio of suspended particulate matter and sediment trap samples to estimate the contribution of chitinaceous OM in the marine environment.

Gluam/Galam ratios are < 2.5 in lake surface and core sediment samples. In sediments, decreasing Gluam/Galam ratios may indicate the decomposition-related accumulation of microbial OM, since Galam is most abundant in microbial cell walls (Kandler 1979). However, the fact that Gluam is present in varying amounts in most OM sources (Benner and Kaiser 2003) may bias the interpretation of Gluam/Galam ratios with respect to microbial contribution. For example, the Tso Moriri core sediments show a relatively low mean Gluam/Galam ratio of 1.3, theoretically indicating high contribution of microbial OM, whereas the Lonar Lake core sediments show a mean ratio of 2.3, indicating less microbial contribution, even though both sediment cores show similar contribution of β -Ala, which suggests similar microbial contribution to the two core sediments (Lee and Cronin 1982). The high contribution of terrestrial OM to Lonar Lake sediments might be the reason for high amounts of Gluam. Fresh leaf samples from Tso Moriri and Lonar Lake catchments reveal relatively low Gluam contents and have AA/Gluam ratios of 112 – 880. But, a sample of dry grass from Lonar Lake reveals an AA/Gluam ratio of 9.5, and wood samples potentially show similar or even lower AA/Gluam ratios, which is corroborated by the positive correlation of Gluam/Galam ratios and C/N (Table 2.5). The mean ratio between AA and Galam of the Tso Moriri core samples is 29.3, which is very similar to the mean AA/Galam ratio of 27.8 of Lonar Lake. We surmise that the AA/Galam ratio may be a better proxy of microbial contribution than the Gluam/Galam ratio in lakes, as it is not biased by high variability of Gluam contents in land plants.

2.5.5. Redox index

Different degradation mechanisms during aerobic and anaerobic decomposition potentially affect the monomeric AA assemblage of OM (Cowie et al. 1995; Menzel et al. 2013). According to findings of changes in monomeric AA assemblages due to different redox conditions (Cowie et al. 1995), Menzel et al. (2013) calculated a simple ratio between AAs that become relatively enriched and those that become relatively depleted during aerobic degradation:

$$\text{Ox/Anox} = \frac{\text{Asp} + \text{Glu} + \beta\text{-Ala} + \gamma\text{-Aba} + \text{Lys}}{\text{Ser} + \text{Met} + \text{Ile} + \text{Leu} + \text{Tyr} + \text{Phe}} \quad (2.3)$$

The Ox/Anox ratio of the sediment core samples of the four lakes reveals aerobic degradation of OM in the whole Tso Moriri core, in the upper 16.8 m of the Mansar Lake core, in the bottommost 85 cm of the Lonar Lake core, and, to a lesser extent, in most of the samples of the uppermost 42.5 cm of the Pookode Lake core, whereas less oxygenated conditions are indicated for most of the samples of the lower 7.6 m of the Mansar Lake core and for the bottommost ca. 6 cm of the Pookode Lake core. Lowest Ox/Anox values, suggesting anaerobic conditions during degradation, are found in Lonar core sediments down to 9.1 m, especially in the sections 0.85 m – 3.1 m and 6.2 m – 9.1 m. These findings agree with palaeo-environmental reconstructions of Tso Moriri (Mishra et al. submitted), Mansar Lake (Das et al. 2010), Lonar Lake (Prasad et al. 2014; Menzel et al. submitted), and Pookode Lake (Veena et al. 2014).

2.5.6. Ratios between proteinogenic AAs and their non-proteinogenic degradation products

Commonly, ratios between protein AAs and their non-protein degradation products or intermediates, namely Asp/ β -Ala, Glu/ γ -Aba, and Arg/Orn, or equivalent combinations of

these (Gupta and Kawahata 2007) are used to compare the state of degradation of different samples (Lee and Cronin 1982; Cowie and Hedges 1994; Dauwe and Middelburg 1998; Das et al. 2010). However, varying OM sources in terrestrial environments potentially bias these ratios by contributing relatively high amounts of non-protein AAs, as for example elevated γ -Aba and Orn percentages of terrestrial OM. Also, the relative enrichment of Asp and Glu during aerobic degradation (Cowie et al. 1995) might lead to elevated Asp/ β -Ala and Glu/ γ -Aba ratios, as for example in the bottommost part of the Lonar Lake sediment core, which comprises a palaeosol on top of an underlying hard clay. Both samples indicate strong microbial degradation under aerobic conditions, and whereas the palaeosol shows respective Asp/ β -Ala and Glu/ γ -Aba ratios of 4.0 and 5.3, indicating strong degradation, the hard clay shows ratios of 8.0 and 16.1. A low to moderate degradation of the hard clay is not supported by other indices, such as AA-N, RI, Ox/Anox, Gluam/Galam, or %Gly/(Gly+Ser+Thr). Hence, the ratios between protein AAs and their non-protein degradation products and intermediates exhibit some weaknesses in deciphering the state of OM degradation in terrestrial environments.

Nevertheless, the contribution of β -Ala to fresh OM of both aquatic and terrestrial origin is relatively low and increases during progressing degradation with slightly elevated values in surface sediments and higher values in more degraded sediment core samples (Cowie and Hedges 1992; Menzel et al. 2013). Hence, the contribution of β -Ala seems to be more sensitive to OM degradation than to OM origin and might be used to trace OM decomposition even in less degraded samples, whereas the ratios between protein AAs and their non-protein degradation products, the molar percentage of γ -Aba, or the sum of non-protein AAs might only be useful to identify moderately or highly degraded samples. However, different redox conditions during OM degradation can have considerable influence on the formation of β -Ala and other non-protein AAs in sediments and should be considered during interpretation (Cowie et al. 1995).

2.6. Conclusions

The investigation of sediment cores of four Indian lakes from different climatic regimes confirms that AA-based indices are capable of deciphering the state of OM degradation and can also be used to identify specific sources of OM to lake sediments. However, some commonly used proxies show limitations in lacustrine environments, dominantly due to their interference with varying amounts of different OM sources. During our study, the following proxies have proven to be applicable to lake sediment studies comprising samples from different climate regimes with varying contribution of aquatic and terrestrial OM and of different OM degradation state.

- AA-N shows high potential in deciphering the state of OM degradation. Fresh OM dominantly shows AA-N values of $\geq 50\%$, linearly decreasing with progressing degradation. AA-C on the other hand is highly depending on the percentage of terrestrial vs. aquatic OM, typically showing values $\geq 30\%$ in aquatic and values $\leq 15\%$ in terrestrial OM, and should not be used as a degradation proxy.
- The RI and the newly calculated LDI are applicable to identify the freshness of OM in lake sediments. The DI, invented on the basis of marine sediment, shows some weaknesses in sediments with high terrestrial OM contribution. Thus, the use of RI and LDI should be preferred.
- The relative contribution of the non-protein AA β -Ala to the AA assemblage of sediments seems to be dominantly attributed to the state of OM degradation. The non-protein AAs γ -Aba and Orn, which also accumulate during degradation, can be significantly enriched in terrestrial OM compared to β -Ala and might therefore potentially be biased when it comes to the assessment of OM degradation.

- To identify the percentage of terrestrial and aquatic OM contribution to lake sediments, the commonly used C/N ratio should be used, since AA-based indices might not contribute superior information.
- The accumulation of microbial OM, often a by-product of progressing OM degradation, might be assessed using $\%Gly/(Gly+Ser+Thr)$, with values $> 60 \%$ usually pointing to enhanced microbial contribution. Also, the AA/Galam ratio might be used to decipher the contribution of microbial OM to sediment samples. In our data set, an AA/Galam ratio of approximately 30 seems to sub-divide the samples, with samples showing ratios < 30 being relatively enriched in microbial OM and samples showing ratios > 30 being relatively depleted.
- Sediments that show notable contribution of siliceous OM are usually characterised by elevated percentages Gly+Ser+Thr. Values of $> 27 \text{ mol}\%$ seem to identify such sediments in our data set, as long as $\%Gly/(Gly+Ser+Thr)$ does not indicate prominent contribution of microbial OM, which would bias this interpretation. Thus, Gly+Ser+Thr might also be applicable to other lacustrine studies and more reliable than the Asp/Gly ratio, which can be biased by microbial OM contribution, different state of degradation, as well as different redox conditions during degradation.
- The use of the Ox/Anox ratio provides reliable information about the dominant redox conditions during OM degradation in our data set, with approximate values > 1 indicating aerobic degradation and < 1 indicating anaerobic degradation. Thus, this ratio might be applicable to other study sites too.
- Furthermore, the calculation of an individual PCA of any AA data set is highly recommended, as it yields fundamental information about the most important factors controlling the variability in AA assemblages and might help to identify anomalies within the investigated system.

3. Influence of bottom water anoxia on nitrogen isotopic ratios and amino acid contribution of recent sediments from small eutrophic Lonar Lake, central India

Abstract

Lonar Lake is a eutrophic, saline soda lake with permanently anoxic deep water. The high pH and deoxygenation result in very elevated $\delta^{15}\text{N}$ of suspended particulate matter (SPM) and sediments due to denitrification and pH related loss of gaseous ammonia. SPM and sinking particles are predominantly aquatic in origin, whereas surface sediments are of mixed terrestrial plant and planktonic source. An indicator of degradation intensity was derived from a principal component analysis of the spectral distribution of amino acids and named Lonar degradation index (LI). A ratio of individual amino acids (Ox/Anox ratio) was additionally used to determine the relative degree of aerobic vs. anaerobic degradation. These two biogeochemical indicators can be used to detect changes in degradation intensity and redox conditions in the geological history, and thus the palaeo-climatic interpretation of Lonar sediments. Surface sediments can be divided into three zones: (1) a near shore, oxic zone of predominantly aquatic organic matter, in which oxidation leads to a strong diagenetic increase of $\delta^{15}\text{N}$; (2) an alluvial zone with a predominance of isotopically depleted land plant and soil organic matter degraded under oxic conditions, and (3) an anoxic, deep zone, which receives aquatic organic matter and land plant derived material transported near the bottom and in which organic matter is well preserved due to anoxic diagenetic conditions.

3.1. Introduction

Lonar Lake is a crater lake with small streams and surface runoff as major water sources and no outflow. It is saline, alkaline, eutrophic, and below ca. 4 m water depth permanently sub- to anoxic, which is typical for closed basin saline lakes (Eugster and Hardie 1978). The laminated sediments in the deep, permanently anoxic part of the lake provide one of the very scarce climate records in Central India (Prasad et al. 2014). Due to their high resolution, these sediments provide an excellent archive of recent climate change. We tested common productivity and degradation proxies that are based on nitrogen isotopic ratios and amino acid assemblages for their applicability in Lonar Lake. For the current investigation, terrestrial plants and soils from the inner Lonar crater as well as suspended particulate matter (SPM) were sampled. Sediment traps were installed to sample sinking particles in seasonal resolution and to study the effect of early degradation on sinking organic matter (OM). Surface sediments were analysed to determine the state of degradation and to understand the differences in effect of early degradation under oxic and sub- to anoxic conditions. Furthermore, the ratio of the two stable carbon isotopes was used to determine the percentage of terrestrial and aquatic OM in the surface sediments and the pathways of CO₂ uptake of different plants.

The nitrogen cycle in aquatic systems is often investigated using the ratio of nitrogen isotopes ¹⁵N/¹⁴N of OM. This ratio, expressed as $\delta^{15}\text{N}$, can serve as an indicator of the inorganic nitrogen source of aquatic plankton, and it reflects isotopic fractionation of the different transformation processes within the nitrogen cycle (Brandes and Devol 2002). In small, isolated waterbodies short-term changes in the water chemistry, catchment ecology, or nitrogen source or cycle can alter the $\delta^{15}\text{N}$ of the sediment quickly (Hodell and Schelske 1998). Trend and magnitude of OM nitrogen isotopic ratio alteration during early degradation depend on the availability of oxygen (Macko and Estep 1984; Freudenthal et al. 2001;

Lehmann et al. 2002). In this study, the differences of aerobic and anaerobic degradation of similar source sediments in a natural environment were discovered.

Amino acids are important components in biochemical research as they are ubiquitous in OM and are the major constituent of nitrogen in fresh OM (Lee 1988). Frequently they are used to determine the state of degradation in marine OM since the distribution of individual amino acids shows characteristic changes during degradation. Hence, degradation indices based on the amino acid assemblages in OM were developed, such as the degradation index (DI) introduced by Dauwe and Middelburg (1998) and Dauwe et al. (1999) as well as the reactivity index (RI) established by Jennerjahn and Ittekkot (1997). These proxies were also applied to terrestrial aquatic systems (Verma and Subramanian 2002; Meckler et al. 2004; Unger et al. 2005). However, due to differences in amino acid spectra between terrestrial and marine OM, common degradation indices have to be tested and possibly modified in terrestrial dominated environments (Gaye et al. 2007). Differences in amino acid assemblages of OM degraded under aerobic and OM degraded under anaerobic conditions as observed by Cowie et al. (1995) could also be detected in Lonar Lake sediments. Therefore, we used the ratio between the amino acids that become relatively enriched during aerobic decomposition and the amino acids relatively enriched during anaerobic decomposition. This results in high ratios if sediments are degraded under aerated conditions and low ratios if degraded in permanently anoxic sediments; this ratio might also be applicable to palaeo-records.

3.2. Study site

3.2.1. Geology

Lonar Lake, located at 19°58'N and 76°30'E, occupies the floor of a Middle to Late Pleistocene meteorite impact crater on the Deccan Plateau in Buldhana District, Maharashtra, Central India (Figure 3.1 A). Origin and formation age of the crater were subject to various investigations (Misra et al. 2010). The crater is almost circular and its rim to rim diameter averages 1880 m (Figure 3.1B). The modern crater floor is located at ca. 470 m above sea level, which is around 140 m below the rim crest elevation. The inner rim wall is fairly steep with slopes of 15° – 18° in the east and up to ~ 30° in the west and southwest. The shape of the crater floor is almost planar dipping only very slightly to the west due to the impact direction of the meteorite, which struck the target rock from the east with an angle of 30° – 45° (Misra et al. 2010). The inner crater wall is characterised by erosion features such as rills and gullies. In the northeast, an incised channel developed in consequence of two small streams flowing into the lake. Erosion by these streams has led to an incision on the scale of 30 – 40 m depth and some 300 m distance.

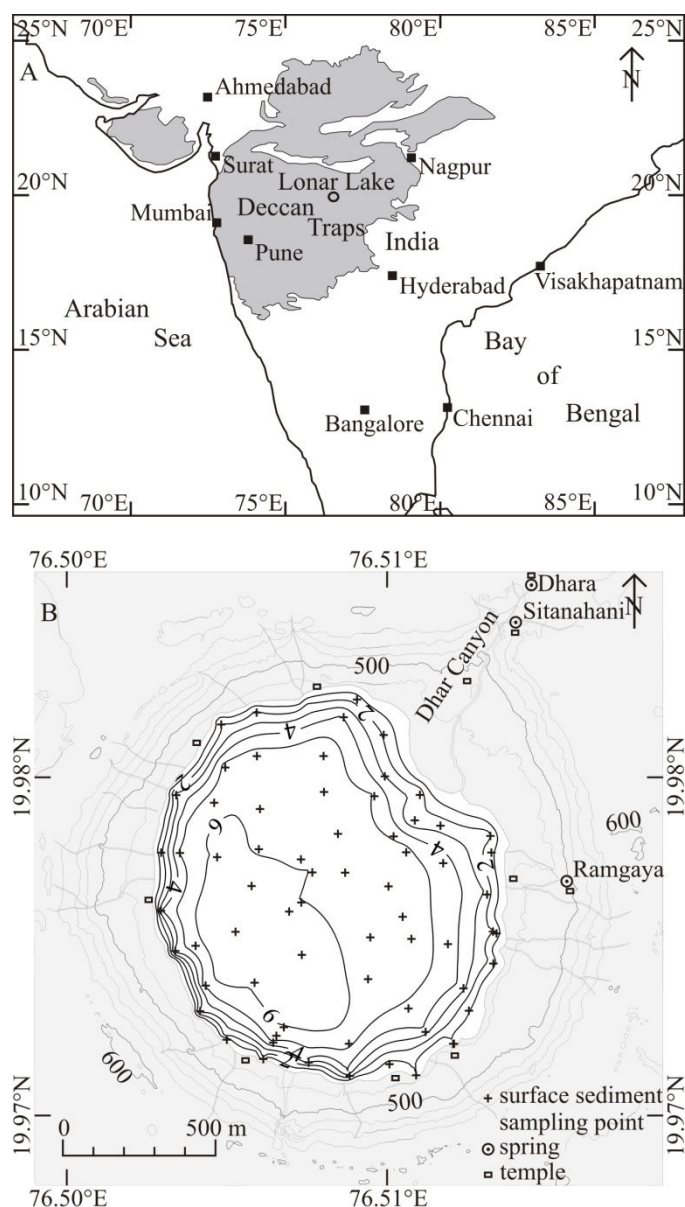


Figure 3.1: Location map showing the position of Lonar Lake on the Deccan Traps in Central India (A). Map of Lonar Lake showing the bathymetry (m) and surface sediment sampling points (B).

3.2.2. Climate and hydrology

Lonar Lake is located in India's core monsoon zone. The annual climate can be divided into three periods: (1) hot (average temperature: 31°C) and dry weather during the pre-monsoon from March to beginning of June, (2) hot (average temperature: 27°C) and wet weather from June to end of September (south west monsoon) with strong winds and rainfall

averaging 680 mm, and (3) relatively cool (average temperature: 23°C) and dry weather during post-monsoon from October to February (Basavaiah et al. 2014).

The lake itself covers an area of nearly 1 km² and is fed by three perennial streams (Figure 3.1 B). Two of them, the Dhara spring and the Sitanahani spring, are entering the crater from the northeast. They formed the Dhar Canyon, an erosive incision, and built up an alluvial fan into the lake. On this fan, crops such as banana (*Musa X paradisiaca*), millet (*Setaria italica*), corn (*Zea mays*), custard-apple (*Annona reticulata*), and papaya (*Carica papaya*) are cultivated. The third stream feeding the lake springs from the inner crater wall and enters the lake from the eastern shore. Today the three streams are diverted toward the Dhara fan to irrigate the agricultural fields. Apart from these streams, ephemeral runoff during the monsoon rainfalls and seepage of water from the country rocks are contributing to the water supply. Water discharge is only conducted by evapotranspiration. No outflowing stream is present and no seepage loss occurs since the lake level is below the local groundwater level (Nandy and Deo 1961).

During our investigations, the lake water was brackish (salinity: 8.0‰ – 12.3‰) and alkaline with pH values between 8.7 and 10.7 (Basavaiah et al. 2014). The lake groups into the Na-Cl-CO₃ subtype of saline lakes (Eugster and Hardie 1978). Since no outflow is present, the lake level fluctuates seasonally with highest level after and lowest level before the southwest monsoon. However, since 1985 the lake level has increased significantly (Badve et al. 1993), which is obvious from dead trees drowned in the shallow water of the modern lake. Given that precipitation has been relatively reduced during the first half of the 1980s (Badve et al. 1993), the main cause of the lake level increase is likely to be seepage of water along fractures into the lake from the Kalapani Dam, a large rainwater reservoir that was constructed near the southwestern rim of the crater in 1970 – 1973 (Surakasi et al. 2007). This seepage may also explain the gradual reduction of the lake's salinity as noticed by Badve et al. (1993) and Surakasi et al. (2007). Enhanced lake level fluctuation in the recent past is not

only indicated by the drowned trees but also by trona ($\text{Na}_3(\text{HCO}_3)(\text{CO}_3) \times 2\text{H}_2\text{O}$) precipitates covering the walls of shore temples, which were built in medieval times during the rule of the Yadavas (Malu et al. 2005).

3.2.3. Biology

The algal assemblage is dominated by Cyanophyceae (> 98%); minor species are largely pennate diatoms, such as *Cymbella*, *Cocconeis*, *Nitzschia*, and *Navicula*, as well as Euglenophyceae and Chlorophyceae (Badve et al. 1993). The non-nitrogen-fixing, filamentous *Arthrothrix fusilini* (formerly *Spirulina platensis*) was reported to be the major Cyanophyceae species in Lonar Lake; also *Planktothrix agardhii* (formerly *Oscillatoria agardhii*) and *Dactylococcopsis* sp. were found to be abundant (Badve et al. 1993; Mahajan 2005). Dense and locally surface-floating blooms were observed particularly after the monsoon (Badve et al. 1993). Mahajan (2005) reported that zooplankton in Lonar Lake are restricted to a few species and are generally low in number. Beside some protozoans, mainly ciliates, identified zooplankton species are the rotifers *Brachionus* sp., *Philodina* sp., and *Testudinella* sp., culicid larvae, and very few exemplars of the ostracod *Cypris subglobosa* (Badve et al. 1993; Mahajan 2005). Branchiopoda have not been observed (Mahajan 2005). The lake is fishless, and only one gastropod species (*Lymnea acuminata*) was found (Badve et al. 1993). The non-Cyanophyceae microbial community consists of thermophilic, halophilic, and alkalophilic bacteria (10^2 to 10^4 viable cells mL^{-1} ; Joshi et al. 2008). Also, methanogenic archaea were reported (Surakasi et al. 2007).

The vicinity of Lonar crater is characterised by semi arid vegetation, but at the present time most of the area is under agricultural land use. Within the crater, the vegetation is more diverse. The rim is overgrown by grass, shrub, and dry deciduous forest. A plain of alluvial material surrounding the lake has formed at the crater floor. This plain predominantly hosts

semi-evergreen forest and is ca. 5 – 100 m broad except at the Dhara fan in the northeast, where it reaches a breadth of > 300 m. The Dhara fan is mostly under land use with crop plantations and meadows for grazing cattle. Also, swamp vegetation is common on the Dhara fan. Most trees growing in the Lonar crater were afforested during 1986 to 1992 by the Forest Department (Malu et al. 2005). In addition to native species, like *Acacia nilotica*, *Azadirachta indica*, *Dendrocalamus strictus*, and *Tectona grandis*, non-indigenous species were planted, such as *Eucalyptus* sp., *Delonix regia*, and *Prosopis juliflora*.

3.3. Methods

3.3.1. Sampling

Surface sediment samples were collected in January 2007 and May 2008 at 68 locations using a Wildco Ponar-type grab sampler with a maximum penetration depth of 5 – 7 cm. Additionally, 28 samples were taken along the shoreline consisting of soil, terrestrial plants, and plankton.

Water samples were taken in May 2008 and February 2011 with a Niskin 1011 water sampler activated by a General Oceanics Devil messenger (model 1000MG) attached to a hydrocable that was marked in 10 cm intervals. The samples were filtered immediately after retrieval onto pre-combusted and pre-weighed Whatman GF/F filters (0.45 µm) and air dried. Water samples were stored frozen until further analysis in the laboratory.

Sediment traps were deployed at two stations from February 2011 to May 2011 and from May 2011 to October 2011~ 70 cm above the lake floor. The trap bottles were not poisoned because the study location is a natural heritage site, and the use of toxic chemicals is prohibited.

Data on air temperature, rainfall, evapotranspiration, wind speed, and wind direction were acquired from the India Meteorological Department, Pune, and from the India Water Portal (http://indiawaterportal.org/met_data/)

Surface samples from the Himalayan lakes Rewalsar, Renuka, and Mansar were taken with grabs or short corers by B. K. Das over the last decades, and sampling details as well as further information on the lakes are available in Das et al. (2008).

3.3.2. Analytical methods

Prior to analyses, the surface sediment, soil, and plankton samples were rinsed with distilled water and centrifuged at 4000 revolutions min^{-1} until the supernatant water was clear and attained an electrical conductance coefficient of $< 1000 \mu\text{S}$. This treatment was done to remove any salts dissolved in the pore water. Subsequently, the samples were freeze-dried for 72 hours and aliquots were ground manually in an agate mortar.

Total carbon and nitrogen (TC, TN) were measured on a Carlo Erba Nitrogen Analyzer (NA) 1500 elemental analyzer; the standard deviation of the duplicate analyses was 0.15% for carbon and 0.005% for nitrogen. Total organic carbon (TOC) analyses were performed on the same instrument after pre-treating the samples with 2 mol L^{-1} HCl to eliminate inorganic carbon. The relative error of this method was $\pm 5\%$. Inorganic carbon (IC) was defined as the difference between total and organic carbon; the values were converted to calcite as this was the only carbonate phase detected in the sediments.

$^{13}\text{C}/^{12}\text{C}$ isotope ratios were determined using a Finnigan MAT 252 gas isotope mass spectrometer after high-temperature flash combustion in a Carlo Erba NA-2500 elemental analyzer at 1100°C . Values are expressed as:

$$\delta^{13}\text{C} (\text{‰}) = [(R_{\text{sam}} / R_{\text{std}}) - 1] \times 10^3 \quad (3.1)$$

With $R_{\text{sam}} = {}^{13}\text{C}/{}^{12}\text{C}$ ratio of the sample and $R_{\text{std}} = {}^{13}\text{C}/{}^{12}\text{C}$ ratio of the reference standard VPDB (Vienna Pee Dee Belemnite). Analytical precision was better than 0.1‰ based on replicate measurements of a reference standard; duplicate measurements of samples resulted in a mean deviation of 0.2‰.

The ratio of the two stable nitrogen isotopes (${}^{15}\text{N}/{}^{14}\text{N}$) is expressed as $\delta^{15}\text{N}$ after determining the abundance of the two isotopes in samples (after combustion and reduction of NO_x to N_2) by mass spectrometry:

$$\delta^{15}\text{N} (\text{‰}) = [(R_{\text{sam}} / R_{\text{std}}) - 1] \times 10^3 \quad (3.2)$$

With $R_{\text{sam}} = {}^{15}\text{N}/{}^{14}\text{N}$ ratio of the sample and $R_{\text{std}} = {}^{15}\text{N}/{}^{14}\text{N}$ ratio of the reference standard, atmospheric N_2 ($\delta^{15}\text{N} = 0\text{‰}$). $\delta^{15}\text{N}$ values were determined using a Finnigan MAT 252 gas isotope mass spectrometer after high-temperature flash combustion in a Carlo Erba NA-2500 elemental analyzer at 1100°C. Pure tank N_2 calibrated against two reference standards of the International Atomic Energy Agency (IAEA), IAEA-N-1, and IAEA-N-2, as well as a sediment standard was used as a working standard. Analytical precision was better than 0.1‰ based on replicate measurements of a reference standard. Duplicate measurements of samples resulted in a mean standard deviation of 0.11‰.

Nitrate and nitrite concentrations of filtered water samples were measured with standard colorimetric techniques (Grasshoff et al. 1999) on an AutoAnalyzer 3 by Bran and Luebbe. Detection limit of nitrate and nitrite concentration was 0.15 and 0.02 $\mu\text{mol L}^{-1}$, respectively.

Amino acid analyses were carried out on a Biochrom 30 Amino Acid Analyzer according to the method described in chapter 2.3.2 and in Lahajnar et al. (2007).

3.4. Results

3.4.1. TOC, TN, IC, C/N

The TOC, TN, IC, and atomic TOC/TN (C/N) ratio values of the analysed samples are shown in Table 3.1. The surface sediment data were reported by Basavaiah et al. (2014). TOC and TN of the surface sediments show values of 0.25% to 6.28% and 0.02% to 0.88%, respectively. IC values of the sediments vary between 0.23% and 2.48% and the atomic C/N ratios range from 7.8 to 17.6.

Table 3.1: Bulk biogeochemical parameters, AA and HA concentrations of different Lonar samples. IC values of surface sediment samples as well as TOC, TN, C/N, and $\delta^{13}\text{C}$ values of all samples except for those of sediment traps were taken from Basavaiah et al. (2014).

Abbreviations: THAA, total hydrolysable amino acids in mg/g dry sample; AA-C, percentage of organic carbon present as amino acids; AA-N, percentage of total nitrogen present as amino acids; THHA, total hydrolysable hexosamines in mg/g dry sample; nd, not detected; *, number of samples analyzed for amino acids.

Sample type	TOC (%)	TN (%)	C/N (atomic)	IC (%)	$\delta^{13}\text{C}$ (‰)	$\delta^{15}\text{N}$ (‰)	THAA (mg/g)	AA-C (%)	AA-N (%)	THHA (mg/g)
Surface sediments ($n=66$; 26*)	2.65 ± 1.47	0.30 ± 0.19	10.71 ± 1.66	1.23 ± 0.42	-18.32 ± 1.81	12.62 ± 2.64	11.33 ± 7.35	18.23 ± 5.02	49.98 ± 8.32	0.82 ± 0.63
Soil samples ($n=17$; 6*)	0.52 ± 0.62	0.08 ± 0.07	15.77 ± 24.03	0.33 ± 0.54	-22.56 ± 2.95	5.84 ± 1.53	3.02 ± 3.77	13.39 ± 9.90	38.01 ± 24.31	0.59 ± 0.83
Suspended particulate matter (SPM)										
Shallow water SPM (0.5 m; $n=2$)	28.72 ± 2.48	4.54 ± 0.24	7.41 ± 1.02	nd	-8.79 ± 0.83	10.18 ± 0.15	250.18 ± 15.95	38.90 ± 5.82	73.55 ± 1.23	2.40 ± 0.23
Deep water SPM (4 m; $n=2$)	35.17 ± 5.39	5.23 ± 0.69	7.99 ± 2.26	nd	-8.97 ± 0.61	10.59 ± 0.35	317.55 ± 38.45	41.02 ± 10.88	81.67 ± 0.66	2.24 ± 0.29
Sediment trap samples										
Western trap Feb – May 2011	17.24	3.21	6.26	0.24	-4.96	16.09	135.15	34.48	56.42	2.04
Eastern trap Feb – May 2011	26.82	5.68	5.90	0.04	-6.99	18.57	157.01	35.65	53.97	2.87
Western trap Jun – Oct 2011	20.98	3.56	6.88	0.08	-8.49	18.17	170.30	36.07	64.33	2.80
Eastern trap Jun – Oct 2011	30.16	4.39	8.59	0.11	-8.45	16.49	323.34	37.52	83.25	4.62
Vascular plant samples										
<i>Prosopis juliflora</i> leaves	45.09	4.58	11.49	nd	-30.52	-1.64	176.74	17.55	52.61	0.62
<i>Tectona grandis</i> leaves	38.99	1.04	43.74	nd	-28.65	2.66	39.31	4.58	50.83	0.50
<i>Azadirachta indica</i> leaves	44.94	3.13	16.74	nd	-28.52	5.17	138.64	13.81	60.39	0.66
<i>Acacia nilotica</i> leaves	43.89	1.24	41.45	nd	-28.71	-2.75	49.09	5.09	54.52	0.37
<i>Heteropogon</i> sp.	42.49	0.59	84.59	nd	-12.13	10.03	24.29	2.60	37.79	3.67

3.4.2. $\delta^{13}\text{C}$

The $\delta^{13}\text{C}$ values of surface sediments were investigated by Basavaiah et al. (2014). $\delta^{13}\text{C}$ of surface sediments range between -23.1‰ and -15.2‰ with lowest values off the Dhara river mouth and along the westernmost lakeshore and highest values in the deep central part of the lake. SPM filtered from shallow (0.5 m) as well as from deep (4 m) water has $\delta^{13}\text{C}$ values of -9.4‰ to -8.2‰ . Sediment trap material shows $\delta^{13}\text{C}$ values of -8.5‰ to -5.0‰ . Terrestrial C_3 and C_4 plants have mean $\delta^{13}\text{C}$ values of -29.1‰ and -12.1‰ , respectively. Depending on the percentage of C_3 and C_4 plant material in the soils, their $\delta^{13}\text{C}$ values vary between -26.7‰ and -18.1‰ .

3.4.3. $\delta^{15}\text{N}$

The $\delta^{15}\text{N}$ values of the surface sediments show a clear correlation with water depth (Figure 3.2 A). Samples from depths > 4 m have values of 7.8‰ to 13.6‰ (mean: 10.8‰). $\delta^{15}\text{N}$ of samples from stations shallower than 4 m range between 10.5‰ and 18.2‰ (mean: 15.3‰ ; Figure 3.2 B). $\delta^{15}\text{N}$ of SPM group in a narrow range of 10.1‰ – 10.8‰ . Sediment trap material has $\delta^{15}\text{N}$ values of 16.1‰ to 18.6‰ and does not show a systematic difference between the two stations or the two sampling intervals. The analysed vegetation samples have a wide range of $\delta^{15}\text{N}$ values from -2.8‰ to 12.1‰ with a mean of 4.4‰ , which is well in the range of terrestrial plants (Maksymowska et al. 2000). 5 of the 12 vegetation samples show relatively ^{15}N -depleted values between -2.8‰ and 0.9‰ , indicating N_2 -fixation. In fact, these vegetation samples were taken from genera of the family Fabaceae, which is known to form root nodules associated with symbiotic nitrogen-fixing bacteria (Soltis et al. 1995), including the species *Acacia nilotica*, *Prosopis juliflora*, and *Tamarindus indica*. The remaining 7 vegetation samples have $\delta^{15}\text{N}$ values of 2.7‰ to 12.1‰ (mean: 7.4‰). The sampled soils

show diverse $\delta^{15}\text{N}$ values of -0.4‰ to 16.1‰ (mean: 6.2‰), mostly depending on the vegetation close to the sampling points.

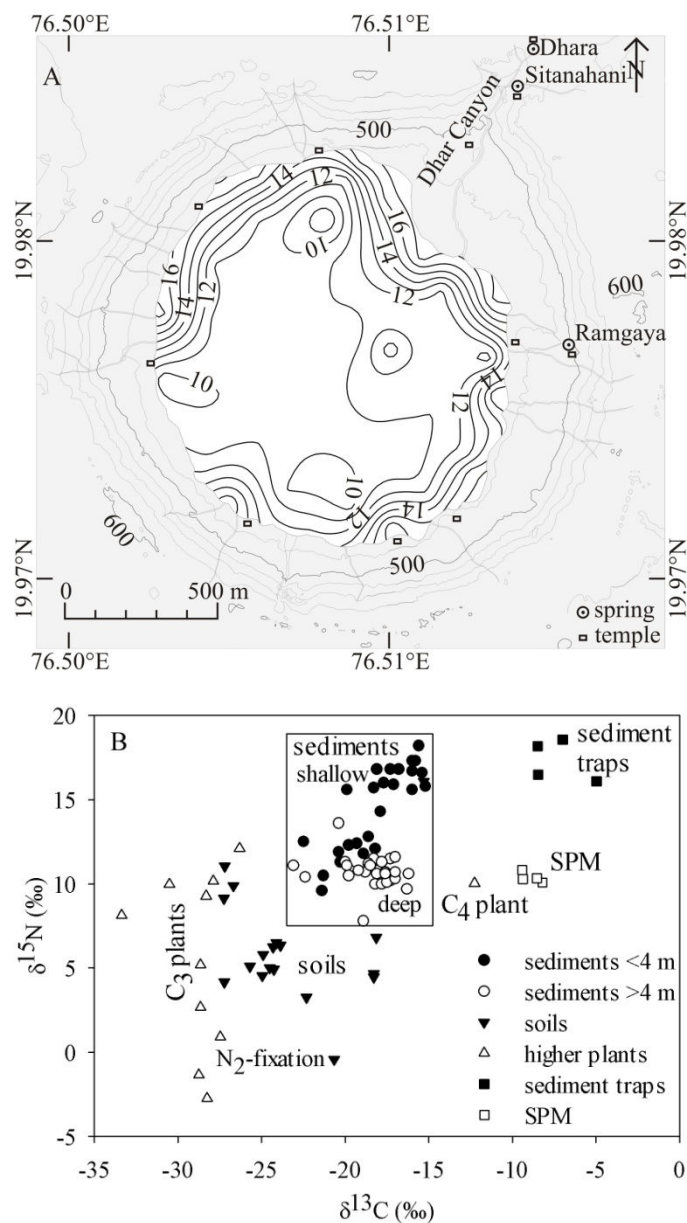


Figure 3.2: Spatial distribution of $\delta^{15}\text{N}$ (‰) in Lonar surface sediment organic matter (A). Stable carbon vs. nitrogen isotopic ratios of the different Lonar samples (B).

3.4.4. Amino acids

The amounts of total hydrolysable amino acids and hexosamines of the different samples are shown in Table 3.1. Amino acid contents in the surface sediments range between 1.1 and 31.4 mg g⁻¹ and are significantly correlated with organic carbon content. The amount of organic carbon and total nitrogen incorporated into amino acids (AA-C; AA-N) is 10.3% to 33.5% (mean: 18.2%) and 36.8% to 73.4% (mean: 50.0%), respectively. Sediment trap samples and SPM are relatively enriched in total amino acid content and also show elevated AA-C and AA-N values compared to surface sediments. The analysed soils are the most depleted samples in terms of amino acid content and AA-C and AA-N percentages. The average distribution of the individual amino acids in surface sediments, sediment traps, SPM, terrestrial plants, and soils are given in Table 3.2.

Table 3.2: Amino acid composition of the different Lonar samples.

Abbreviations: Asp, aspartic acid; Thr, threonine; Ser, serine; Glu, glutamic acid; Gly, glycine; Ala, alanine; Val, valine; Met, methionine; Ile, isoleucine; Leu, leucine; Tyr, tyrosine; Phe, phenylalanine; β -Ala, β -alanine; γ -Aba, γ -aminobutyric acid; His, histidine; Trp, tryptophan; Orn, ornithine; Lys, lysine; Arg, arginine.

Sample type	Asp	Thr	Ser	Glu	Gly	Ala	Val	Met	Ile	Leu	Tyr	Phe	β -Ala	γ -Aba	His	Trp	Orn	Lys	Arg
	(mol %)																		
Surface sediments ($n=26$)	12.99	5.62	6.06	11.90	12.60	10.97	6.72	0.38	4.30	7.30	2.49	4.29	0.54	0.48	2.57	0.22	0.58	3.81	4.24
	± 0.73	± 0.45	± 0.58	± 0.45	± 1.12	± 0.51	± 1.09	± 0.17	± 0.92	± 0.71	± 0.34	± 0.47	± 0.19	± 0.13	± 0.69	± 0.09	± 0.17	± 0.35	± 0.54
Soil samples ($n=6$)	16.57	5.71	6.80	12.17	15.07	10.51	5.02	0.43	2.78	5.33	1.44	2.80	1.60	0.71	4.80	0.48	0.71	3.73	3.33
	± 0.69	± 0.19	± 0.47	± 0.77	± 0.69	± 0.26	± 0.16	± 0.25	± 0.13	± 0.36	± 0.23	± 0.13	± 0.62	± 0.18	± 0.98	± 0.27	± 0.33	± 0.23	± 0.35
Suspended particulate matter																			
Shallow water SPM (0.5 m; $n=2$)	10.75	5.59	6.15	18.01	9.12	11.18	7.83	0.53	5.64	8.80	2.69	3.76	0.10	0.06	1.58	0.10	0.09	2.81	5.20
	± 0.27	± 0.02	± 0.22	± 0.16	± 0.02	± 0.19	± 0.20	± 0.06	± 0.01	± 0.16	± 0.06	± 0.03	± 0.00	± 0.00	± 0.02	± 0.00	± 0.00	± 0.10	± 0.23
Deep water SPM (4 m; $n=2$)	10.77	5.51	6.17	17.28	9.05	11.38	7.79	0.46	5.65	8.95	2.87	3.71	0.07	0.04	1.48	0.10	0.09	3.18	5.43
	± 0.45	± 0.15	± 0.26	± 1.76	± 0.22	± 0.66	± 0.38	± 0.07	± 0.31	± 0.35	± 0.10	± 0.07	± 0.01	± 0.01	± 0.01	± 0.02	± 0.07	± 0.30	± 0.55
Sediment trap samples																			
Western trap Feb – May 2011	12.42	6.80	5.53	12.49	10.82	10.95	8.36	0.28	5.74	8.06	3.10	4.64	0.11	0.11	1.99	0.09	0.10	4.01	4.39
Eastern trap Feb – May 2011	12.38	6.65	5.74	12.79	10.96	10.79	8.04	1.12	5.51	7.88	3.28	4.57	0.10	0.23	1.86	0.07	0.13	3.55	4.36
Western trap Jun – Oct 2011	12.14	6.74	5.76	12.38	10.94	10.80	8.39	0.16	5.66	8.26	3.10	4.77	0.09	0.10	1.82	0.08	0.20	3.96	4.66
Eastern trap Jun – Oct 2011	12.05	6.68	5.67	12.90	10.74	10.74	8.39	0.25	5.65	8.15	3.22	4.63	0.09	0.11	1.85	0.08	0.10	3.89	4.78
Vascular plant samples																			
<i>Prosopis juliflora</i> leaves	17.66	5.23	6.17	10.93	9.43	8.33	6.44	0.18	4.46	8.74	3.27	4.94	0.15	0.65	2.31	0.25	0.00	5.97	4.90
<i>Tectona grandis</i> leaves	10.63	5.78	6.94	11.80	10.62	9.30	7.50	1.04	5.70	9.97	3.49	5.02	0.38	0.44	2.21	0.17	0.00	4.73	4.28
<i>Azadirachta indica</i> leaves	11.39	4.82	6.07	17.14	9.28	9.42	6.21	0.43	4.69	8.34	3.24	4.44	0.31	0.90	2.32	0.13	0.07	5.57	5.23
<i>Acacia nilotica</i> leaves	10.38	5.41	7.31	11.29	10.32	9.49	7.36	0.44	5.29	9.35	3.57	5.19	0.30	0.57	2.50	0.15	0.00	6.61	4.48
<i>Heteropogon</i> sp.	10.08	7.13	7.82	13.06	10.58	10.29	7.41	1.50	5.12	8.08	2.85	3.39	0.43	0.59	2.87	0.25	0.74	4.63	3.20

3.5. Discussion

3.5.1. TOC, TN, IC, C/N

Despite eutrophic conditions, TOC and TN values in the modern Lonar Lake sediments are low compared to most reported values for eutrophic lakes (Dean and Gorham 1998). The low TOC and TN concentrations of the sediments are due to the high input of lithogenic material, which is eroded from the steep slopes of the crater and transported into the lake during monsoonal rainfall events. The IC sources are carbonate crystals formed during lake level decline in dry years and during maximum photosynthesis. Similar to TOC and TN concentrations, IC concentrations are related to lithogenic matter input and are therefore higher in the central and lower in the nearshore area.

The C/N ratio is often used in lake studies to estimate the terrestrial and aquatic fraction of OM in the sediments (Meyers 1994). C/N ratios of aquatic OM vary between 4 and 10, whereas C/N ratios of terrestrial vascular plant material show values of 20 and greater (Meyers 1994). The surface sediments of Lonar Lake have C/N ratios of 7.8 to 17.6 with a mean value of 10.7, indicating a dominance of aquatic OM. C/N ratios may increase during early diagenesis as N-bearing components (proteins, peptides, and free amino acids), particularly in protein-rich OM derived from aquatic source, are preferentially decomposed (Meyers 1997). On the other hand, C/N ratios of OM of terrestrial origin may decrease during degradation as a consequence of preferential removal of C-rich lipids and sugars (Meyers 1997). In organic-poor sediments, ammonium sorbed by clay minerals can be a significant N-contributor, reducing C/N ratios (Müller 1977). Since these diagenetic effects usually are of minor magnitude, the C/N ratio still serves as a good indicator of the OM source. However, as $\delta^{13}\text{C}$ of aquatic and terrestrial OM in Lonar Lake and its catchment are fairly different and in

a narrower range than C/N, $\delta^{13}\text{C}$ of organic carbon seems to be a better proxy to identify the source of surface sediment OM in Lonar Lake (Table 3.1).

3.5.2. $\delta^{13}\text{C}$ and $\delta^{15}\text{N}$

Compared to the majority of lakes from the literature, both $\delta^{13}\text{C}$ and $\delta^{15}\text{N}$ are considerably enriched in Lonar surface sediments (Meyers and Teranes 2002). Figure 3.3 shows a comparison of the Lonar data to those from Himalayan lakes of similar altitude but of different trophic status. The $\delta^{13}\text{C}$ of the oligotrophic lake Rewalsar and the mesotrophic lakes Renuka and Mansar are in the range of C_3 plants with admixture of C_4 plants (-28‰ to -22‰), and $\delta^{15}\text{N}$ values vary around 4‰, generally considered as the average of land plants (Maksymowska et al. 2000). Lonar SPM is highly enriched in ^{13}C , with $\delta^{13}\text{C}$ values of -9.4‰ to -8.2‰. These values are consistent with reported $\delta^{13}\text{C}$ values of Lonar dissolved inorganic carbon (DIC), being in the high range of 11‰ to 14.8‰ (Anoop et al. 2013b), as plankton are usually depleted in ^{13}C by 20‰ compared to their DIC source (O'Leary 1988). As discussed by Basavaiah et al. (2014), the high $\delta^{13}\text{C}$ values of Lonar DIC are due to the high pH of the lake water. In this case, lake water is depleted in $\text{CO}_2(\text{aq})$, and plankton utilise HCO_3^- for photosynthesis, which is enriched in ^{13}C by ca. 8.7‰ (at 25°C) compared to $\text{CO}_2(\text{aq})$ (Zhang et al. 1995). With an aquatic $\delta^{13}\text{C}$ endmember of -9‰ and a terrestrial endmember of -28‰, Basavaiah et al. (2014) calculated the percentages of terrestrial OM in Lonar surface sediments (32.5% – 74.0%; mean: 49.1%) by a $\delta^{13}\text{C}$ two end-member mixing equation.

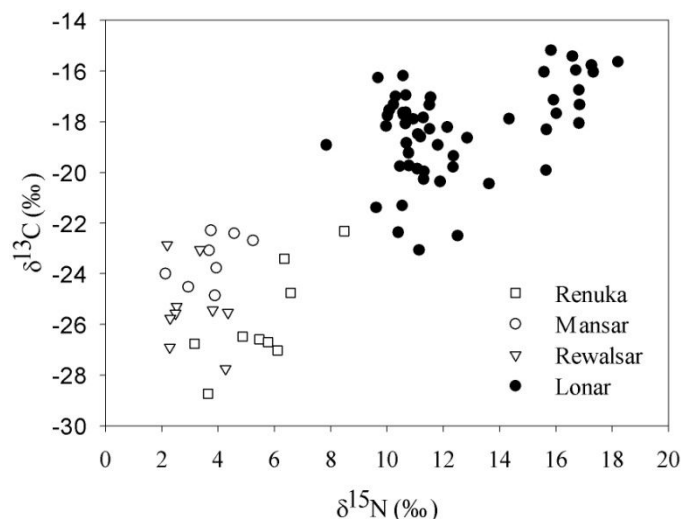


Figure 3.3: Comparison of the stable carbon vs. nitrogen isotopic ratios of Lonar Lake and Renuka, Mansar, and Rewalsar Lakes.

$\delta^{13}\text{C}$ in combination with C/N ratio and AA-C is used to identify the source of the sediment trap material. These parameters indicate that the contribution of resuspended surface sediment, soil OM, and terrestrial plants to the sediment trap samples is low (Table 3.1). Thus, the dominant source of sediment trap samples is SPM and microorganisms decomposing it, as discussed in chapter 3.5.4. Degradation processes may affect $\delta^{13}\text{C}$ during early diagenesis as, for example, the hydrolysis of proteins is accompanied by an enrichment of ^{13}C in the residual material (Silfer et al. 1992). This effect might be responsible for the slight increase in $\delta^{13}\text{C}$ values between SPM and sediment trap material. The sediment trap material is enriched in ^{13}C by 2.5‰ before the onset of the monsoon compared to the monsoon despite the higher productivity during the monsoon season. As the lower summer $\delta^{13}\text{C}$ values are accompanied by C/N ratios elevated by 1.7 (Table 3.1), we assume that the relative amount of terrestrial OM is slightly higher, related to ephemeral runoff causing enhanced erosion and transport of terrestrial OM into the lake.

The elevated $\delta^{15}\text{N}$ values in Lonar SPM and surface sediments can be attributed to the sub-to anoxic conditions in the hypolimnion in conjunction with the high pH (Heaton 1986). Nitrate in the hypolimnion becomes denitrified associated with a fractionation factor of $\epsilon = -$

30‰ to -22‰ (Brandes et al. 1998), leaving the remaining nitrate pool enriched in ^{15}N . Elevated $\delta^{15}\text{N}$ values are also related to high salinity and the associated high pH of Lonar Lake (Heaton 1986). At high pH values, the equilibrium of NH_4^+ and NH_3 shifts towards NH_3 (pKa of $\text{NH}_4^+ = 9.3$), leading to ^{15}N enrichment of NH_4^+ relative to NH_3 by 20‰ – 35‰ (Casciotti et al. 2011). The pH values of ~ 9.3 below 4 m water depth and ~ 10.5 at shallower depth result in ~ 50% to 90% NH_3 , respectively, which can escape the water column. Concentrations of nitrate and nitrite were very low in the epi- and hypolimnion in February 2011, with values between < 0.15 to 0.94 $\mu\text{mol L}^{-1}$ and 0.24 to 0.52 $\mu\text{mol L}^{-1}$, respectively. This property may be related to uptake in surface waters and to anoxia below 4 m water depth. The high $\delta^{15}\text{N}$ values of plankton (mean: 10.4‰) sampled in February 2011 when nitrate and nitrite were almost depleted in the epilimnion do not suggest that N_2 -fixation is a dominant nitrogen source in Lonar Lake. Whereas the intense plankton blooms during the monsoon are related to the in-wash of nutrients from the ephemeral runoff, the nutrient source during post-monsoon may be small streams and recycling of nutrients in the water column and the surface sediments.

The spatial variability of $\delta^{15}\text{N}$ of surface sediment is depth dependent (Figure 3.2 A) and is most likely linked to the stratification of the lake, with oxic surface water up to about 4 m depth and sub- to anoxic water in > 4 m depth (Basavaiah et al. 2014). Lehmann et al. (2002) found a $\delta^{15}\text{N}$ decrease by 3‰ during anoxic incubation and an increase of $\delta^{15}\text{N}$ by > 3‰ within the first months of oxic incubation before $\delta^{15}\text{N}$ slowly dropped to the initial source values. Since the traps at Lonar Lake were not poisoned, microbial growth and related OM degradation could occur during the time of deployment (3 – 4 months). While installing the traps, oxic surface water filled the sampling bottles so that, at least to some extent, degradation under oxic conditions could play a role in OM respiration in the traps and explain the elevated $\delta^{15}\text{N}$ values compared to SPM and surface sediments from anoxic sampling points. Macko and Estep (1984) analysed the effect of aerobic microbial degradation on

different nitrogen-containing substrates. Their findings show that deamination and transamination of different amino acids can result in both elevated and reduced $\delta^{15}\text{N}$ values of the residual OM. Comparison with the results of the amino acid analysis of the Lonar Lake samples shows that the elevated $\delta^{15}\text{N}$ values in shallow surface sediments and sediment trap material can be attributed to aerobic microbial degradation. Further indications of degradation processes derived from the analysis of amino acids are given in the following section.

3.5.3. Amino acid concentrations

Since most amino acids in fresh OM are more labile than other carbon compounds present in particulate matter (Lee 1988), they are preferentially lost during degradation. The mean amino acid content in sediment trap samples is 87.4 mg g^{-1} lower compared to that of SPM (Table 3.1), which is a reduction by 30%. TOC and TN content in the trap samples are reduced by 25% and 20% compared to SPM, respectively. C/N ratio, $\delta^{13}\text{C}$ values, and AA-C are in the same range in sediment trap and SPM samples, corroborating the assumption that the sediment trap material is dominated by SPM derived OM with only very minor contribution of land-derived OM sources. Thus, the loss of amino acids must be due to the preferential removal of amino acids during early decomposition. In surface sediments only about 8% of the TOC, 6% of the TN, and 4% of the amino acid content found in SPM are present, which is partly due to degradation but also to enhanced contribution of amino acid-poor terrestrial OM as indicated by enhanced C/N ratios, depleted $\delta^{13}\text{C}$ values, and decreased AA-C (Table 3.1). In environments with varying amounts of terrestrial OM, such as the Lonar Lake, AA-C values are strongly influenced by the distribution of aquatic- and terrestrial-derived OM in the sediments (Haake et al. 1992; Verma and Subramanian 2002), whereas AA-N is more sensitive to degradation (Henrichs et al. 1984; Cowie and Hedges 1992). Terrestrial OM, particularly woody fragments, has lower AA-C values than plankton due to

the lower percentage of proteins, peptides, and free amino acids in terrestrial plants and the higher percentage of nitrogen deficient organic compounds (Rashid 1985).

3.5.4. Individual amino acid assemblages

Sources of the OM of the sediments are terrestrial plant tissue of differing reactivity, moderately to intensely degraded soils, dead plankton degraded during sinking, bacterial OM, and resuspended lake sediment. The most important processes, modulating the amino acid assemblage of source material, are aerobic microbial degradation at the water-sediment interface in the shallow oxic part of Lonar Lake, anaerobic microbial degradation within the sediments and at the water sediment interface in the deeper sub- to anoxic part of the lake, and lysis of cells and cell compounds. Generally, the amino acid spectra indicate that Lonar sediments are less degraded than sediments in other shallow freshwater environments (Verma and Subramanian 2002; Unger et al. 2005; Das et al. 2010) and resemble those of suspended matter or plankton (Lee 1988; Cowie and Hedges 1992). This difference is most likely attributable to the high productivity in combination with high sedimentation rates due to slope erosion during the southwest monsoon, leading to fast burial of the OM in the sediment where anoxic conditions prevent enhanced degradation (Hulthe et al. 1998; Lehmann et al. 2002; Moodley et al. 2005). The lack of higher organisms that feed on the suspended and surface sediment OM may additionally diminish the state of degradation.

The amino acid assemblages of Lonar SPM differ from those reported for marine SPM (Lee 1988). Lonar SPM is comparatively enriched in glutamic acid (Glu), alanine (Ala), valine (Val), leucine (Leu), and iso-leucine (Ile) and depleted in lysine (Lys), serine (Ser), aspartic acid (Asp), and glycine (Gly). These differences can be attributed to dominance of cyanobacteria in the plankton community of Lonar Lake. In diatom-dominated marine sediments, Asp/Gly ratios are 0.6 – 0.8 (Ittekkot et al. 1984a) whereas Lonar sediments have

Asp/Gly ratios of 0.86 to 1.16. The most abundant cyanobacterium in Lonar Lake is *Arthrothrix fusilini*, which is enriched in Ile, Ala, Val, and Leu and depleted in Gly, Glu, Lys, Asp, and Ser (Becker 2007) compared to marine plankton (Lee 1988). Glu is highly enriched in many microbes, especially in gram-positive bacteria (Tempest et al. 1970). In summary, the difference between amino acids spectra of Lonar SPM, trap material, and surface sediments compared to other lacustrine and marine samples results from the high amounts of bacterial biomass.

The amino acid assemblages of the analysed vascular plant samples are quite different from those of the SPM samples as they show significantly lower values of Glu and markedly higher values of histidine (His), Lys, and the non-protein amino acids β -alanine (β -Ala) and γ -aminobutyric acid (γ -Aba) (Table 3.2). The elevated Glu values in Lonar SPM are related to high microbial OM contribution in the lake. His is usually more abundant in plants than in phytoplankton and even more in fungi (Cowie and Hedges 1992). Lys, being an essential amino acid to most animals, is synthesised in higher plants from Asp by the enzyme aspartate kinase (Azevedo and Lea 2001). Elevated β -Ala and γ -Aba values in vascular plant tissue compared to plankton were reported by Cowie and Hedges (1992). In addition, γ -Aba is known to be produced by plants as a response to environmental stress linked to heat, salt, and flooded soil (Kinnersley and Turano 2000), which regularly occur in the Lonar crater.

Characteristic changes in amino acid spectra, such as relative increases in Asp, Gly, and non-protein amino acids as well as decreases of the essential amino acids Val, Ile, Leu, and arginine (Arg), indicate that degradation is progressing from SPM to sediment trap samples to surface sediments and that soils are even more degraded than lake sediments (Figure 3.4). Higher plants are an additional amino acid source for the sediments with a wide range of amino acid spectra (Table 3.2). However, although terrestrial plants contribute about 50% of organic carbon to lake sediments (*see* chapter 3.5.2), their contribution to total amino acids is lower due to the low amino acid content of most higher plants (Rashid, 1985).

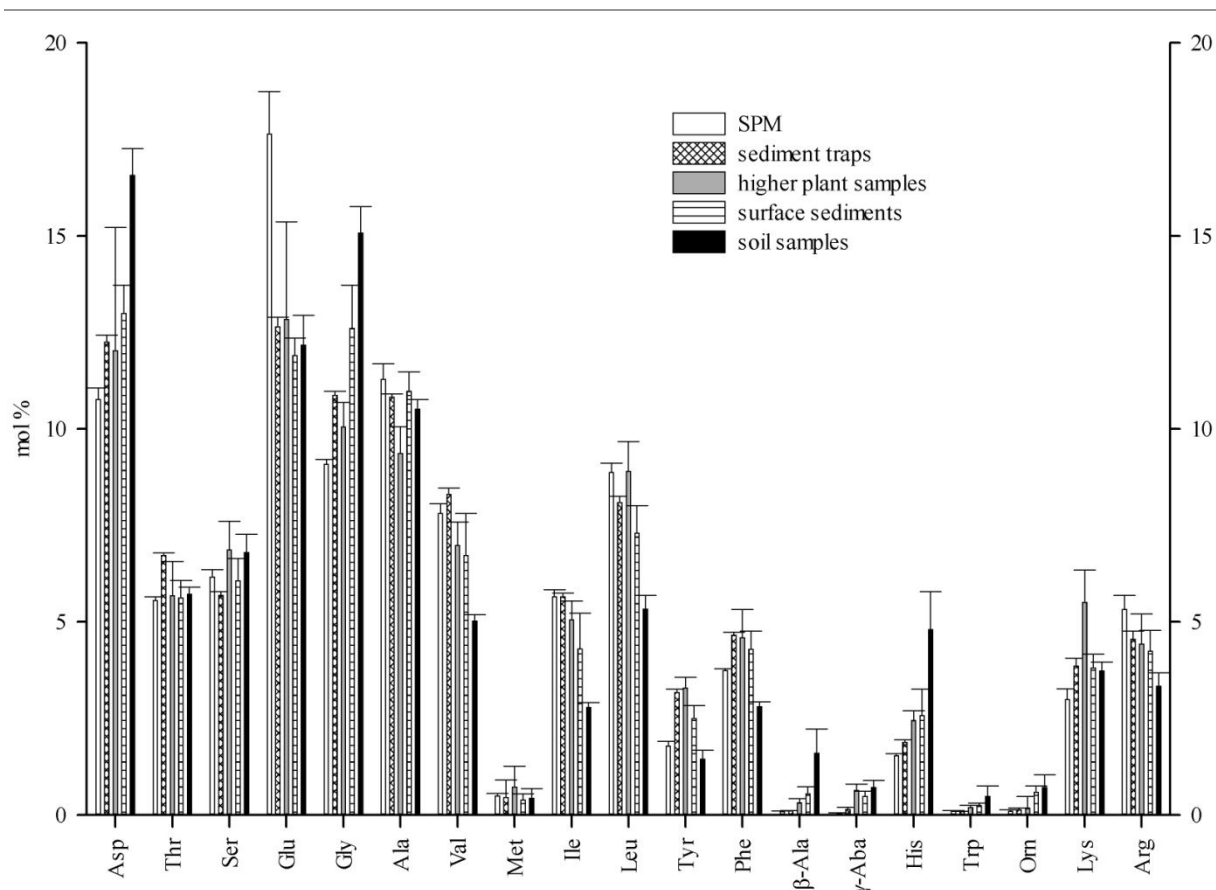


Figure 3.4: Mean contributions (mol %) of the individual amino acids to the total hydrolysable amino acid pool of the different Lonar samples. Error bars denote the standard deviation. Amino acid abbreviations as defined in Table 3.2.

One of the prominent changes from SPM to trap material is the drop of Glu by 5 mol%. When attributing this difference to the preferential microbial removal of Glu from the aquatic OM, the elevated $\delta^{15}\text{N}$ values in the sediment trap samples and in the oxic shallow-water sediments could be explained as follows. Macko and Estep (1984) showed that amino acid degradation by aerobic heterotrophic bacteria occurs via different pathways, depending on the substrate amino acids. Whereas bacteria that utilise Glu and Asp can incorporate these amino acids into the metabolic pathways without preceding deamination, Ala, Ser, and threonine (Thr) have to be deaminated and transformed to glutamate or aspartate. Both pathways are associated with a release of ^{13}C -depleted CO_2 , which is reflected in the Lonar sediment trap samples as these show $\delta^{13}\text{C}$ elevated by 1.7‰ relative to SPM (Table 3.1). The Glu- and Asp-based aerobic metabolism is accompanied by the excretion of ^{15}N depleted ammonia, whereas

during aerobic Ala, Ser, and Thr decomposition ^{15}N -enriched ammonia is excreted (Macko and Estep 1984). Thus, microbial OM predominantly growing on Glu and Asp shows elevated $\delta^{15}\text{N}$ values compared to its substrate, which seems to be the case for the Lonar sediment trap and shallow-water surface sediments. Enhanced microbial contribution to the sediment trap material is also evident by diminished C/N ratios as bacterial OM is characterised by low C/N ratios of about 5 (Goldman et al. 1987) and by a 33% increase in hexosamines from SPM to trap material (Table 3.1), especially in galactosamine, which is mostly associated with bacterial cell walls (Kandler 1979; Haake et al. 1992). Thus, the ratio of glucosamines and galactosamines (Gluam/Galam) can be used to identify the sources of hexosamines to sediments and trap samples; bacterial OM is associated with Gluam/Galam ratios of 1 to 3, whereas higher ratios are present in chitinaceous OM, which is usually most abundant in zooplankton. Gluam/Galam ratios of Lonar sediment trap and surface sediment samples range between 1.4 and 2.0, indicating bacterial origin of the hexosamines (Haake et al. 1992). This corroborates the finding of Mahajan (2005), who reported only sparse zooplankton abundances in Lonar Lake.

To integrate the degradation trends and attribute a degradation state to each sample, we carried out a principal component analysis (PCA) of the amino acid assemblage of the different Lonar samples. The Lonar degradation index (LI) follows the approach of the DI calculation by Dauwe et al. (1999) with the additional amino acids Lys, tryptophan (Trp), β -Ala, γ -Aba, and ornithine (Orn). The LI of a sample is defined as:

$$\text{LI} = \sum_i \left[\frac{\text{var}_i - \text{AVGvar}_i}{\text{STDvar}_i} \right] \times \text{fac.coef.}_i \quad (3.3)$$

Where var_i is the mole percentage of amino acid i , AVGvar_i and STDvar_i are its mean and standard deviation in all samples, and fac.coef._i is the factor coefficient of the first axis of the PCA (values shown in Table 3.3).

Table 3.3: Parameters of the principal component analysis (PCA) of the Lonar sample set.

Abbreviations: Amino acid abbreviations as defined in Table 3.2. AVG, mean contribution of individual amino acids to the amino acid assemblage in mol percent; SD, standard deviation.

Amino acids	First axis factor		
	coefficient	AVG	SD
Asp	0.091	13.089	1.907
Thr	-0.016	5.686	0.550
Ser	0.053	6.205	0.641
Glu	-0.049	12.690	1.840
Gly	0.099	12.100	1.879
Ala	0.002	10.781	0.715
Val	-0.096	6.856	1.203
Met	-0.011	0.438	0.276
Ile	-0.103	4.486	1.093
Leu	-0.105	7.465	1.201
Tyr	-0.088	2.491	0.596
Phe	-0.082	4.144	0.716
β -Ala	0.104	0.573	0.511
γ -Aba	0.077	0.456	0.229
His	0.104	2.653	1.098
Trp	0.073	0.225	0.157
Orn	0.080	0.458	0.293
Lys	-0.001	3.867	0.733
Arg	-0.076	4.232	0.691

The first axis explains 46% of the total variance, and most negative LI values are representative for the freshest (SPM) samples. Trap samples and terrestrial plant samples also have negative values. The most degraded samples, thus represented by the highest LI values, are soil samples from the lake's vicinity. The surface sediments show values varying between -0.8 to 0.8 with one exceptional high value of 1.28 off the perennial streams in the east. Most elevated values, thus the most degraded sediments, occur in the northeast and east off the Dhara fan and the perennial streams (Figure 3.5), indicating the supply of degraded terrestrial OM (e.g., soils) to the eastern part of the lake. Lowest LI values are present in the centre of

the lake, where input of terrestrial sediment is less and sub- to anoxic water reduces the effects of early degradation.

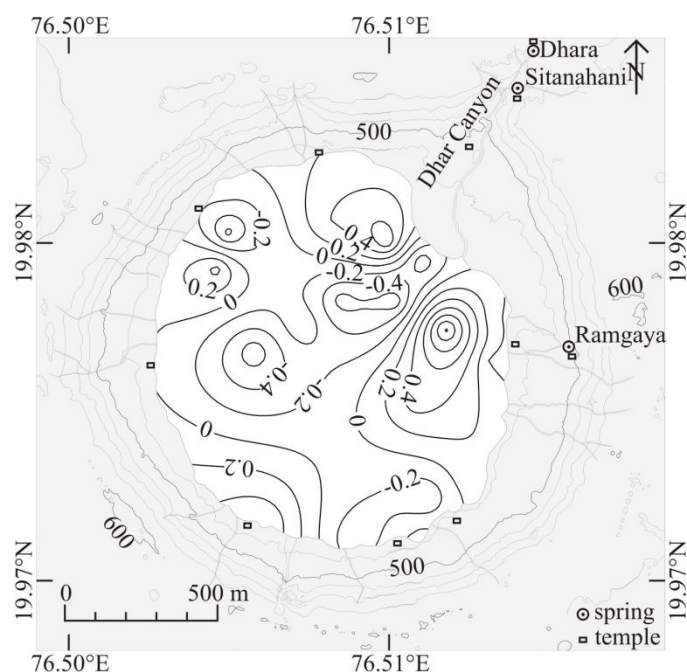


Figure 3.5: Spatial distribution of the Lonar degradation index (LI) in Lonar surface sediment organic matter.

The influence of aerobic and anaerobic degradation on the amino acid assemblage seems to play a significant role in Lonar Lake. Therefore, we decided to use the differences in the amino acid assemblage most probably related to the degree of oxygenation to calculate an indicator of degradation under oxic vs. anoxic conditions. Our calculation is based on the observations made by Cowie et al. (1995), who investigated the differences of anaerobic and aerobic degradation on the amino acid assemblage of identical turbiditic sediments. The Ox/Anox ratio uses the sum of amino acids (mol%) relatively enriched during aerobic degradation and those relatively depleted during anaerobic degradation (Asp, Glu, β -Ala, γ -Aba, Lys) divided by the sum of amino acids relatively depleted during aerobic and relatively enriched during anaerobic degradation (Ser, Ile, Leu, methionine [Met], tyrosine [Tyr], phenylalanine [Phe]). The Ox/Anox ratio of the predominantly undegraded SPM, sediment trap, and higher plant samples are in the range of 0.87 to 1.30 (mean: 1.09). The soil samples,

degraded mostly under oxic conditions, have Ox/Anox values of 1.66 to 2.05. The values of surface sediment Ox/Anox ratios vary between 0.98 and 1.44 with highest values in the shallowest parts of the lake and especially off the Dhara fan, where input of aerobically degraded terrestrial OM is highest and the permanent supply of stream freshwater prevents the development of anoxic lake water (Figure 3.6). Samples from deeper water stations in the centre of the lake show lowest Ox/Anox ratios due to almost permanently anoxic conditions as observed by Basavaiah et al. (2014). The Ox/Anox ratio of surface sediments correlates with the LI, thus suggesting that aerobic amino acid degradation is stronger and leads to an overall enhanced state of OM degradation compared to anaerobic degradation.

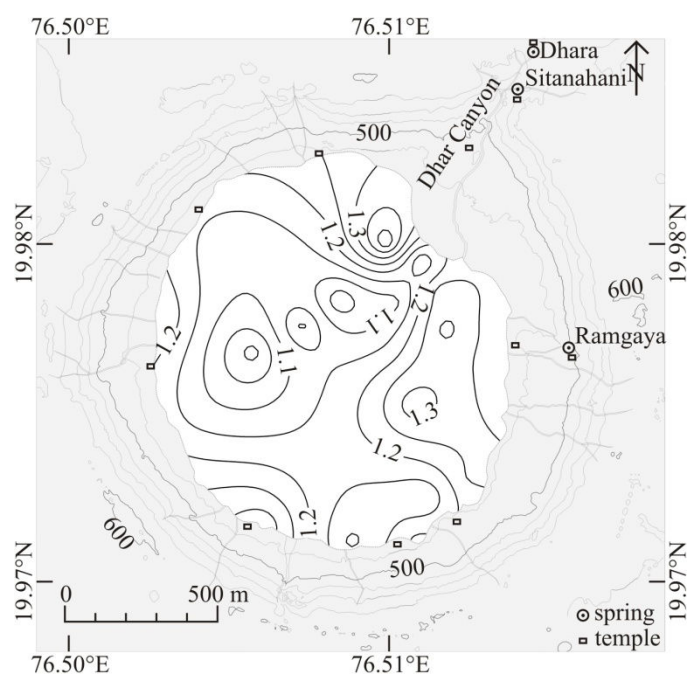


Figure 3.6: Spatial distribution of the Ox/Anox ratio in Lonar surface sediment organic matter.

3.5.5. Depositional environments

According to the spatial differences in Lonar Lake's sedimentation and degradation processes, the lake can roughly be divided into three zones (Figure 3.7). These zones do not have distinct boundaries but merge seamlessly. The three zones are (1) the shallow (< 4 m water depth), nearshore parts of the lake; (2) the eastern part of the lake influenced by the inflow of the perennial streams entering the lake from the east and northeast; and (3) the deep (≥ 5 m water depth) part in the central and southwestern lake. The characteristics of the different zones are discussed below, and the corresponding values are shown in Table 3.4.

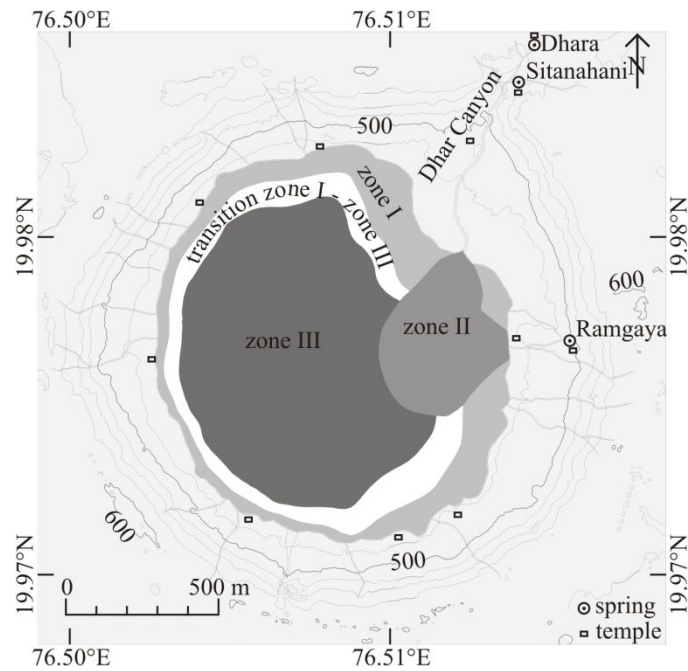


Figure 3.7: Map showing the different depositional zones of Lonar Lake.

Table 3.4: Bulk biogeochemical parameters, amino acid and amino sugar concentrations, and degradation indices of the different depositional environments of Lonar Lake. TOC, TN, C/N, IC, $\delta^{13}\text{C}$, and Terr. TOC values were calculated from data reported by Basavaiah et al. (2014).

Abbreviations: THAA, AA-C, AA-N, THHA as defined in Table 3.1; Terr. TOC, calculated percentage of organic carbon derived from terrestrial source; Gluam/Galam, ratio of the two hexosamines glucosamines and galactosamines; LI, Lonar degradation index; Ox/Anox, ratio of amino acids relatively enriched during aerobic degradation and amino acids relatively enriched during anaerobic degradation; *, number of samples analyzed for amino acids.

Surface sediments	TOC (%)	TN (%)	C/N (atomic)	IC (%)	$\delta^{13}\text{C}$ (‰)	$\delta^{15}\text{N}$ (‰)	Terr. TOC (%)	THAA (mg/g)	AA-C (%)	AA-N (%)	THHA (mg/g)	Gluam/Galam	LI	Ox/Anox
Whole lake ($n=66$; 26*)	2.65 ± 1.47	0.30 ± 0.19	10.71 ± 1.66	1.23 ± 0.42	-18.32 ± 1.81	12.62 ± 2.64	49.06 ± 9.50	11.33 ± 7.35	18.23 ± 5.02	49.98 ± 8.32	0.82 ± 0.63	1.66 ± 0.12	0.03 ± 0.49	1.20 ± 0.11
Zone I ($n=24$; 10*)	3.14 ± 1.81	0.40 ± 0.24	9.63 ± 1.22	1.23 ± 0.50	-17.48 ± 1.94	15.67 ± 1.59	44.64 ± 10.22	16.97 ± 8.13	21.30 ± 4.88	53.30 ± 8.88	1.34 ± 0.62	1.62 ± 0.10	0.15 ± 0.36	1.25 ± 0.09
Zone II ($n=8$; 5*)	1.24 ± 0.43	0.12 ± 0.05	12.35 ± 2.51	0.90 ± 0.19	-20.40 ± 1.58	11.51 ± 0.93	59.99 ± 8.31	4.27 ± 1.88	14.66 ± 3.14	47.81 ± 5.99	0.28 ± 0.12	1.69 ± 0.13	0.39 ± 0.54	1.27 ± 0.07
Zone III ($n=26$; 8*)	2.47 ± 0.98	0.26 ± 0.11	11.31 ± 1.19	1.25 ± 0.32	-17.97 ± 0.95	10.48 ± 0.72	47.24 ± 4.99	8.93 ± 4.88	16.96 ± 4.99	48.52 ± 8.91	0.60 ± 0.48	1.67 ± 0.15	-0.13 ± 0.50	1.12 ± 0.09

3.5.5.1. Zone I: shallow, nearshore lake

The most striking features of this zone are the exceptionally high $\delta^{15}\text{N}$ values, elevated $\delta^{13}\text{C}$, TOC, TN, and amino acid content values, and relatively low C/N ratios, indicating the deposition of predominantly aquatic organic matter, mostly floating cyanobacterial mats drifting to the shores by wind and by inflow-driven surficial currents. These algal mats are heavily microbially reworked as indicated by slightly elevated LI values and especially by the highest contribution of hexosamines with lowest Gluam/Galam ratios. Due to the oxic water conditions in zone I, the Ox/Anox ratios are elevated.

3.5.5.2. Zone II: the eastern part of the lake at the stream mouths

The sediments of this zone are characterised by high C/N ratios and low $\delta^{13}\text{C}$ values, indicating relatively high contributions of terrestrial OM from the streams. Additionally, dilution with lithogenic material input is obvious from the low TOC, TN, and IC values in the surface sediments. Although aerobic degradation is suggested to occur, the $\delta^{15}\text{N}$ values of zone II sediments are much more depleted compared to the values from shallow zone I. This feature can be attributed to the higher contribution of relatively ^{15}N -depleted terrestrial OM and the faster burial of the OM into the anoxic sediments according to stream-controlled elevated sedimentation rates. Recently, the streams have been diverted to the alluvial fan at the northeastern shore for irrigation purposes. However, their influence on the distribution of the OM can still be seen in zone II. Delineating the TOC and TN values, the amino acid content in zone II sediments is lowest. The input of more degraded soil and terrestrial plant remains results in highest LI values and lowest AA-C and AA-N percentages. The calculated Ox/Anox ratios are elevated due to the influence of oxic stream water and the incorporation of high amounts of terrestrial OM that was exposed to subaerial degradation.

3.5.5.3. Zone III: deep, sub- to anoxic part of the lake

The deepest part of the lake is characterised by sub- to anoxic waters, which is reflected by high sulphur contents and low Mn/Fe ratios in the surface sediments (Basavaiah et al. 2014). TOC, TN, C/N, and $\delta^{13}\text{C}$ values of zone III sediments are in the range of the whole-lake mean values and lie between those of zone I and zone II. $\delta^{15}\text{N}$ values are lowest in this zone, which is consistent with the findings that ^{15}N enrichment is restricted to degradation under oxic conditions, whereas under anoxic conditions no changes or even decreasing trends were observed (Freudenthal et al. 2001; Lehmann et al. 2002). The mean amino acid concentrations in the sediments in zone III are lower than the lake mean. This may be due to dilution with fine clays, which accumulate in the deep lake in addition to some coarse material bypassing the lake slopes (Basavaiah et al. 2014). Lowest LI values confirm that reduced degradation of organic matter in sediments is related to the anoxic conditions in zone III with its lowest Ox/Anox ratios.

3.6. Implications of our results

High pH, brackish water, constantly elevated temperatures, eutrophic conditions, and water column stratification with oxic waters in ~ 0 – 4 m depth and sub- to anoxic waters in ~ 4 – 6 m depth result in unusually high $\delta^{15}\text{N}$ values and amino acid assemblages of Lonar Lake OM that differ from most marine and lacustrine environments. The high $\delta^{15}\text{N}$ values are due to denitrification in the anoxic deep water resulting in strongly elevated $\delta^{15}\text{N}$ of the residual NO_3^- . Furthermore, at the high pH, the $\text{NH}_4^+ - \text{NH}_3$ equilibrium shifts towards NH_3 , which is depleted in ^{15}N and can escape from the lake water. As these two mechanisms are associated with high fractionation factors, they mainly control the ^{15}N enrichment of the inorganic nitrogen pool of Lonar Lake, and thus the ^{15}N enrichment of the phytoplankton.

Differences in amino acid assemblage between SPM of Lonar Lake and other aquatic environments can be attributed to the unique ecosystem. The exceptional conditions have yielded an aquatic ecosystem sparse in species but rich in individuals of adapted organisms. Hence, the absence or underrepresentation of common species, such as diatoms and most zooplankton, and the dominance of adapted species, such as cyanobacteria, as well as the contribution of terrestrial OM have led to the development of a unique amino acid assemblage of the Lonar Lake OM. Comparison with amino acid assemblages of other aquatic environments is therefore problematic. This is also indicated by the poor correlation of the two commonly used degradation indices DI and RI. Thus, we calculated a specific Lonar degradation index (LI) on the basis of the DI calculation (Dauwe et al. 1999).

The comparison of $\delta^{15}\text{N}$ values of potential sources of OM to the lake sediments, i.e., terrestrial plants, soils, SPM, and sediment trap material, to $\delta^{15}\text{N}$ values of the sediments from different regions of the lake showed that $\delta^{15}\text{N}$ of OM changes during early degradation as a function of local redox conditions. During anaerobic degradation, apparently no change or only a slight increase occurs whereas aerobic degradation yields $\delta^{15}\text{N}$ increases of 5‰ to 9‰.

A Previous study of Macko and Estep (1984) examined the effect of aerobic microbial degradation on $\delta^{15}\text{N}$ of individual amino acids. According to their findings, we can relate the $\delta^{15}\text{N}$ increase during aerobic degradation mostly to the preferential microbial remineralisation of ^{15}N depleted Glu.

To understand the redox-related changes during early degradation, we calculated a ratio based on the study by Cowie et al. (1995), who identified amino acids that become relatively enriched during anaerobic decomposition and amino acids relatively enriched during anaerobic decomposition. This ratio (Ox/Anox) successfully distinguished samples from the oxic shallow water from samples from the anoxic deep water. For future consideration, the calculation of this ratio might be improved by the incorporation of additional data sets from other sites with varying redox conditions and the weighting of the individual amino acids on basis of a PCA calculation.

4. Linking Holocene drying trends from Lonar Lake in monsoonal central India to North Atlantic cooling events

Abstract

We present the results of biogeochemical and mineralogical analyses on a sediment core that covers the Holocene sedimentation history of the climatically sensitive, closed, saline, and alkaline Lonar Lake in the core monsoon zone in central India. We compare our results of C/N ratios, stable carbon and nitrogen isotopes, grain-size, as well as amino acid derived degradation proxies with climatically sensitive proxies of other records from South Asia and the North Atlantic region. The comparison reveals some more or less contemporaneous climate shifts. At Lonar Lake, a general long term climate transition from wet conditions during the early Holocene to drier conditions during the late Holocene, delineating the insolation curve, can be reconstructed. In addition to the previously identified periods of prolonged drought between 4.6 – 3.9 and 2.0 – 0.6 cal ka that have been attributed to temperature changes in the Indo Pacific Warm Pool, several additional phases of shorter term climate alteration superimposed upon the general climate trend can be identified. These correlate with cold phases in the North Atlantic region. The most pronounced climate deteriorations indicated by our data occurred during 6.2 – 5.2, 4.6 – 3.9, and 2.0 – 0.6 cal ka BP. The strong dry phase during 4.6 – 3.9 cal ka BP at Lonar Lake corroborates the hypothesis that severe climate deterioration contributed to the decline of the Indus Civilisation about 3.9 ka BP.

4.1. Introduction

The increasing demand for reliable climate projections due to the challenges related to global warming calls for enhanced investigation of the relationship between climate change and its effect on the environment. To assess future interaction between climate and environment, it is necessary to understand their interactions in the present and past. But, while modern observations are increasing rapidly and cover almost the whole world in high spatial and temporal resolution, the identification and investigation of suitable sites for palaeoclimate reconstruction is more difficult and requires great effort. Hence, several regions still lack a sufficient cover of investigated areas to help the scientific community in reconstructing the past climate and its influence on the former environment. One of these regions is India, which highly depends on the annual rainfall delivered by the Indian summer monsoon (ISM). This meteorological phenomenon affects a human population of more than one billion and is highly sensitive to climate change. In order to assess and to interpret potential future modifications of the Indian monsoon system, the knowledge of Holocene monsoon variability, its extremes, and their underlying causal mechanisms is crucial. And while terrestrial palaeorecords are available from the northern Indian subcontinent and the Himalayan region (Gasse et al. 1991; Gasse et al. 1996; Enzel et al. 1999; Denniston et al. 2000; Thompson et al. 2000; Bookhagen et al. 2005b; Prasad and Enzel 2006; Clift et al. 2008; Demske et al. 2009; Wünnemann et al. 2010; Alizai et al. 2012), the number and length of comparable records from central and south India are limited (Yadava and Ramesh 2005; Caner et al. 2007; Sinha et al. 2007; Berkelhammer et al. 2010). To address this issue, we have investigated the Holocene sedimentation history of Lonar Lake from central India with special focus on palaeoclimate reconstruction.

Based on mineralogical, palynological, and biogeochemical investigations on the ca. 10 m long sediment core, the longest, well dated palaeo-climate archive from India's core monsoon

zone, Prasad et al. (2014) reconstructed the broad, Holocene climatic development of the Lonar Lake region, identified two millennial scale dry phases, and discussed the stability of the ISM – El Niño Southern Oscillation (ENSO) links and the influence of shifts in the position of the Indo Pacific Warm Pool (IPWP) on the prolonged droughts in ISM realm. Here we present stable carbon and nitrogen isotope data from Prasad et al. (2014) as well as new data from amino acid, sediment composition, and grain-size analysis and interpret them with respect to centennial scale, Holocene climate variability and its tele-connections with the North Atlantic climate.

Bond et al. (2001) hypothesised a connection between North Atlantic cooling events and cosmogenic nuclide production rates, the latter indicating small changes in solar output. Additionally, they found virtually synchronous “quasi-periodic” ~ 1500 year cyclicality in both their palaeorecord as well as in the nuclide production rates. Thus, they postulated a reaction of climate to small changes in solar output, which would not be limited to the North Atlantic region but which would affect the global climate system (Bond et al. 2001). Correlations between the high and mid latitude climate, as reconstructed from Greenland ice cores (Stuiver and Grootes 2000; Johnsen et al. 2001) and ice-rafted debris in North Atlantic deep sea records (Bond et al. 1997), and the low latitude tropical climate have been found in various climate reconstructions (Haug et al. 2001; Gupta et al. 2003; Hong et al. 2003; Dykoski et al. 2005; Wang et al. 2005; Fleitmann et al. 2007; Koutavas and Sachs 2008) supporting the assumption that different climate systems react to the same cause, like solar output variation, (Bond et al. 2001; Soon et al. 2014) either independently or via tele-connections. However, since many palaeoclimate investigations concerning the correlations between tropical climate and North Atlantic climate were carried out in peripheral ISM regions (Hong et al. 2003; Fleitmann et al. 2007), these records could not indicate if the change in moisture availability was exclusively linked to an alteration in monsoonal summer rainfall rather than to altered winter westerly precipitation. Lonar Lake is one of very few natural lakes located in the core

monsoon zone in central India, and it is fed exclusively by precipitation of the Indian summer monsoon and stream inflow that is closely linked to monsoon rainfall (Anoop et al. 2013b). Additionally, available precipitation data from the region close to Lonar Lake indicate a good correlation with the all Indian rainfall record of the last century (1901 – 2002). Correlation between the all Indian rainfall record (<ftp://www.tropmet.res.in/pub/data/rain/iitm-regionrf.txt>) and the annual precipitation data of the meteorological stations in Buldana, Jalna, Hingoli, and Washim (http://www.indiawaterportal.org/met_data/) varies between 0.62 and 0.69 ($p < 0.001$), making Lonar Lake a key site to investigate the connection between Indian monsoon strength and its connection to North Atlantic climate change.

4.2. Study site

Lonar Lake is a closed basin lake situated at the floor of a meteorite impact crater that formed during the Pleistocene ($\sim 570 \pm 47$ ka) on the Deccan Plateau basalts (Jourdan et al. 2011). The lake is located at Buldhana District in Maharashtra, central India at 19.98° N and 76.51° E (Figure 4.1). The meteorite crater has a diameter of ca. 1880 m, and the almost circular lake covers an area of about 1 km². The modern crater floor is located at ca. 470 m above sea level, which is around 140 m below the rim crest elevation. The inner rim wall is fairly steep with slopes of $15 - 18^\circ$ in the east and up to $\sim 30^\circ$ in the west and southwest (Basavaiah et al. 2014).

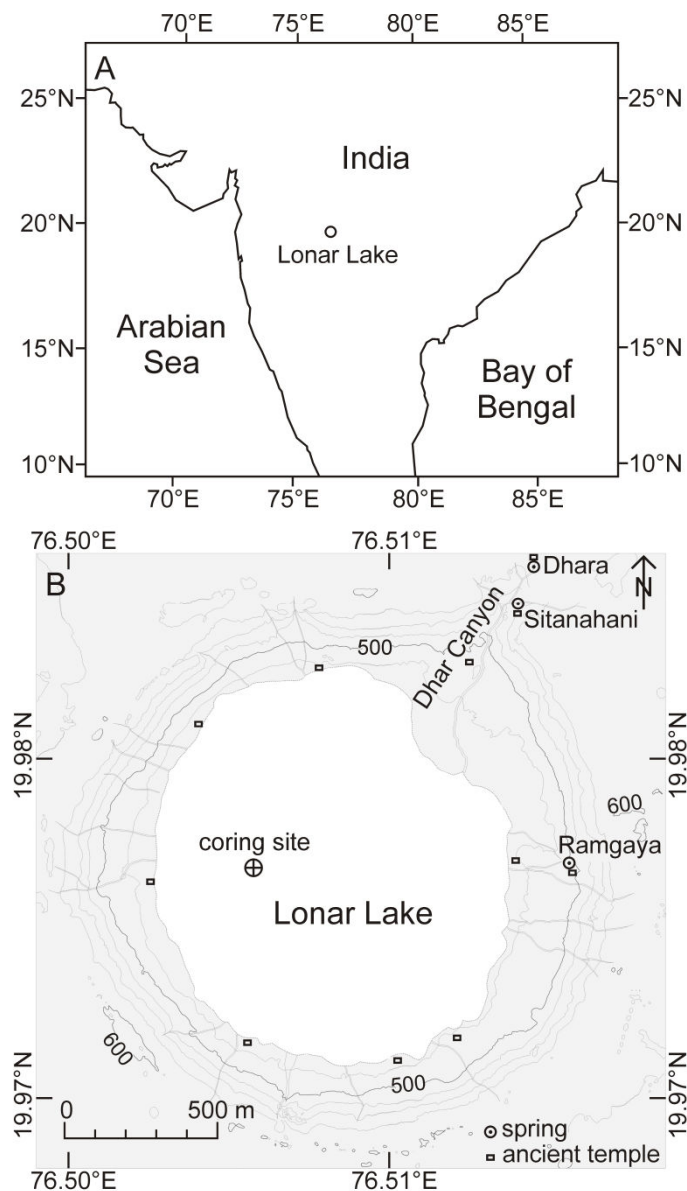


Figure 4.1: Regional overview and location of Lonar Lake (A). Study area showing the coring site (B).

Lonar Lake is located in the ‘core monsoon zone’ of the Indian summer monsoon (Gadgil 2003). The southwest monsoon from June to end of September is characterised by strong winds and brings in average rainfall of ~ 700 mm. Precipitation during December to April occurs only in rare cases. The temperature can exceed 40°C before the onset of the monsoon and declines during the monsoon phase to an average of approximately 27°C . The post monsoon from October to February is characterised by relatively low temperatures at an average of 23°C (http://indiawaterportal.org/met_data/). The lake is fed by surface runoff during the monsoon season and three perennial streams that are closely linked to monsoon

rainfall as indicated by tritium dating (Anoop et al. 2013b). Two of them, the Dhara stream and the Sitanahani stream are entering the crater from the northeast. They have formed the Dhara Canyon, an erosive incision, and have built up an alluvial fan into the lake. Today this fan is used for agricultural plantation. The Ramgaya stream, the third stream feeding the lake, springs from the inner crater wall and enters the lake from the eastern shore. Nowadays the three streams are diverted towards the Dhara fan to irrigate the agricultural fields. Water discharge is only conducted by evapotranspiration; no outflowing stream is present and no loss due to seepage occurs as the lake level is below the local groundwater level (Nandy and Deo 1961).

The modern lake is ca. 6 m deep, brackish, alkaline, and eutrophic with permanent bottom water anoxia (Basavaiah et al. 2014). The eutrophication promotes phytoplankton blooms especially during and subsequent to the monsoon when nutrients are washed into the lake. The algal assemblage is primarily made up of cyanophyceae (Badve et al. 1993). Thermophilic, halophilic, and alkalophilic bacteria in numbers of 10^2 to 10^4 viable cells/ml (Joshi et al. 2008) and methanogenic archaea (Surakasi et al. 2007) were reported from Lonar Lake. The lake lacks most zooplankton species and higher organisms. The zooplankton community within the lake consists of ciliates, culicid larvae, and rotifers (Mahajan 2005). Only few exemplars of the ostracod *Cypris subglobosa* and the gastropod *Lymnea acuminata* have been observed in the lake (Badve et al. 1993).

The vegetation of the inner crater walls changes from the upper part near the rim crest to the bottom part close to the lake shore. The upper part of the inner crater walls is covered by drought tolerant grass and thorn shrub species, further down grows teak (*Tectona grandis*) dominated dry deciduous forest, and the bottom part of the inner crater walls is overgrown by semi evergreen forests. The alluvial fan, which has formed due to riverine erosion in the northeast of the lake, is used for crop plantation and cattle grazing. The fan is characterised by vegetation cover of grasses, sedges, and crop plants like banana (*Musa x paradisiaca*), millet

(*Setaria italica*), corn (*Zea mays*), custard-apple (*Annona reticulata*), and papaya (*Carica papaya*) (Menzel et al. 2013).

4.3. Methods and material

4.3.1. Sampling

Two parallel ca. 10 m long cores were retrieved in May-June 2008 at 5.4 m water depth using a UWITEC sediment piston corer. The cores were opened in the laboratory; a composite core was constructed and sub-sampled in 0.5 cm resolution using L-channel sampling procedure. All samples despite those for grain-size analyses were freeze-dried and ground manually in an agate mortar.

4.3.2. Analytical methods

The total carbon (TC), total nitrogen (TN), and total organic carbon (TOC) contents and the $\delta^{15}\text{N}$ and $\delta^{13}\text{C}_{\text{org}}$ isotopic composition were determined using an elemental analyzer (NC2500 Carlo Erba) coupled with a ConFlowIII interface on a DELTAplusXL mass spectrometer (ThermoFischer Scientific). The isotopic composition is given in the delta (δ) notation indicating the difference, in per mil (‰), between the isotopic ratios of the sample relative to an international standard:

$$\delta (\text{‰}) = [(R_{\text{sample}} / R_{\text{standard}}) - 1] \times 1000 \quad (4.1)$$

The ratio and standard for carbon is $^{13}\text{C}/^{12}\text{C}$ and VPDB (Vienna Pee Dee Belemnite) and for nitrogen $^{15}\text{N}/^{14}\text{N}$ and air N_2 .

For TC, TN and $\delta^{15}\text{N}$ determination, around 20 mg of sample material were loaded in tin capsules and burned in the elemental analyzer. The TC and TN content were calibrated against acetanilide whereas for the nitrogen isotopic composition two ammonium sulphate standards (e.g. IAEA N-1 and N-2) were used. The results were proofed with an internal soil reference sample (Boden3). Replicate measurements resulted in a standard deviation better than 0.1 % for N and 0.2 ‰ for $\delta^{15}\text{N}$.

The TOC contents and $\delta^{13}\text{C}_{\text{org}}$ values were determined on *insitu* decalcified samples. Around 3 mg of sample material were weighted into Ag-capsules, dropped with 20 % HCl, heated for 3 h at 75 °C, and finally wrapped into the Ag-capsules and measured as described above. The calibration was performed using elemental (Urea) and certified isotopic standards (USGS24, IAEA CH-7) and proofed with an internal soil reference sample (Boden3). The reproducibility for replicate analyses is 0.1 % for TOC and 0.2 ‰ for $\delta^{13}\text{C}_{\text{org}}$.

Inorganic carbon (IC) was defined as the difference between TC and TOC. IC was converted to carbonate by multiplying with 8.33, since calcium carbonate was the only carbonate phase detected in the sediments despite three distinct zones of the core where gaylussite crystals were found (1.58 – 4.22 m, 6.42 – 7.60 m, 9.10 – 9.25 m). These crystals were handpicked under microscope prior to analyses. The percentage of lithogenic material in the sediments was calculated using the formula:

$$\text{Lith (\%)} = 100 \% - (\text{total organic matter [\%]} + \text{carbonate [\%]}) \quad (4.2)$$

Analyses of AA and HA were carried out on a Biochrom 30 Amino Acid Analyser according to the method described by Lahajnar et al. (2007). Briefly, after hydrolysis of the samples with 6 mol L⁻¹ HCl for 22h at 110°C under a pure argon atmosphere, HCl was removed from an aliquot by repeated evaporation using a vacuum rotating evaporator (Büchi 011) and subsequent dissolution of the residue in distilled water. After evaporating the aliquot three times, the residue was taken up in an acidic buffer (pH: 2.2) and injected into the

analyser. The individual monomers were separated with a cation exchange resin and detected fluorometrically according to the procedure described by Roth and Hampai (1973). Duplicate analysis of a standard solution according to this method results in a relative error of 0.1 to 1.3 % for the concentration of individual AA monomers. Duplicate measurement of a sediment sample revealed a relative error of < 1 % for AA and HA concentrations, < 10 % for molar contribution of low concentrated (< 1 mol%) AA monomers, and < 2.5 % for higher concentrated (> 1 mol%) AA monomers.

Grain-size distribution of the core samples was determined using a Malvern Mastersizer 2000 analyser. The pre-treatment of sediments included the wet-oxidizing of the organic matter and the chemical dissolution of carbonates at room temperature. Ca. 0.3 g freeze-dried sample aliquots were treated with 10 ml H₂O₂ (30%) which was added in two steps. The excess oxidising agent was removed by repeated washing with Millipore water (18.2 MΩcm), centrifugation (6000 rpm, 5min) and suction of the supernatant. The carbonates of the solid residues were dissolved by addition of 3.5 ml 1 M HCl over night. The solid residues were repeatedly washed (*see* above) and suspended in 20 ml Millipore water. The de-acidified samples were kept in an ultrasonic vibrator for 15 min. to disaggregate all grains. The instrument measured the grain-size of the suspended particles from 0.02 to 2000 μm for 100 grain-size classes. The content of coarse particles (> 200 μm) in the small aliquots exposed to measurement cannot be representative for the entire sample. Therefore, we re-calculated the volume-percentage for the grain-size fraction 0.02 to 200 μm.

4.3.3. Statistical method

To assess the interrelation of climatic changes in central India and the North Atlantic region as well as the concurrence of climate changes in central India and the solar output we have calculated the major frequencies in our climate proxy data as well as the correlation between the BCI and the ^{14}C production rate. Before the spectral analysis, the long term climate trend was removed from the whole time series by applying a Gaussian kernel based filter with a kernel bandwidth of 500 years. The spectral analysis is then performed as the Fourier transform of the auto-correlation function. Since the sampling of the time series is irregular, the auto-correlation estimation is also based on a Gaussian kernel (bandwidth of 0.5 years), allowing us to directly apply this method without preceding interpolation (Rehfeld et al. 2011; software NESToolbox for MATLAB used).

4.3.4. Chronology

The age model for the core is based on 19 AMS ^{14}C dated samples of wood, leaves, gaylussite crystals, and bulk organic matter (Table 4.1; Prasad et al. 2014). The oldest dated sample of the core shows an age of 11016 ± 161 cal a BP, suggesting that the core covers the complete Holocene sedimentation history of the Lonar Lake. The radiocarbon dating was carried out at Poznan radiocarbon laboratory, Poland. Since the catchment geology comprises carbonate free basaltic rocks of the Deccan Traps, no correction for hard water effect was conducted. However, the elevated salinity and pH in combination with stratification of the water body led to an ageing of the bulk organic matter samples (Prasad et al. 2014). Calibration of the ^{14}C dates was carried out using the program OxCal, interpolating with the INTCAL04 and NH3 calibration curves (Bronk Ramsey 2008).

Table 4.1: Radiocarbon ages from the Lonar Lake core; first published by Prasad et al. (2014). Calibration of the ^{14}C dates was carried out using the program OxCal, interpolating with the INTCAL04 and NH3 calibration curves (Bronk Ramsey 2008).

Lab No.	Material	Composite Depth (cm)	^{14}C date (2σ) (^{14}C yr BP)	Calendar age range (2σ) (cal yr BP)
Poz 44133	Bulk	0	116.79 ± 0.84	-55 – -59
Poz 44142	Wood	20	143.51 ± 0.0086	-16 – -28
Poz 44143	Bulk		107.88 ± 0.76	
Poz 27189	Wood	163.5	564 ± 60	669 – 505
Poz 41602	Bulk		760 ± 360	
Poz 41605	Gaylussite crystal	266	1105 ± 60	1076 – 944
Poz 27190	Wood	266.5	1105 ± 60	1079 – 947
Poz 41603	Bulk		1075 ± 60	
Poz 41604	Wood	267.5	1100 ± 60	1086 – 950
Poz 41607	Wood	383.5	1840 ± 70	1924 – 1624
Poz 27236	Wood	482	2315 ± 70	2696 – 2192
Poz 44141	Bulk	511.5	2680 ± 70	2944 – 2580
Poz 44226	Bulk	612	3470 ± 70	3867 – 3531
Poz 27237	Wood	778	4185 ± 70	4911 – 4583
Poz 27191	Wood	820	4600 ± 120	5479 – 4867
Poz 41611	Wood	870	7420 ± 80	8396 – 8096
Poz 27193	Wood	870.5	7460 ± 180	8412 – 8104
Poz 27194	Wood	872	7410 ± 200	8476 – 8100
Poz 27373	Wood	882.5	8880 ± 120	10197 – 9529
Poz 27253	Wood	899	8990 ± 160	10707 – 9867
Poz 27238	Leaf	902	9740 ± 100	11274 – 10670
Poz 27192	Wood	904	9570 ± 200	11338 – 10694

4.3.5. Mineralogical and biogeochemical proxies

Our reconstruction of the climatic history of the Lonar Lake region and its comparison to the North Atlantic region is mainly based on lithogenic contribution to the sediments, grain-size, atomic organic carbon to total nitrogen ratio (C/N), $\delta^{13}\text{C}_{\text{org}}$, $\delta^{15}\text{N}$, and amino acid derived indices. The C/N, $\delta^{13}\text{C}_{\text{org}}$, and $\delta^{15}\text{N}$ data were reported and interpreted with respect to climate variability and climatic tele-connections of the Lonar Lake region with the Pacific by Prasad et al. (2014). Additionally, the occurrence of evaporitic gaylussite crystals in the sediments, as

reported by Anoop et al. (2013b), was used for the climate reconstruction. The mechanisms driving the changes in the parameters are shortly summarised in the following sections.

4.3.5.1. Lithogenic contribution

The lithogenic contribution to lake sediments mostly depends on the erosion that takes place in the catchment area, transport energy, and shore line proximity (Koinig et al. 2003; Magny et al. 2012). The intensity of erosion at a lake, which is not affected by temperatures below the freezing point, is mostly driven by the amount of rainfall, the occurrence of heavy rainfall events, and the density of vegetation that prevents erosion (Kauppila and Salonen 1997; Anoop et al. 2013a). Human interferences like deforestation, agricultural land use, and construction activity must be considered as potential causes of enhanced erosion especially in the younger past (Wilmshurst 1997). Counterintuitive, phases of enhanced precipitation potentially triggering stronger erosion do not necessarily coincide with elevated lithogenic percentages in the lake sediments. This is due to the spreading of vegetation during climatically wet phases, but can also be controlled by changes in lake level. During wet phases, the lake level increases, which also increases the distance between a sampling site and the lake shore. Thus, high proportions of the eroded material from the catchment are deposited relatively close to the shore in shallow water and do not reach the deeper sampling site. These mechanisms seem to dominate at Lonar Lake, since time slices of the Lonar core that show strong evidence of dry climate coincide with high lithogenic contribution to the sediments.

Thus, the lithogenic contribution seems to be a good proxy for the climate reconstruction at Lonar Lake with high values indicating low lake level during drier climate and low values indicating high lake level during wetter climate.

4.3.5.2. Grain-size

The grain-size of lake sediments depends much on the source of the sediment load. But if the source of the sediments does not change, the grain-size can give information about changes in the hydrodynamics of inflowing streams, the amount of precipitation, the occurrence of heavy rainfall events, seasonality, shore line or sediment source (e.g., river mouth) proximity, changes in the internal hydrodynamics (e.g., currents), and external factors affecting the catchment erosion (McLaren and Bowles 1985; Sun et al. 2002; Peng et al. 2005). The sorting of the sediments can be used to reconstruct the transport distance and the rate of deposition.

The grain-size data are particularly useful for the broad, Holocene climate reconstruction at Lonar Lake since they depend on changes in monsoon strength. However, for the reconstruction of smaller scale climate variability, the resolution of grain-size data might not be high enough, especially in the lower part of the core, where sedimentation rates are low.

4.3.5.3. C/N

The C/N ratio is often used to determine the source of organic matter (OM) in lake and coastal sediments (Meyers 1997). Since aquatic OM is relatively enriched in nitrogen rich proteins, and vascular plant OM is relatively enriched in nitrogen depleted lignin and cellulose, the ratio of carbon to nitrogen is much lower in aquatic OM than in OM of terrestrial origin. C/N ratios of 4-10 indicate origin of aquatic OM source, whereas C/N ratios of >20 typically indicate dominant contribution of terrestrial plants (Meyers and Ishiwatari 1993). However, the use of C/N ratios as OM source indicator can be biased since C/N ratios can be altered during degradation. This can shift the C/N ratio to higher values if the degraded OM is enriched in labile nitrogen rich compounds like proteins, peptides, and free amino

acids, which are most abundant in planktonic OM. On the other hand, OM of terrestrial origin tends to become relatively depleted in carbon during degradation, since nitrogen deficient components like carbohydrates and lipids are preferentially decomposed (Meyers and Lallier-Vergès 1999). Nevertheless, these alterations are usually of minor magnitude, hence, the source information of the C/N ratio are mainly preserved.

At the modern Lonar Lake, soils show a tendency towards low C/N ratios (Menzel et al. 2013). This is related to the aforementioned preferential degradation of nitrogen depleted components in combination with the immobilization of re-mineralised nitrogen, which can be absorbed by clay minerals in the form of NH_4^+ (Sollins et al. 1984; Mengel 1996). This effect has strongest influence on sediments that show low TOC contents.

The C/N ratio does not provide much direct information for the climate reconstruction. It is particularly useful for determining the OM source, which is not much climate depending. During wet conditions, more terrestrial OM might be washed into the lake due to denser vegetation and stronger rainfall, but this could also cause more nutrient in-wash into the lake promoting the production of aquatic OM. Thus, the C/N ratio can not be used as a climate proxy but identifies changes in OM source and supports the interpretation of other palaeoclimate proxies that are affected by changes in OM source.

4.3.5.4. $\delta^{13}\text{C}_{\text{org}}$

$\delta^{13}\text{C}_{\text{org}}$ in lake sediments is influenced by the abundances of land plant OM and aquatic OM in the sediments. The $\delta^{13}\text{C}$ of terrestrial OM is mainly driven by the percentage of plants using the C_3 pathway and plants using the C_4 pathway of CO_2 assimilation. C_3 plants show $\delta^{13}\text{C}$ values of -23 to -35 ‰, whereas C_4 plants have $\delta^{13}\text{C}$ values of -10 to -16 ‰ (O'Leary 1988). C_3 plants are more abundant during wet conditions whereas C_4 plants usually spread during phases of dry climate (Tieszen et al. 1979).

$\delta^{13}\text{C}$ of the aquatic OM depend on the $\delta^{13}\text{C}$ of dissolved inorganic carbon (DIC) and on the concentration of $\text{CO}_2(\text{aq.})$ in the photic zone. Lower $p\text{CO}_2(\text{aq.})$ lead to reduced fractionation during CO_2 uptake by phytoplankton, and thus to ^{13}C enrichment in aquatic OM (Lehmann et al. 2004). The factors controlling the isotopic composition of DIC in Lonar Lake are (1) the aquatic productivity driven by nutrient supply to the lake, (2) redox conditions of surface sediments and lake water, determining the mechanisms and inorganic products of OM decomposition, (3) the pH of lake water, shifting the equilibrium of the three types of DIC ($\text{CO}_2(\text{aq.})$, HCO_3^- , and CO_3^{2-}), (4) the development and stability of lake stratification, affecting the exchange of DIC between the photic and aphotic zones, and (5) CO_2 degassing caused by lake level decline during climatically dry phases. Generally, factors enriching the DIC in ^{13}C are linked to eutrophication, dryer climate, and lake stratification. In highly productive lakes, ^{13}C deficient OM is transported into the sediments, leaving the DIC in the photic zone enriched in ^{13}C (Hodell and Schelske 1998). This effect can be expedited by strong lake stratification, hampering the convection of lake water, and thus the transport of ^{13}C depleted CO_2 , which is produced during OM degradation mostly in the aphotic zone, into the photic zone. Additionally, eutrophic conditions and lake stratification support the development of anoxia in deep waters. This causes the production of highly ^{13}C depleted methane during OM degradation, which can escape the lake system in gaseous state if it is not re-oxidized. Methanogenesis in anoxic sediments is accompanied by the release of ^{13}C enriched CO_2 at the expense of ^{13}C depleted methane. Thus, if methane is degassed from the lake water and not re-oxidised, anoxia leads to enriched $\delta^{13}\text{C}$ values of lake water DIC (Gu et al. 2004). In response to dryer climate, evaporation intensifies and the lake level lowers; this increases the salinity, and thus the alkalinity and pH of lake water. Under highly alkaline conditions, the equilibrium of the three types of DIC shifts towards HCO_3^- and CO_3^{2-} , which are enriched in ^{13}C compared to $\text{CO}_2(\text{aq.})$ (Zhang et al. 1995). Under these $\text{CO}_2(\text{aq.})$ depleted conditions, the growth of phytoplankton capable of using HCO_3^- as carbon source is promoted

producing ^{13}C enriched aquatic OM (Stuiver 1975). Additionally, exceeding evaporation can cause supersaturation of carbonate in the lake water, and consequently CO_2 degassing, which is accompanied by an increase in $\delta^{13}\text{C}$ of DIC (Lei et al. 2012).

Since $\delta^{13}\text{C}$ increases under dry conditions in both aquatic and terrestrial OM, it is a good climate proxy in our record. The only limitation is the influence of lake water anoxia, which more likely occurs in a deeper lake during wet conditions or as a consequence of eutrophication. The anoxia can cause a change in $\delta^{13}\text{C}$ of aquatic OM due to methane degassing or methane oxidation, factors that disappear in a shallow oxic lake.

4.3.5.5. $\delta^{15}\text{N}$

The introduction and cycling of nitrogen in lakes involves several dissolved inorganic nitrogen (DIN) species and transformation processes, associated with more or less strong isotopic fractionation. Thus, $\delta^{15}\text{N}$ of OM in lakes can exhibit highly diverse values, linked to several processes. Usually, plankton discriminates against ^{15}N during DIN uptake, with the exception of plankton that is capable of fixing molecular nitrogen (Talbot and Lærdal 2000). Hence, phases of intense phytoplankton blooms are associated with increased $\delta^{15}\text{N}$ values of DIN in the photic zone. Comparable to carbon uptake, low concentrations of DIN lead to reduced isotopic fractionation of plankton, amplifying the increase of $\delta^{15}\text{N}$ during phases of high aquatic productivity (Peterson and Fry 1987). However, the most important processes in determining the $\delta^{15}\text{N}$ values of DIN, and thus in $\delta^{15}\text{N}$ of aquatic OM are the conversion processes of the different DIN species. The most prominent processes are nitrification, denitrification, and ammonia volatilization, which are associated with strong fractionation factors. Nitrification occurs under oxic conditions and results in ^{15}N depleted nitrate and ^{15}N enriched ammonium, whereas denitrification, occurring under anoxic conditions, leads to ^{15}N enrichment of nitrate at the expense of ^{15}N depleted molecular nitrogen. The strongest

fractionating process most probably affecting the DIN pool of Lonar Lake is ammonia volatilization. This process becomes important in aquatic environments showing high pH values (>9). Under these conditions, the equilibrium between ammonium and ammonia shifts towards ammonia, which is significantly depleted in ^{15}N compared to ammonium (20-35 ‰) and can escape the water column in gaseous state (Casciotti et al. 2011). Thus, ammonia volatilization leads to increasing $\delta^{15}\text{N}$ values of the remaining DIN in lake water.

Even though terrestrial OM does not contribute as much to the $\delta^{15}\text{N}$ variability in lake sediments as to $\delta^{13}\text{C}_{\text{org}}$ due to the fact that terrestrial OM has much lower nitrogen contents than aquatic OM, changes in $\delta^{15}\text{N}$ during phases of low aquatic productivity and high terrestrial OM contribution to the sediments can indicate shifts in the vascular plant and soil nitrogen isotopic composition. In general, $\delta^{15}\text{N}$ of soil and terrestrial plant OM increase with increasing temperature and decreasing precipitation (Amundson et al. 2003).

The use of $\delta^{15}\text{N}$ as a proxy for climate reconstruction at Lonar Lake is limited since $\delta^{15}\text{N}$ values of aquatic OM depend on the redox conditions of lake water with high values occurring under anoxic conditions but also increasing due to high pH. And whereas anoxic water is more likely accompanying high lake levels during wet conditions, the pH increases during dry conditions when ions become concentrated in the shrinking water body. Additionally, terrestrial OM shows a wide range of $\delta^{15}\text{N}$ values due to different nitrogen uptake mechanisms, making it difficult to interpret in terms of climate variability.

4.3.5.6. Amino acids

The monomeric distribution of the amino acids is commonly used to determine the state of OM degradation in sediments. For the assessment of the OM degradation state, we have calculated the Lonar degradation index (LI), which was first calculated for modern Lonar Lake sediments on the basis of the molar percentages of 19 amino acids (Menzel et al. 2013). The LI compares the amino acid assemblage of the core samples with the data set of Menzel et al. (2013), which includes fresh OM like plankton and vascular plants, moderately degraded sediment trap and surface sediment samples, and highly degraded soil samples from Lonar Lake and its catchment. The calculation of the LI follows the approach of the degradation index (DI) calculation developed by Dauwe and Middelburg (1998) and Dauwe et al. (1999):

$$LI = \sum_i \left[\frac{\text{var}_i - \text{AVGvar}_i}{\text{STDvar}_i} \right] \times \text{fac.coef}_i \quad (4.3)$$

Where var_i is the original mole percentage of each amino acid in the sample, AVGvar_i and STDvar_i are the arithmetic average and the standard deviation and fac.coef_i the factor coefficient of the first axis of a principle component analysis (PCA) of the individual amino acids in the data set of Menzel et al. (2013). Negative values indicate less degraded and positive values more degraded state of the OM compared to the average of the reference data set.

The second amino acids derived proxy we used is a ratio of individual amino acids that are relatively enriched during aerobic degradation and amino acids that are relatively enriched during anaerobic degradation, named Ox/Anox:

$$\text{Ox/Anox} = \frac{\text{Asp} + \text{Glu} + \beta\text{-Ala} + \gamma\text{-Aba} + \text{Lys}}{\text{Ser} + \text{Met} + \text{Ile} + \text{Leu} + \text{Tyr} + \text{Phe}} \quad (4.4)$$

This ratio has been applied to the modern Lonar Lake sediments (Menzel et al. 2013) to evaluate the redox conditions during OM degradation and is based on a study of Cowie et al. (1995).

The amino acid derived indices seem to be good proxies for climate reconstruction as they can be used to identify phases of aerobic degradation within the sediments. Especially during wet phases that induce a deep anoxic lake, elevated values of these indices identify relatively short term, dry anomalies. Highest values are most probably related to subaerial degradation, and thus to phases of lake desiccation. In rare cases, the indices could be biased by input of eroded soils, which would cause elevated values. In addition, eutrophication causes low LI and Ox/Anox values due to strong aquatic production and the consequent development of lake water anoxia.

4.4. Results and discussion

The results of our investigation of the biogeochemical and lithological properties of the Holocene sediments from Lonar Lake are shown in Figure 4.2. The percentages of the different grain-size classes indicate sediments dominated by clayey silt with few exceptions showing sandy silt (Figure 4.3). The sandy silt samples are from 863 – 900 cm depth (10.5 – 7.8 cal ka BP). Based on the changes in biogeochemical properties, lithology, and sedimentation rate, Prasad et al. (2014) have identified the large scale climate development over the whole Holocene as well as two phases of prolonged drought. Here we present several shorter phases of climate changes superimposed on the large scale trend. The identified phases of drier and wetter climate can be correlated with other Asian palaeomonsoon records and palaeoclimate records from the North Atlantic region. A detailed description is given below (chapter 4.4.2) after a summary of the large scale climate development with additional remarks regarding the grain-size and amino acid data.

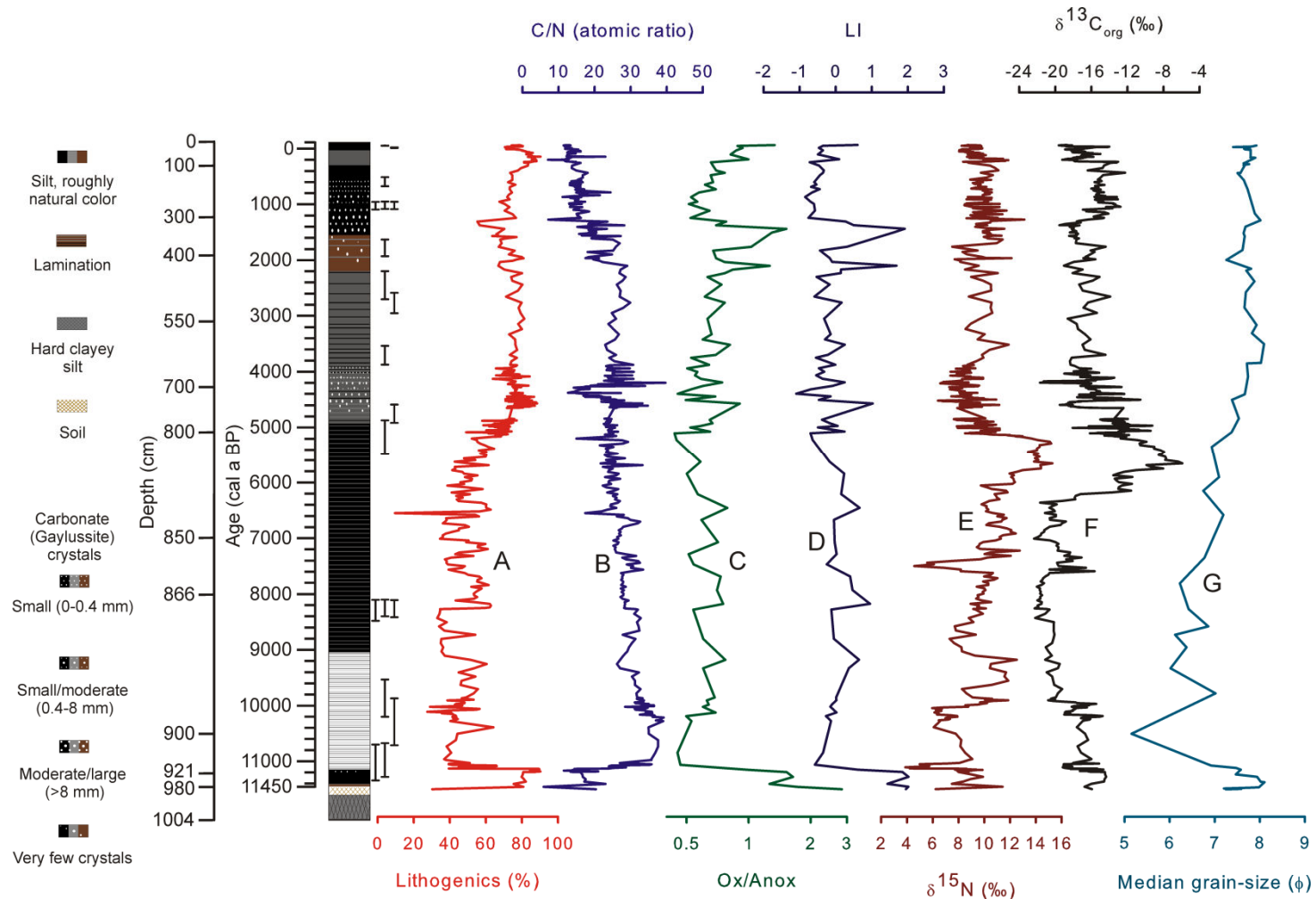


Figure 4.2: Summary of the analytical results. Schematic lithology of the Lonar Lake core and down-core variation in lithogenic contribution (A), C/N ratio (B), amino acid derived indices Ox/Anox (C) and LI (D), stable nitrogen (E) and carbon (F) isotopic ratios of bulk organic matter, and median grain-size (G). C/N, $\delta^{13}\text{C}$, and $\delta^{15}\text{N}$ were reported by Prasad et al. (2014); gaylussite crystal occurrence was reported by Anoop et al. (2013b). Error bars indicate the standard deviation range (2σ) of calibrated radiocarbon dates.

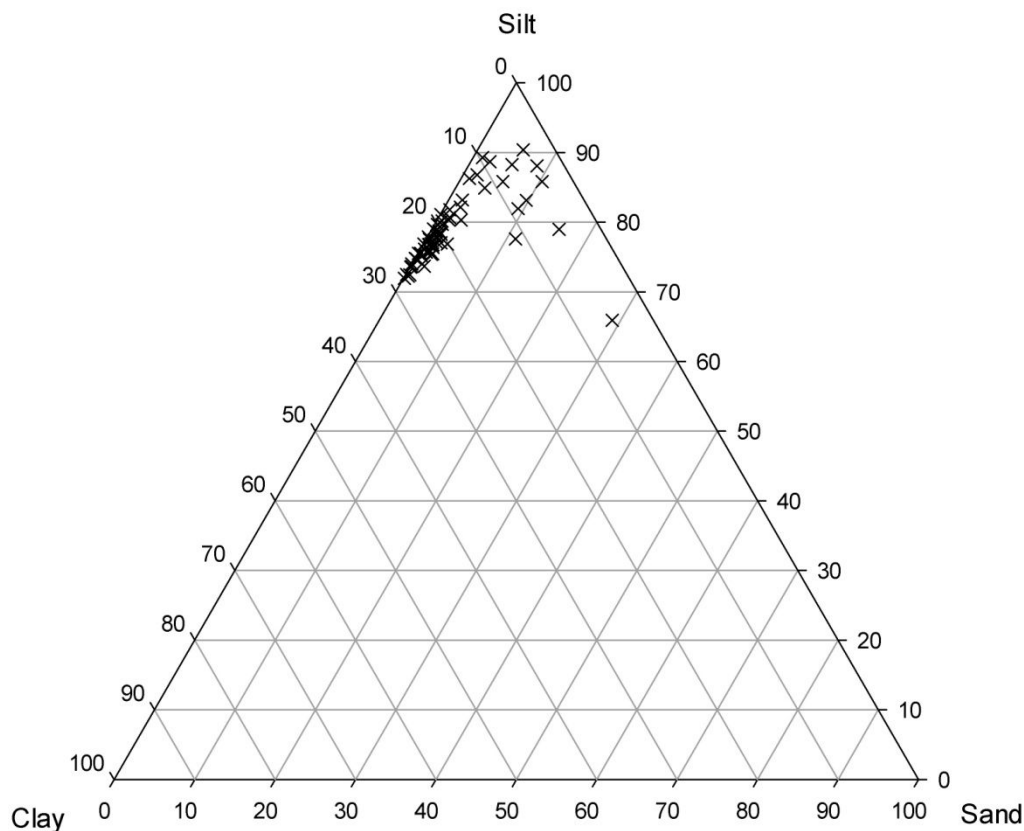


Figure 4.3: Ternary diagram showing the percentages of the different grain-size classes (clay, silt, sand) of the analysed sediment samples of the Lonar Lake core.

4.4.1. Large scale Holocene climate transition

The general long term palaeoclimate trend at the climatically sensitive Lonar Lake reconstructed by Prasad et al. (2014) starts with a drying period that probably coincides with the Younger Dryas at ~ 11.4 cal ka BP, which marks a dry period prior to the beginning of the Holocene in many geological records of India and adjacent regions (Overpeck et al. 1996; Bar-Matthews et al. 1997; Wei and Gasse 1999; Gasse 2000; Wang et al. 2001; Morrill et al. 2003; Sharma et al. 2004; Dykoski et al. 2005; Demske et al. 2009). Median grain-size of this section is low indicating low energy transport, which is probably due to dry conditions with reduced sediment input by run-off and precipitation fed streams and enhanced aeolian

deposition. High LI values indicate strongly degraded OM in these sediments, and the high Ox/Anox ratios point to subaerial decomposition of the OM. Thus, the bottommost sediment section most likely represents a palaeosol.

The beginning of the Holocene is marked by a transition from dry to wet climate with an abrupt increase in monsoon strength after ~11.4 cal ka BP (Prasad et al. 2014). The phase of monsoon onset and strengthening is reflected in the sediments by high lithogenic input, which was eroded from the sparsely vegetated crater walls and transported to the dried out lake bed. The values of the biogeochemical parameters and the grain-sizes are comparable to those of the underlying soil, and thus indicate high contribution of eroded soil material to the sediments. On top of this section, few gaylussite crystals can be found, denoting a drier phase at ~ 11.1 cal ka BP.

Subsequently, the early Holocene between 11.1 and 6.2 cal ka BP is characterised by wet conditions (Figure 4.4). The sediments of this section show low lithogenic contribution, and consequently low sedimentation rates. Thus, the section represents a deep lake with less eroded material reaching the sampling site. A deep lake developed quickly after 11.1 cal ka BP as is obvious from seasonally laminated sediments (Prasad et al. 2014). The median grain-size values indicate a shift to medium silt, and thus to slightly coarser material. This might be due to higher energy transport during strong rainfall events. The aquatic productivity was low during this phase, as shown by the high C/N ratios (mean: 30.1), which denote dominant contribution of terrestrial OM. Since 9.9 cal ka BP the $\delta^{13}\text{C}_{\text{org}}$ values stabilised on a relatively low level (mean: -20.9‰) indicating a C_3 dominated vegetation in the catchment of the lake. The predominantly low LI and Ox/Anox values of the section and the increasing $\delta^{15}\text{N}$ values between 9.1 and 6.2 cal ka BP point to extended anoxia in the water column and the sediments.

The time slice between 6.2 and 3.9 cal ka BP is regarded as being a transitional phase between wet climate during the early Holocene and dry climate during the late Holocene. This

time slice shows two drying phases accompanied by strong water body reduction between 6.2 and 5.2 cal ka BP and between 4.6 and 3.9 cal ka BP, respectively. The former drying phase is most obvious from high $\delta^{13}\text{C}_{\text{org}}$ and $\delta^{15}\text{N}$ values, whereas the latter shows elevated lithogenic contribution and gaylussite crystal precipitation (Figure 4.4), which indicates strongest lake level decline.

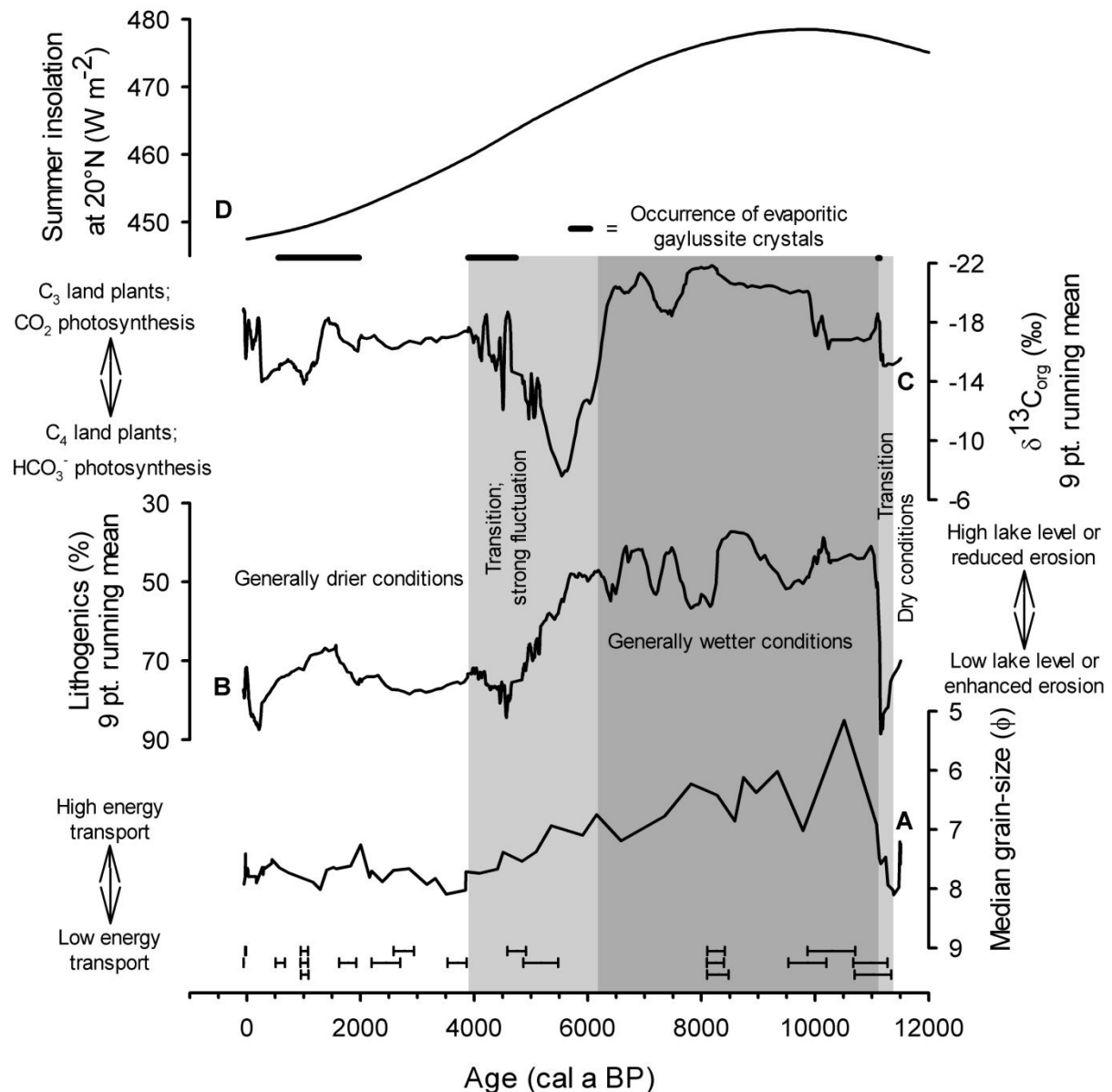


Figure 4.4: Long term Holocene climate trend at Lonar Lake as interpreted from our data. Comparison of median grain-size (A), lithogenic contribution (B), $\delta^{13}\text{C}$ values (C) (Prasad et al. 2014), and summer (JJA) insolation at 20°N (D) (Berger and Loutre 1991). Error bars indicate the standard deviation range (2σ) of calibrated radiocarbon dates.

Following the climate transition between 6.2 and 3.9 cal ka BP, evidence of relatively dry climate persists until today. Elevated $\delta^{13}\text{C}_{\text{org}}$ values, lithogenic contribution, Ox/Anox ratios, and finer median grain-sizes indicate drier conditions compared to the early Holocene. The lithogenic contribution and the Ox/Anox ratios denote a shallow lake, and the $\delta^{13}\text{C}_{\text{org}}$ values imply a dominance of C_4 catchment vegetation. The grain-size data indicate weaker monsoon rains causing lower transport energy. Additionally, the alluvial fan in the northeast of the lake might have been exposed due to the lower lake level, possibly reducing the velocity of the streams that enter the lake from the northeast and east. Probably, this effect has also reduced the distance between the sampling site and the source of fine sediment (alluvial fan/stream mouth) causing a shift to finer grain-sizes and increasing the sedimentation rate. A phase of exceedingly dry conditions is indicated by the reoccurrence of evaporitic gaylussite crystals between 2.0 and 0.6 cal ka BP (Anoop et al. 2013b; Prasad et al. 2014). The climate information of the younger part of the core might be mirrored to some extent due to anthropogenic interferences, as for example eutrophication and deforestation. A persistent decrease in C/N ratio since 1.3 cal ka BP indicates permanently elevated nutrient supply to the lake, which cannot be observed in the older parts of the core. Thus, a natural source of these additional nutrients seems unlikely. Since ca. 0.8 cal ka BP strong anthropogenic interference is evident from several near shore temples that have been built during the Yadavan rule approximately in the 12th century (Malu et al. 2005).

In general, the impact of long term Holocene climate change on palaeolimnology becomes notably obvious from the $\delta^{13}\text{C}_{\text{org}}$, lithogenic contribution, and grain-size values in our record and quite well delineates the insolation curve since the end of the Younger Dryas (Figure 4.4), which additionally seems to drive the position of the summer Inter-Tropical Convergence Zone (ITCZ), and thus the strength and northwards extent of the summer monsoon rainfall (Fleitmann et al. 2007). One point that might be questioned is the characteristic of the climate deterioration at 6.2 cal ka BP, which is reflected in the Lonar Lake record by a sharp increase

in $\delta^{13}\text{C}_{\text{org}}$, and thus points to an abrupt change, which was also reported from other records (Morrill et al. 2003). Nevertheless, we believe that this abrupt change is related to short term climate variability and that the sudden increase in $\delta^{13}\text{C}_{\text{org}}$ at 6.2 cal ka BP most likely represents the transgression of a threshold in annual precipitation that led to the decline in terrestrial C_3 plant vegetation and the increase in C_4 plant contribution. Also, the changes in lake level as displayed by the lithogenic content in the sediments show a relatively smooth transition from a deep to a shallow lake. Additionally, the relatively short term of the interval of drying between 6.2 and 3.9 cal ka BP is obvious from the subsequent change to wetter conditions indicated by subaquatic sedimentation and the disappearance of the gaylussite minerals. Thus, the transition from generally wet to drier climate after the Holocene climate optimum seems to occur gradually, and abrupt changes in the biogeochemical parameters are due to relatively short-term climate anomalies as postulated by Fleitmann et al. (2007) and reported from several regions (Hodell et al. 1999; Gupta et al. 2003; Hong et al. 2003; Gupta et al. 2005; Demske et al. 2009; Wünnemann et al. 2010).

4.4.2. Centennial scale Holocene climate variability

Beside the large scale millennial climate trend, several smaller centennial scale climate variations can be reconstructed from the Lonar Lake bioclastic record. While the role of ENSO and shifts in the position of the Indo Pacific Warm Pool (IPWP) in causing the prolonged droughts during 4.6 – 3.9 and 2.0 – 0.6 cal ka have been discussed by Prasad et al. (2014), the short term climate variability identified in our new dataset cannot be explained by the same mechanism necessitating the search for alternative causal mechanisms. Several studies have identified links between Asian monsoon and North Atlantic palaeoclimate with cold events in the North Atlantic region, as identified by ice-rafted debris in deep sea cores (Bond et al. 1997; Bond et al. 2001), being linked to decreases in monsoon strength over Asia

(Gupta et al. 2003; Hong et al. 2003; Dykoski et al. 2005; Wang et al. 2005; Fleitmann et al. 2007). Nearly all Bond events are isochronally reflected by indications of short term changes in monsoon strength in the proxies from Lonar Lake sediment core (Figure 4.5).

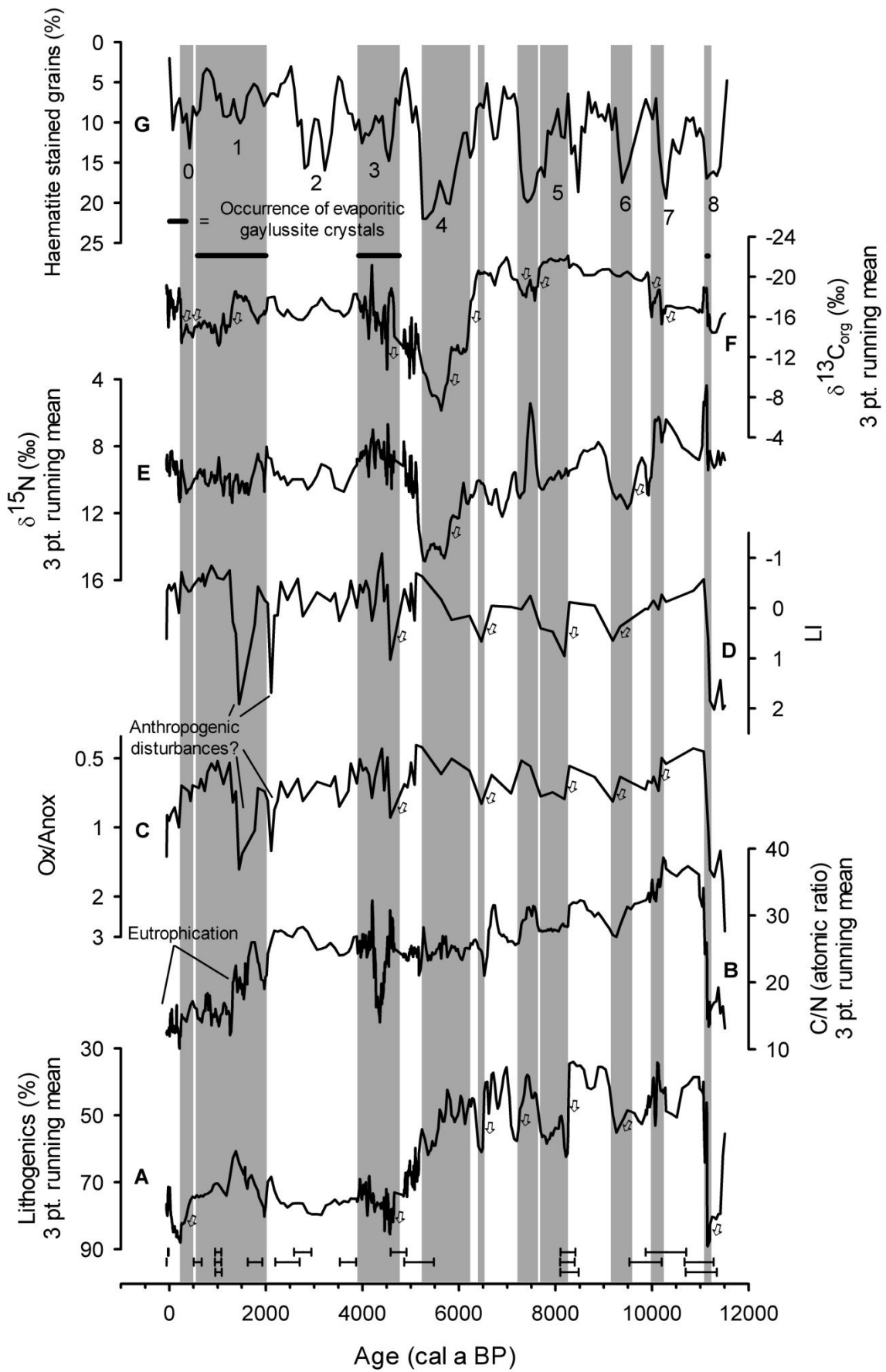


Figure 4.5: Comparison of our data of lithogenic contribution (A), C/N ratio (B), Ox/Anox ratio (C), LI (D), $\delta^{15}\text{N}$ (E), and $\delta^{13}\text{C}$ (F) to the percentage of haematite stained grains (G) in core MC52, a climate record from the North Atlantic region (Bond et al. 2001). C/N, $\delta^{13}\text{C}$, and $\delta^{15}\text{N}$ were reported by Prasad et al. (2014); gaylussite crystal occurrence was reported by Anoop et al. (2013b). Numbers 0 – 8 designate cold events in the North Atlantic region (Bond events). Small arrows denote increases in climate sensitive proxies that are interpreted to indicate phases of climate deterioration at Lonar Lake (grey shaded intervals). Error bars indicate the standard deviation range (2σ) of calibrated radiocarbon dates.

Since the centennial scale climate variations at Lonar Lake are reflected in different proxies and not all proxies show every phase of climate change, we calculated a Bioclastic Climate Index (BCI) that combines the Holocene course of the independent and climatically sensitive $\delta^{13}\text{C}_{\text{org}}$, lithogenic contribution, and combined amino acid proxy values. Since the variations in $\delta^{15}\text{N}$ and C/N values within the Lonar Lake record seem not to be predominantly driven by climate change or at least are considerably biased by other processes (*see* chapters 4.3.5.3 and 4.3.5.5), we did not include them into the BCI calculation. The BCI shows the deviation from the mean values given in percent of the maximum variation of the respective proxy in the data set according to the formula:

$$\text{BCI} (\%) = \frac{\Delta^{13}\text{C}_{\text{org}} (\%) + \Delta\text{lith} (\%) + 0.5 \times [\Delta\text{LI} (\%) + \Delta\text{Ox/Anox} (\%)]}{3} \quad (4.5)$$

High values indicate drier and low values indicate wetter conditions. We used half of the sum of the LI and Ox/Anox values to not overstate the variability in amino acid data as both values are calculated from the same data set, and thus are not fully independent. Further, linearly interpolated values for the amino acid derived proxies were used as these proxies were measured in a lower resolution than $\delta^{13}\text{C}_{\text{org}}$ and lithogenic contribution. Since the BCI also shows the long term palaeoclimate trend, a detrended curve was calculated to emphasize the centennial scale palaeoclimate variations (Figure 4.6). In addition to the BCI, the occurrence of evaporitic gaylussite crystals (Anoop et al. 2013b) was used to interpret the climatic changes at Lonar Lake since the gaylussite crystals exclusively indicate changes in Lonar Lake hydrology related to reduced available effective moisture.

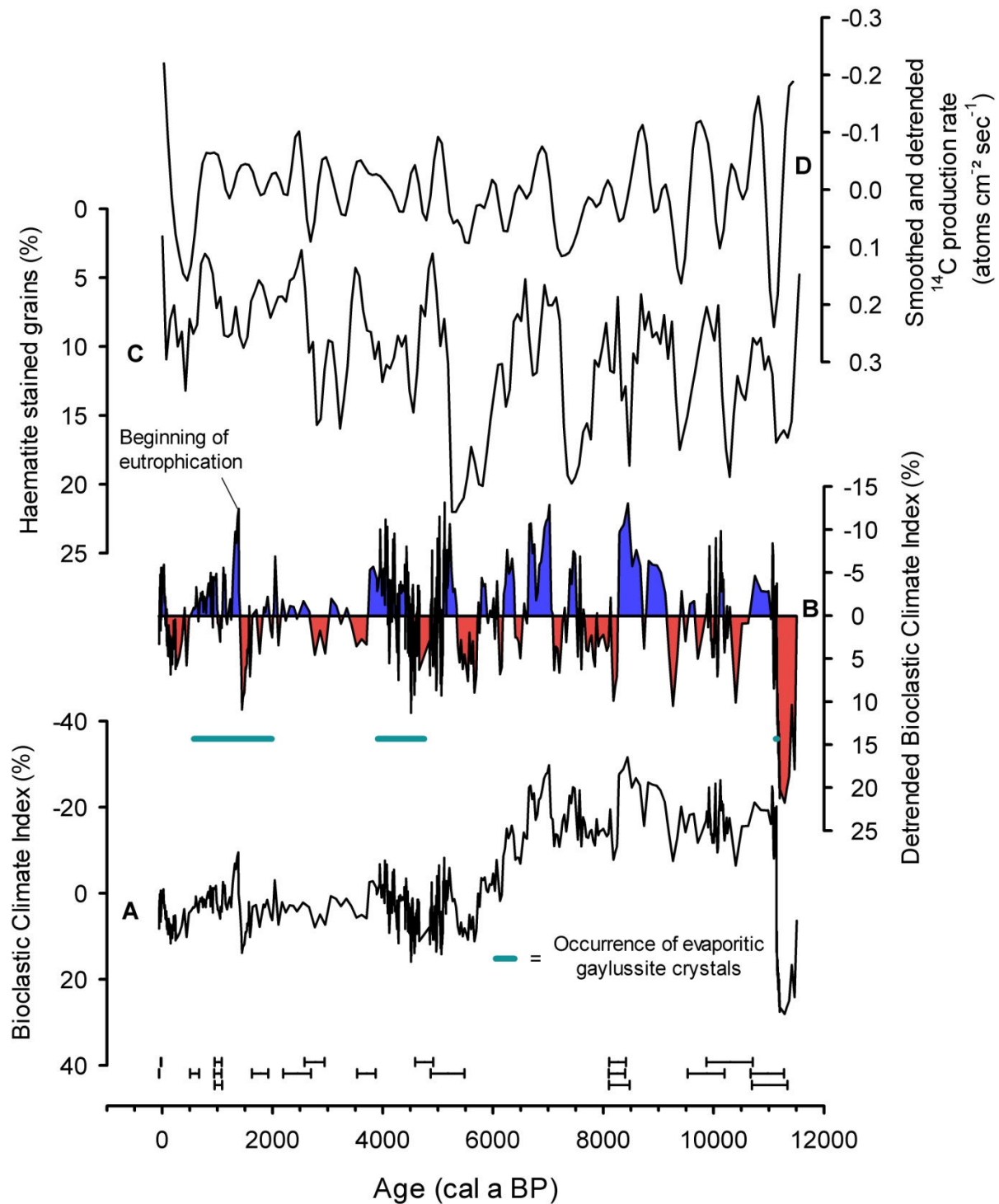


Figure 4.6: Comparison between the Bioclastic Climate Index (BCI) (A), the detrended BCI (B), the climate record from the North Atlantic Region (C), and the detrended and smoothed ^{14}C production rate (D) (Bond et al. 2001). Detrending of the BCI was performed by applying a Gaussian kernel based filter with a kernel bandwidth of 500 years to the values of the time slice <11.14 cal ka BP. The values of the time slice ≥ 11.14 cal ka BP were adjusted by subtracting the lowest value of this time slice from the data since a rapid shift in BCI values at 11.14 cal ka BP occurs. Red and blue colour fills indicate relatively dry and wet phases, respectively. Lines between the BCI and the haematite stained grains plots denote some approximately contemporaneous climate shifts in both records that are interpreted to be linked. Error bars indicate the standard deviation range (2σ) of calibrated radiocarbon dates.

Largely, the changes in the de-trended BCI are coincident with the intervals of increased ice rafted debris in the north Atlantic (Bond et al. 2001). The oldest of the Holocene cooling events in the North Atlantic region, the Bond event 8, can be correlated with the occurrence of gaylussite crystals in the Lonar Lake core on top of the section that represents the phase of climate transition and monsoon onset after the soil formation (Figure 4.5). The Bond event 7 is concurrently correlated to a double-peaked increase in $\delta^{13}\text{C}_{\text{org}}$ and to an increase in lithogenic contribution. The $\delta^{13}\text{C}_{\text{org}}$ increases are interpreted as changes in terrestrial vegetation to more C_4 plant abundance, indicating drier conditions. The subsequent decrease in $\delta^{13}\text{C}_{\text{org}}$ denotes the transition to C_3 plant domination, and thus wetter conditions during the early Holocene. A concurrent climate variation to Bond event 6 is indicated by elevated LI and Ox/Anox values as well as high $\delta^{15}\text{N}$ values (Figure 4.5). The amino acid based indices reveal an increase in oxygen supply to the sediments at 9.15 cal ka BP, and the pollen record points to a dry phase, during which the whole sediment section of this subunit became exposed to oxic or even subaerial conditions, since only few pollen that are resistant to aerobic decomposition are preserved in the sediments older than 9.2 cal ka BP (Riedel and Stebich in preparation). Enhanced oxygen supply could also be responsible for the elevated $\delta^{15}\text{N}$ values, since an increase in $\delta^{15}\text{N}$ during aerobic degradation was reported from in vitro (Lehmann et al. 2002) as well as from in vivo (Freudenthal et al. 2001) investigations. A drying trend in the Asian tropical region during this so called 9.2 ka event was reported before and also related to a cooling trend in the North Atlantic region (Dykoski et al. 2005; Fleitmann et al. 2008). Elevated LI, Ox/Anox, and lithogenic contribution values in the Lonar Lake core comparable to the values at 9.2 cal ka BP can be found during 8.2 – 7.7 cal ka BP (Figure 4.5). This phase correlates within dating uncertainties with a cool phase in the North Atlantic situated at the early stage of Bond event 5. The relatively short cool phase during the early stage of Bond event 5 is also known as the 8.2 ka event. Similarly to the 9.2 ka event, a cooling trend in the North Atlantic region was accompanied by a drying trend in monsoon

influenced Asia (Alley et al. 1997; Wang et al. 2005). It is widely accepted that the cooling during the 8.2 ka event was caused by a pulse of freshwater that burst out of the Lakes Agassiz and Ojibway through the Hudson Strait, which weakened the thermohaline Atlantic meridional overturning circulation, thus leading to the climate anomaly (Barber et al. 1999; Teller et al. 2002; Kendall et al. 2008). The peak at the later stage of Bond event 5 is correlated with elevated $\delta^{13}\text{C}_{\text{org}}$ values and an increase in lithogenic contribution (Figure 4.5). Elevated LI, Ox/Anox, and lithogenic contribution at 6.45 cal ka BP correlates within dating uncertainties with a cool phase at the beginning of Bond event 4. The following intensification of the North Atlantic cold spell (Bond event 4) and the Bond event 3 are reflected by the most obvious centennial scale climate changes shown by our data. These two phases constitute the climate transition from generally wet to generally drier conditions during the mid Holocene (*see* chapter 4.4.1) at 6.2 – 5.2 cal ka BP and 4.6 – 3.9 cal ka BP, respectively, which is consistent with the reports of southward migration of the ITCZ, monsoon weakening, and related drying trends from various locations of the Asian monsoon realm (Enzel et al. 1999; Morrill et al. 2003; Parker et al. 2004; Prasad and Enzel 2006; Staubwasser and Weiss 2006; Fleitmann et al. 2007; Demske et al. 2009; V. Prasad et al. 2014). The older phase, concordant with Bond event 4, is characterised by a strong increase in $\delta^{13}\text{C}_{\text{org}}$ with two sudden shifts, the first by $\sim 8\text{‰}$ at about 6.2 cal ka BP and the second by $\sim 4\text{‰}$ at about 5.7 cal ka BP. The second shift in $\delta^{13}\text{C}_{\text{org}}$ is accompanied by an increase in $\delta^{15}\text{N}$ of $\sim 2\text{‰}$. The increase in $\delta^{13}\text{C}_{\text{org}}$ is most likely linked to two major factors. A shift in terrestrial vegetation from C_3 dominance to more C_4 contribution seems to explain the increase in $\delta^{13}\text{C}_{\text{org}}$ at 6.2 cal ka BP since S. Sarkar (in preparation) found an increase in $\delta^{13}\text{C}$ of long chain n-alkanes. The second increase in $\delta^{13}\text{C}_{\text{org}}$ at 5.8 cal ka BP results in $\delta^{13}\text{C}_{\text{org}}$ values that even exceed the values of C_4 land plants, and thus the second shift cannot be explained by a further change in the terrestrial fraction of the OM alone. Hence, the elevated $\delta^{13}\text{C}_{\text{org}}$ values seem to be related to a change in the aquatic system. A reasonable explanation

is an increase in pH, as a result of increased salt concentration in the water during lake level decline in response to relatively dry conditions, and a related shift in the dominant photosynthetic inorganic carbon source from CO_2 to HCO_3^- (Prasad et al. 2014). The assumption that elevated pH is responsible for the $\delta^{13}\text{C}_{\text{org}}$ increase is corroborated by the concurrent increase in $\delta^{15}\text{N}$. In anoxic waters, which most probably were present during the related time as indicated by the low Ox/Anox ratios, high pH causes ammonia volatilization that leads to a $\delta^{15}\text{N}$ increase of aquatic OM (Casciotti et al. 2011). After 5.2 cal ka BP, the $\delta^{13}\text{C}_{\text{org}}$ and $\delta^{15}\text{N}$ values gradually decrease, which could indicate a slightly wetter period from 5.2 – 4.6 cal ka BP but which could also be due to the disappearance of the anoxic water layer as a response to further lake level decline. Subsequently, the dry phase between 4.6 and 3.9 cal ka BP, which has been correlated with an expansion of the IPWP (Prasad et al. 2014) but also partly correlates with Bond event 3, does not show as elevated $\delta^{13}\text{C}_{\text{org}}$ and $\delta^{15}\text{N}$ values as the previous dry episode. This seems to be related to the disappearance of the anoxic water layer, and hence the lack of ammonia volatilization, producing ^{15}N enriched ammonium, and the lack of methanogenesis, producing ^{13}C enriched CO_2 . The strongest indications for dry climate during this period are the occurrence of evaporitic gaylussite crystals throughout this zone (Anoop et al. 2013b) and the elevated lithogenic content in the sediments indicating low lake level. However, the decreased $\delta^{13}\text{C}_{\text{org}}$ values are responsible for the lower BCI values during this time slice even though the occurrence of gaylussite crystals indicates drier conditions compared to the time slice 6.2 – 5.2 cal ka BP (Figure 4.6). Subsequently, the only Bond event that does not show a marked complement in the Lonar Lake record is Bond event 2 between ca. 3.5 and 2.7 cal ka BP. This might be due to the fact that generally drier conditions had been established after the very dry period correlated with Bond events 4 and 3. Thus, the wetter period during ca. 3.9 – 3.5 cal ka BP did not provide enough excess in precipitation over evaporation to establish a high lake level with strong anoxic hypolimnion and vegetation dominated by C_3 plants. Hence, if the period between 3.5 and 2.7 cal ka BP

was drier at Lonar Lake compared to the period 3.9 – 3.5 cal ka BP, no significant changes in our proxies could be expected as long as the lake does not desiccate. Nevertheless, two minor positive shifts in $\delta^{13}\text{C}_{\text{org}}$ and contemporaneous increases in the amino acid derived indices result in two BCI peaks that possibly indicate drier conditions at Lonar Lake corresponding to the double-peaked North Atlantic cooling event during Bond event 2 (Figure 4.6). The following period of strong evidence of climate deterioration at Lonar Lake is again marked by evaporitic gaylussite crystals and was dated at an age of 2.0 – 0.6 cal a BP (Anoop et al. 2013b; Prasad et al. 2014). Thus, it can be correlated with Bond event 1 but exceeds the time span of the Bond event by about 500 years, which is in accordance with the report of decadal scale famines in India during the 14th and 15th century (Sinha et al. 2007). However, this strong drying event is also coincident with an increase in ENSO like conditions (Moy et al. 2002; Rein et al. 2005) in the Pacific (Prasad et al. 2014) suggesting complex links to the North Atlantic and to the Pacific forcings. The dry climate of this period, as indicated by the gaylussite precipitation, is not well reflected in the BCI. This is due to the eutrophication, which causes the development of lake water anoxia and a related descent of the amino acid derived proxy values. The BCI indicates an abrupt transition to wet climate at 1.3 cal ka BP (Figure 4.6), which is due to the biased amino acid indices. Thus, the BCI values during the phase of strongest anoxia between 1.3 and 0.3 cal ka BP, as indicated by the Ox/Anox ratio, are shifted to lower values, hence indicating wetter climate than actually prevailed. Finally, Bond event 0 is concurrently correlated to increased $\delta^{13}\text{C}_{\text{org}}$ and lithogenic contribution values between 440 and 240 cal a BP (Figure 4.5). Again, anthropogenic interference cannot be ruled out here in the younger part of the core. But, since the two-step increase in $\delta^{13}\text{C}_{\text{org}}$ at 440 and 260 – 245 cal a BP and the subsequent decrease in $\delta^{13}\text{C}_{\text{org}}$ correlate with two minima in solar activity, the Spörer Minimum and the Maunder Minimum, and a subsequent increase in solar activity, it seems likely that these changes are driven by monsoon strength weakening during

the ‘Little Ice Age’ (Bond event 0) and the subsequent climate amelioration (Anderson et al. 2002; Agnihotri et al. 2008).

Multiple proxies (Prasad et al. 2014; this study) indicate that there are both tropical and high latitude influences on the ISM that can be finally linked to solar variability. The fact that all phases of climate cooling in the North Atlantic region identified by Bond et al. (2001) are largely contemporaneously (within dating uncertainties) accompanied by climate deteriorations at Lonar Lake, as inferred from changes in BCI and evaporative gypsum crystal precipitation, indicates that the North Atlantic and the Indian monsoon climate systems were linked during the Holocene. Evidence for contemporaneous climate variability in the Asian tropics and the North Atlantic region during the Holocene have also been reported from annually laminated, precisely dated stalagmites (Liu et al. 2013). A reasonable explanation for such a concurrent linkage is an atmospheric tele-connection, which has the potential to connect the two systems without substantial delay. Coupled ocean-atmosphere climate simulations could show that cooling of the northern hemisphere results in reduced summer monsoon rainfall over India (Broccoli et al. 2006; Pausata et al. 2011). This is due to the development of an asymmetric Hadley cell accompanied by a southwards shift of the ITCZ, which causes an enhanced net energy (heat) transport from the tropics to the cooled northern hemisphere (Broccoli et al. 2006). Such a southwards shift of the ITCZ would lead to weaker-than-normal Asian summer monsoon, and thus might be the mechanism responsible for the Asian-North Atlantic climate connection indicated by our data. Another mechanism that might have contributed to the connection could be the effect of northern hemisphere cooling on Eurasian snow cover if the cold phases recorded in the North Atlantic region have caused enhanced snow accumulation over Eurasia. Modern observations and model calculations show that extent and duration of Eurasian snow cover affect the Asian monsoon system (Barnett et al. 1989; Bamzai and Shukla 1999). Prolonged Eurasian snow cover during spring

cools the overlying air since energy is used to melt the snow and to evaporate the melt water instead of warming the land surface, thus having a downwind effect on South Asian landmasses and weakening the thermal gradients between land and ocean, which causes a weaker-than-normal summer monsoon (Barnett et al. 1989).

The reason for the North Atlantic cooling events might be reduction in insolation triggered by reduced solar output. This was postulated by Bond et al. (2001) who found that the North Atlantic cooling events correlate with smoothed and detrended ^{14}C and ^{10}Be production rates (^{14}C shown in Figure 4.6), which are inversely correlated with solar output (Beer 2000). They also found a ca. 1500 year periodicity of the palaeoclimate variation in their record, which is in agreement with palaeoclimate variations reconstructed from other records (*see* Mayewski et al. 2004) and the link between periodicities in climate archives and solar activity (Soon et al. 2014). To compare these findings with our data, we have calculated the major frequencies in our climate proxy data as well as the correlation between the BCI and the ^{14}C production rate. Before the spectral analysis, the long term climate trend was removed from the whole time series by applying a Gaussian kernel based filter with a kernel bandwidth of 500 years. The correlation between the detrended ^{14}C production rate (Bond et al. 2001) and the detrended BCI is relatively high (0.63), thus supporting the hypothesis that climate variability in India is influenced by changes in solar irradiance (Gupta et al. 2005). The power spectral analysis revealed a 1519 year periodicity besides 274 year, multiples of 274 year, and 435 year periodicities in our data set (Figure 4.7). Thus, a periodicity in climate variability similar to the “1500-year cycle” observed by Bond et al. (2001) is present in our record and corroborates the connection of the North Atlantic and the Indian monsoon palaeoclimates. We conclude that while IPWP forcings are important in causing millennial scale periods of prolonged dryness during the mid and late Holocene in central India (Prasad et al. 2014), the subtle short term changes identified by the BCI indicate the presence of North Atlantic forcings as well.

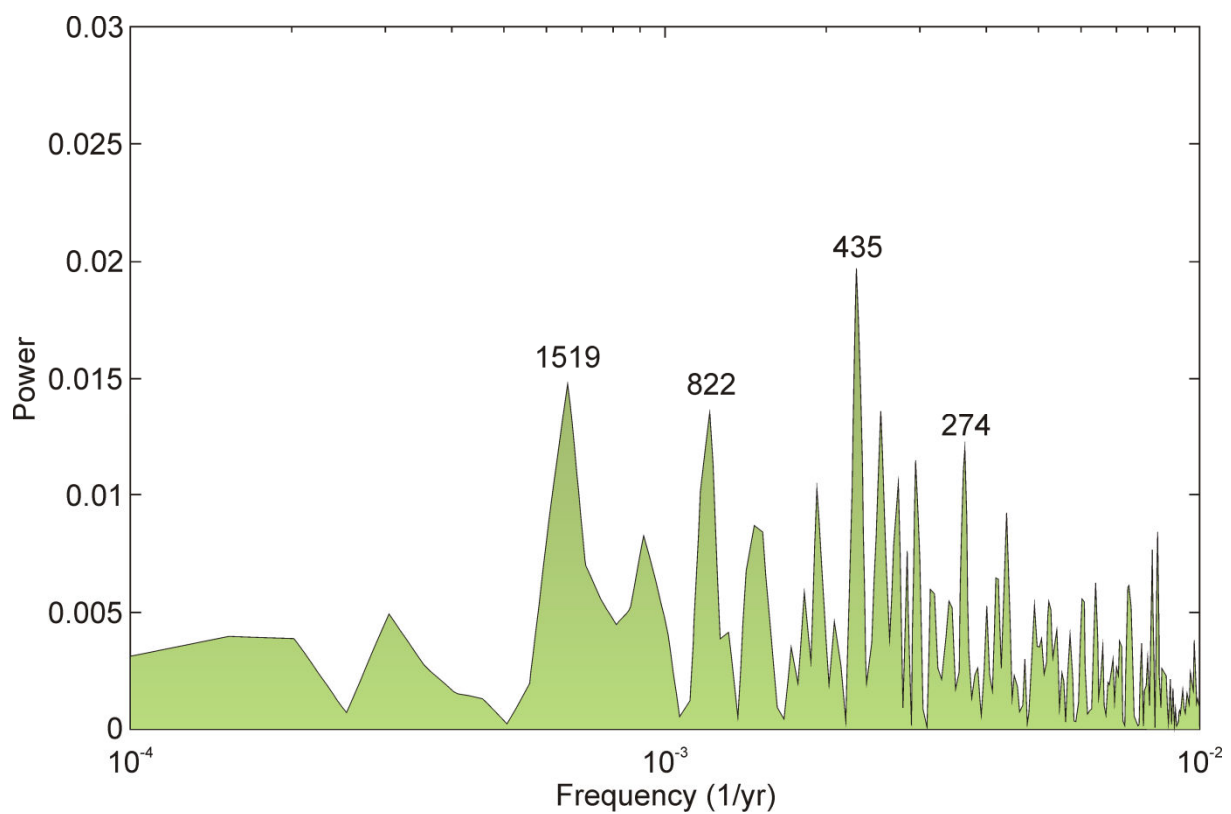


Figure 4.7: Powerspectrum indicating the most prominent cyclicities within the Bioclastic Climate Index data set.

4.4.3. Implication for the archaeological history

Our palaeoclimate reconstruction from Lonar Lake gives some clues according to the ongoing discussion about the role of mid-Holocene climate change on the de-urbanisation and abandonment of most Mature Harappan cities in the Indus valley region and the dislocation of settlements during the Late Harappan phase after 3.9 cal ka BP especially to the western Ganga Plains (Possehl 1997). Singh (1971) postulated that the development and expansion of the Harappan Civilisation was strongly related to favourable climate conditions and to severe climate deterioration during its decline. However, Possehl (1997) and Enzel et al. (1999) proposed that the influence of climate to the fate of the Harappan Civilisation was minimal or absent. But, since the capture of rivers that contributed to the water supply of the Harappan cities caused by tectonic activity during the time of Harappan decline could not be confirmed

(Clift et al. 2012) and since almost all of these rivers were monsoon fed (Tripathi et al. 2004; Giosan et al. 2012), vulnerability of the urban Harappan sites to weakened monsoon seems likely. And while Staubwasser and Weiss (2006) argue for a direct link between the decline of the Harappan Civilisation and the relatively short dry episode at about 4.2 cal ka BP, others hypothesise that the gradual climatic decline between ~ 5 and 4 cal ka BP caused an adaption of the cultivation methods to reduced summer monsoon rainfall (Gupta et al. 2006; Madella and Fuller 2006; MacDonald 2011) and related diminution in seasonal flooding (Giosan et al. 2012).

Our data support the view that the rise of the Harappan Civilisation did not occur during a phase of wettest climate (Enzel et al. 1999) but that the development of the huge cultural centres was more likely linked to the climate deterioration during the transition from the wetter early Holocene towards the drier late Holocene. A similar development was reconstructed for the rise and fall of the Mayan cities in Central America where the spread of urban centres coincided with a phase of declining humidity between 1.3 and 1.15 ka BP and the abandonment started subsequently at ~ 1.15 ka BP probably due to persistent dry conditions (Kennett et al. 2012). The development of highly populated centres in the Indus Valley was possibly due to the reduction of annual rainfall and the concentration of cultivable acreage along the rivers that provided enough water for agriculture in the form of seasonal flooding to supply the resident population. The fact that diminished available effective moisture at Lonar Lake between 4.6 and 3.9 cal ka BP correlates well with other records from the Asian monsoon realm (Hong et al. 2003; Gupta et al. 2005; Demske et al. 2009; Wünnemann et al. 2010) displays the supra-regional character of this drying trend and corroborates the assumption that the climatically sensitive sites especially in the relatively dry regions of the western Harappan territories were forced to adapt to severe shortages in water supply as for example to rivers that became ephemeral. A consequent change in agricultural strategy towards cultivation of crops that called for a more extensive land use and could not

support the highly populated centres seems to be a reasonable explanation for the gradual decline of the Harappan Civilisation.

4.5. Conclusions

The analyses of the C/N, $\delta^{13}\text{C}_{\text{org}}$, $\delta^{15}\text{N}$, lithogenic contribution, grain-size, and amino acid degradation indices LI and Ox/Anox ratio values in combination with the evaporitic gaylussite crystals from the sediment core samples of the climatically sensitive Lonar Lake revealed several environmental and hydrological changes during the Holocene that can be related to climate shifts.

The long term Holocene climate development at Lonar Lake shows three phases. The first phase is characterised by dry conditions at about 11.4 cal ka BP followed by a transition to wetter conditions during the time of monsoon onset and strengthening (~ 11.4 – 11.1 cal ka BP). The second phase comprises the early Holocene and shows wet conditions with high lake level and C_3 dominated catchment vegetation. A subsequent transition to drier conditions occurs between ca. 6.2 and 3.9 cal ka BP. The late Holocene represents the third phase, which is characterised by relatively dry conditions as indicated by lower lake level and terrestrial vegetation with high C_4 plant contribution. Comparison of these findings with other climate records from South Asia and the North Atlantic region displays a strong similarity, with strong monsoon phases in Asia correlating with warm periods in the North Atlantic region and weak monsoon correlating with colder climate in the North Atlantic region (Johnsen et al. 2001). These climatic conditions seem to be closely related to the northern hemisphere insolation, which additionally seems to drive the position of the ITCZ, and thus the northwards extent of the summer monsoon rainfall (Fleitmann et al. 2007).

The long term climate trend is superimposed by several shorter term climate fluctuations. Some of these fluctuations have also been observed in other high resolution climate records

from Asia, and they can be correlated with the North Atlantic Bond events (Bond et al. 1997; Bond et al. 2001). The correlation is the same as observed for the long term trend with cold periods in the North Atlantic correlating with dry periods over South Asia and vice versa. All the 9 Bond events during the Holocene are isochronally (within dating uncertainties) reflected in the Lonar Lake record. This points to a connection between the two climate systems or to an identical trigger of climate variability. The fact that the Bioclastic Climate Index (BCI) quite well delineates the solar output proxy ^{14}C production rate (Bond et al. 2001) corroborates the assumption that variations in solar activity triggered centennial scale variability of the Indian monsoon climate during the Holocene. However, the amplitude of the BCI not solely depends on the centennial climate variability but is also influenced by the long term Holocene climate variability, other tele-connections (e.g., Pacific climate; Prasad et al. 2014), local climate phenomena, changes in environmental conditions, and anthropogenic interferences. Thus, the amplitude of the BCI curve does not always reliably display the absolute strength of climate variability.

With respect to the archaeological record from India and Pakistan, our results support the hypothesis that the rise of the Harappan Civilisation was linked to the climate deterioration during the transition from wetter climate of the early Holocene to drier climate of the late Holocene. We believe that the decline of the urban centres especially in the western Harappan territories might best be explained by a gradual reduction of summer monsoon between ~ 4.6 and 3.9 cal ka BP and a consequent adoption of new agricultural practices and crops that demanded a social adjustment.

5. Conclusions and outlook

5.1. Conclusions

During the studies presented in this thesis, the general applicability of amino acid-based degradation and organic matter source proxies in lacustrine environments could be confirmed. However, several proxies that are commonly used to classify marine sediments, namely the degradation index (DI), ratios of proteinogenic amino acids and their non-proteinogenic degradation products (Asp/ β -Ala, Glu/ γ -Aba, Arg/Orn), the Asp/Gly ratio, and the Gluam/Galam ratio, show some weaknesses regarding their validity in lacustrine investigations. Nevertheless, other degradation indices, such as AA-N, the RI, The LDI, the molar percentage of β -Ala, and %Gly/(Gly+Ser+Thr), as well as source indices, as for example AA/Galam and Gly+Ser+Thr, were successfully applied to lake sediments of four Indian lakes located in different climatic regimes.

Moreover, an investigation of the present day environmental conditions of the central Indian Lonar Lake was conducted, with the aim to identify the modern biogeochemical cycles, hydrological conditions, and potential distinctive features. Knowledge of the present day conditions of Lonar Lake was required to enable the palaeo-climate reconstruction on the basis of Lonar Lake sediments, which was performed in a further step. Some properties of the modern Lonar Lake, such as its endorheic nature, high pH, brackish water, severe eutrophication, and anoxic bottom water, make it a unique ecosystem and account for specific biogeochemical characteristics of its biota and sediments. For instance, the plankton community of the modern Lonar Lake is highly dominated by alkaliphile and halophile cyanobacteria that determine the amino acid assemblage of SPM and sediments, which differs from amino acid assemblages of marine and most other lake samples. Additionally, high pH and anoxic bottom water have caused a severe increase in $\delta^{15}\text{N}$ of DIN driven by

denitrification and ammonia volatilisation. This increase in $\delta^{15}\text{N}$ of DIN is responsible for elevated $\delta^{15}\text{N}$ values of phytoplankton in Lonar Lake. Additionally, aerobic degradation as well as the inflow of ^{15}N enriched nitrogenous nutrients from the surrounding alluvial plains resulted in strong ^{15}N enrichment (by 5‰ to 9‰) of OM from shallow, oxic, nearshore sediments compared to OM of deeper, anoxic sediments. This increase could partly be attributed to the selective microbial degradation of individual amino acids, particularly Glu, during aerobic decomposition. Based on the different amino acid assemblages of sediments degraded under aerobic conditions compared to sediments degraded under anaerobic conditions reported by Cowie et al. (1995) and confirmed by our investigation of Lonar Lake sediments, we calculated an Ox/Anox ratio, which might be used to reconstruct the dominant redox conditions during OM degradation in sediments.

In a final step, the results of the amino acid and modern hydrology and biogeochemistry investigations of Lonar Lake were used to support the Holocene palaeo-climate reconstruction conducted on the basis of biogeochemical and mineralogical analyses of a 10 m long sediment core from the central part of Lonar Lake. The most climate sensitive proxies, namely $\delta^{13}\text{C}$, lithogenic contribution, and the amino acid based proxies LI and Ox/Anox, were combined in a Bioclastic Climate Index (BCI). Further climate information was gathered from grain size data, $\delta^{15}\text{N}$ values, and the occurrence of evaporitic gaylussite minerals. A long term climate transition delineating the change in northern hemisphere insolation was identified, with a sharp increase of the monsoon strength at the beginning of the Holocene and the establishment of wet climate conditions during the early Holocene. A more or less gradual decline of wet conditions occurred between ca. 6.2 cal ka BP to 3.9 cal ka BP, and relatively dry conditions prevailed during the late Holocene. Superimposed on the long term climate development, several centennial scale climate variations could be identified from the BCI and correlated with climate variability from higher latitudes, as identified on the basis of the contribution of ice rafted debris to North Atlantic sediment cores (Bond et al. 2001). Good

correlation between indication of dry climate anomalies in central India and cool climate indication in the North Atlantic region, suggest a systematic link or synchronous reaction of the different climate systems to similar forcings. The good correlation between the BCI and the ^{14}C production rate, a proxy of solar activity, indicates that changes in solar output are important driving mechanisms of centennial scale climate variability both in South Asia as well as in the North Atlantic region. These palaeo-climate reconstructions from central India support the hypotheses of connections between the urbanisation of the ancient Harappan Civilization and the beginning of climate deterioration during the mid Holocene as well as between the abandonment of the Harappan Cities and the intensification of dry climate conditions after ca. 4.6 cal ka BP (Gupta et al. 2006).

5.2. Outlook

The studies presented in this thesis emphasize the high potential of multiproxy palaeoclimate investigations. Comparable studies from other sites of different climate regimes could be used to distinguish between local and regional climate signals. Additionally, such comprehensive studies might have the potential to identify spatial differences in environmental and climatic response to small scale variations in the monsoon system, which have been identified for the modern Indian monsoon system. Also information on the interplay of different climate forcings and connections, such as the solar output, the mid latitude westerlies, ENSO, or Indian Ocean Dipole, might be identifiable if spatial differences in regional climate could be reconstructed.

The results of the amino acid analyses indicate that commonly used degradation and OM source indices need to be verified for their applicability to terrestrial systems. However, if the amino acid analyses are thoroughly checked and interpreted, they might not only identify the state of OM degradation but potentially reveal additional information about degradation

mechanisms and pathways, environmental conditions, and OM sources. One attempt to gather additional knowledge from amino acid analyses during these studies was the calculation of a ratio between amino acid monomers that become relatively enriched during aerobic degradation and monomers that become relatively enriched during anaerobic degradation (Ox/Anox). And, even though this ratio was successfully applied to different environments, it might still need some adjustment. This could be achieved by the incorporation of factor scores to the individual monomers that are used for the calculation of the Ox/Anox ratio on the basis of a PCA factor that separates environmental samples that are degraded under aerobic conditions from samples that are degraded under anaerobic conditions. Therefore, amino acid analyses of samples from different environments with known redox conditions must be performed and a data set big enough to exhibit statistical significance must be compiled and the PCA factor that separates the samples according to the redox conditions during their degradation must be identified and the factor loadings of the individual monomers extracted.

Acknowledgements

Funding of the HIMPAC project and my work within this project by the DFG is gratefully acknowledged.

I very much appreciate the support given by the other members of the HIMPAC project, some of whom are also listed as co-authors of the scientific articles, I compiled. Especially the collaboration with working groups from GFZ, Senckenberg Research Station of Quaternary Palaeontology, Indian Institute of Geomagnetism, Potsdam Institute of Climate Research, Kashmir University, and Freie Universität Berlin shall be acknowledged.

I'd like to thank Frauke Langenberg and Dr. Niko Lahajnar for their assistance during lab work. Additionally, support during analytical work by 'my' master students Nicole Herrmann, Peter J. Martens, and Amelie Hagen, the bachelor students Manuel Weiher, Natalie Harms, and Stephan Hase, as well as by several HiWis offered valuable help and shall be thanked.

I thank Prof. Dr. Kay-Christian Emeis for his encouragement to apply for a PhD position in his workgroup after earning my Diploma degree, for reviewing this dissertation, and for being part of my examination commission, and thus his support during my first steps in becoming part of the scientific community.

I also like to thank Prof. Dr. Eva-Maria Pfeiffer, Dr. Berit Brockmeyer, Dr. Justus van Beusekom, and Prof. Dr. Jürgen Böhner for their willingness to complete my examination commission, and thus for dedicating their precious time to my disputation.

I am grateful for help, encouragement, discussion, and diversion offered by fellow students, project, institute, and working group collaborators, friends, and family.

Last but not least, I'd like to express my deep gratitude to Dr. Birgit Gaye for her patience and endurance during supervision of my work. I thank her for her effort to support me during my studies and the help to develop the skills and gain the knowledge needed to realise this thesis.

Figure captions

Figure 1.1: Approximate location of the ITCZ and dominant wind directions during boreal summer (A) and boreal winter (B) (Fleitmann et al. 2007).

Figure 1.2: Overview of $\delta^{13}\text{C}$ values of major carbon sources to lakes and resulting $\delta^{13}\text{C}$ values of DIC (modified after Martens (submitted) and Leng et al. (2006)).

Figure 1.3: Schematic nitrogen cycle (modified after Hensen et al. (2000)).

Figure 1.4: Overview of $\delta^{15}\text{N}$ values of major nitrogen sources to lakes (modified after Martens (submitted) and Leng et al. (2006); values after Maksymowska et al. (2000) and Talbot (2001)).

Figure 1.5: Overview of analysed amino acids (modified after Martens (submitted)).

Figure 2.1: Map showing the locations of the four investigated lakes.

Figure 2.2: Monomeric AA and HA assemblages of the sediment core samples of the four lakes.

Figure 2.3: Cross-plot of AA-N and AA-C-values of sediment core, vascular plant, plankton, suspended particulate matter, and macrophyte samples. Macrophyte, 6 plankton, and 11 vascular plant paired values reported by or calculated from Cowie and Hedges (1992).

Figure 2.4: Cross-plot of DI and RI values of the sediment core samples of the four lakes.

Figure 2.5: Cross-plot of first and second PCA axis factors of the PCA of the monomeric AA contribution of the combined data set.

Figure 3.1: Location map showing the position of Lonar Lake on the Deccan Traps in Central India (A). Map of Lonar Lake showing the bathymetry (m) and surface sediment sampling points (B).

Figure 3.2: Spatial distribution of $\delta^{15}\text{N}$ (‰) in Lonar surface sediment organic matter (A). Stable carbon vs. nitrogen isotopic ratios of the different Lonar samples (B).

Figure 3.3: Comparison of the stable carbon vs. nitrogen isotopic ratios of Lonar Lake and Renuka, Mansar, and Rewalsar Lakes.

Figure 3.4: Mean contributions (mol %) of the individual amino acids to the total hydrolysable amino acid pool of the different Lonar samples. Error bars denote the standard deviation. Amino acid abbreviations as defined in Table 3.2.

Figure 3.5: Spatial distribution of the Lonar degradation index (LI) in Lonar surface sediment organic matter.

Figure 3.6: Spatial distribution of the Ox/Anox ratio in Lonar surface sediment organic matter.

Figure 3.7: Map showing the different depositional zones of Lonar Lake.

Figure 4.1: Regional overview and location of Lonar Lake (A). Study area showing the coring site (B).

Figure 4.2: Summary of the analytical results. Schematic lithology of the Lonar Lake core and down-core variation in lithogenic contribution (A), C/N ratio (B), amino acid derived indices Ox/Anox (C) and LI (D), stable nitrogen (E) and carbon (F) isotopic ratios of bulk organic matter, and median grain-size (G). C/N, $\delta^{13}\text{C}$, and $\delta^{15}\text{N}$ were reported by Prasad et al. (2014); gaylussite crystal occurrence was reported by Anoop et al. (2013b). Error bars indicate the standard deviation range (2σ) of calibrated radiocarbon dates.

Figure 4.3: Ternary diagram showing the percentages of the different grain-size classes (clay, silt, sand) of the analysed sediment samples of the Lonar Lake core.

Figure 4.4: Long term Holocene climate trend at Lonar Lake as interpreted from our data. Comparison of median grain-size (A), lithogenic contribution (B), $\delta^{13}\text{C}$ values (C) (Prasad et al. 2014), and summer (JJA) insolation at 20°N (D) (Berger and Loutre 1991). Error bars indicate the standard deviation range (2σ) of calibrated radiocarbon dates.

Figure 4.5: Comparison of our data of lithogenic contribution (A), C/N ratio (B), Ox/Anox ratio (C), LI (D), $\delta^{15}\text{N}$ (E), and $\delta^{13}\text{C}$ (F) to the percentage of haematite stained grains (G) in core MC52, a climate record from the North Atlantic region (Bond et al. 2001). C/N, $\delta^{13}\text{C}$, and $\delta^{15}\text{N}$ were reported by Prasad et al. (2014); gaylussite crystal occurrence was reported by Anoop et al. (2013b). Numbers 0 –

8 designate cold events in the North Atlantic region (Bond events). Small arrows denote increases in climate sensitive proxies that are interpreted to indicate phases of climate deterioration at Lonar Lake (grey shaded intervals). Error bars indicate the standard deviation range (2σ) of calibrated radiocarbon dates.

Figure 4.6: Comparison between the Bioclastic Climate Index (BCI) (A), the detrended BCI (B), the climate record from the North Atlantic Region (C), and the detrended and smoothed ^{14}C production rate (D) (Bond et al. 2001). Detrending of the BCI was performed by applying a Gaussian kernel based filter with a kernel bandwidth of 500 years to the values of the time slice <11.14 cal ka BP. The values of the time slice ≥ 11.14 cal ka BP were adjusted by subtracting the lowest value of this time slice from the data since a rapid shift in BCI values at 11.14 cal ka BP occurs. Red and blue colour fills indicate relatively dry and wet phases, respectively. Lines between the BCI and the haematite stained grains plots denote some approximately contemporaneous climate shifts in both records that are interpreted to be linked. Error bars indicate the standard deviation range (2σ) of calibrated radiocarbon dates.

Figure 4.7: Powerspectrum indicating the most prominent cyclicities within the Bioclastic Climate Index data set.

Table captions

- Table 1.1: Fractionation factors (α) of different nitrogen transformation processes.
- Table 2.1: Locations as well as hydrological and meteorological properties of the four lakes, Tso Moriri, Mansar Lake, Lonar Lake, and Pookode Lake.
- Table 2.2: Average TOC, C/N, AA, AA-C, and AA-N values of specific groups of samples of the four lakes.
- Table 2.3: AA monomer DI coefficients (Dauwe et al. 1999) and first PCA axis loadings of individual PCAs of the four lake sediment cores.
- Table 2.4: Average molar percentages (Avg.), standard deviations (SD), and factor coefficients (fac. coeff.) of each AA monomer used for LDI calculation.
- Table 2.5: Correlation between different AA- and HA-based OM source and degradation indices as well as C/N ratio of the combined data set.
- Table 3.1: Bulk biogeochemical parameters, AA and HA concentrations of different Lonar samples. IC values of surface sediment samples as well as TOC, TN, C/N, and $\delta^{13}\text{C}$ values of all samples except for those of sediment traps were taken from Basavaiah et al. (2014).
- Abbreviations: THAA, total hydrolysable amino acids in mg/g dry sample; AA-C, percentage of organic carbon present as amino acids; AA-N, percentage of total nitrogen present as amino acids; THHA, total hydrolysable hexosamines in

mg/g dry sample; nd, not detected; *, number of samples analyzed for amino acids.

Table 3.2: Amino acid composition of the different Lonar samples.

Abbreviations: Asp, aspartic acid; Thr, threonine; Ser, serine; Glu, glutamic acid; Gly, glycine; Ala, alanine; Val, valine; Met, methionine; Ile, isoleucine; Leu, leucine; Tyr, tyrosine; Phe, phenylalanine; β -Ala, β -alanine; γ -Aba, γ -aminobutyric acid; His, histidine; Trp, tryptophan; Orn, ornithine; Lys, lysine; Arg, arginine.

Table 3.3: Parameters of the principal component analysis (PCA) of the Lonar sample set.

Abbreviations: Amino acid abbreviations as defined in Table 3.2. AVG, mean contribution of individual amino acids to the amino acid assemblage in mol percent; SD, standard deviation.

Table 3.4: Bulk biogeochemical parameters, amino acid and amino sugar concentrations, and degradation indices of the different depositional environments of Lonar Lake.

TOC, TN, C/N, IC, $\delta^{13}\text{C}$, and Terr. TOC values were calculated from data reported by Basavaiah et al. (2014).

Abbreviations: THAA, AA-C, AA-N, THHA as defined in Table 3.1; Terr. TOC, calculated percentage of organic carbon derived from terrestrial source;

Gluam/Galam, ratio of the two hexosamines glucosamines and galactosamines;

LI, Lonar degradation index; Ox/Anox, ratio of amino acids relatively enriched during aerobic degradation and amino acids relatively enriched during anaerobic degradation;

*, number of samples analyzed for amino acids.

Table 4.1: Radiocarbon ages from the Lonar Lake core; first published by Prasad et al. (2014). Calibration of the ^{14}C dates was carried out using the program OxCal, interpolating with the INTCAL04 and NH3 calibration curves (Bronk Ramsey 2008).

List of abbreviations

α	= Fractionation factor
AA	= Amino acid
AA-C	= Amino acid associated carbon
AA-N	= Amino acid associated nitrogen
Ala	= Alanine
AMS	= Accelerator Mass Spectrometry
Arg	= Arginine
Asp	= Aspartic acid
β -Ala	= β -alanine
BCI	= Bioclastic Climate Index
C/N	= Ratio between total organic carbon and total nitrogen
cal a BP	= Calendar years before 1950
Cya	= Cysteic acid
DFG	= Deutsche Forschungsgemeinschaft (German Research Foundation)
DI	= Degradation index
DIC	= Dissolved inorganic carbon
DIN	= Dissolved inorganic nitrogen
DOC	= Dissolved organic carbon
ENSO	= El Niño Southern Oscillation
γ -Aba	= γ -aminobutyric acid
Galam	= Galactosamine
Glu	= Glutamic acid
Gluam	= Glucosamine
Gly	= Glycine

HA	= Hexosamine
HIMPAC	= Himalaya: Modern and Past Climates
His	= Histidine
IC	= Inorganic carbon
Ile	= Iso-leucine
IPWP	= Indo Pacific Warm Pool
ISM	= Indian summer monsoon
ITCZ	= Intertropical Convergence Zone
ka	= Thousand years
LDI	= Lake degradation index
Leu	= Leucine
LI	= Lonar degradation index
Lys	= Lysine
Ma	= Million years
Met	= Methionine
Mso	= Methionine sulfoximine
OM	= Organic matter
Orn	= Ornithine
PCA	= Principal component analysis
Phe	= Phenylalanine
POC	= Particulate organic carbon
R	= Isotope ratio
RI	= Reactivity index
Ser	= Serine
SPM	= Suspended particulate matter
Tau	= Taurine

TC = Total carbon
THAA = Total hydrolysable amino acids
THHA = Total hydrolysable hexosamines
Thr = Threonine
TN = Total nitrogen
TOC = Total organic carbon
Trp = Tryptophan
Tyr = Tyrosine
Val = Valine
VPDB = Vienna Pee Dee Belemnite

References

- Agnihotri, R., S. Kurian, M. Fernandes, K. Reshma, W. D'Souza, and S. W. A. Naqvi. 2008. Variability of subsurface denitrification and surface productivity in the coastal eastern Arabian Sea over the past seven centuries. *The Holocene* **18**: 755-764.
- Al-Mikhlaifi, A., B. Das, and P. Kaur. 2003. Water chemistry of Mansar Lake (India): an indication of source area weathering and seasonal variability. *Environmental Geology* **44**: 645-653.
- Alizai, A., S. Hillier, P. D. Clift, L. Giosan, A. Hurst, S. Vanlaningham, and M. Macklin. 2012. Clay mineral variations in Holocene terrestrial sediments from the Indus Basin. *Quaternary Research* **77**: 368-381.
- Alley, R. B., P. A. Mayewski, T. Sowers, M. Stuiver, K. C. Taylor, and P. U. Clark. 1997. Holocene climatic instability: A prominent, widespread event 8200 yr ago. *Geology* **25**: 483-486.
- Amundson, R., A. T. Austin, E. A. G. Schuur, K. Yoo, V. Matzek, C. Kendall, A. Uebersax, D. Brenner, and W. T. Baisden. 2003. Global patterns of the isotopic composition of soil and plant nitrogen. *Global Biogeochemical Cycles* **17**: 1031.
- Anderson, D. M., J. T. Overpeck, and A. K. Gupta. 2002. Increase in the Asian southwest monsoon during the past four centuries. *Science* **297**: 596-599.
- Anoop, A., S. Prasad, R. Krishnan, R. Naumann, and P. Dulski. 2013a. Intensified monsoon and spatiotemporal changes in precipitation patterns in the NW Himalaya during the early-mid Holocene. *Quaternary International* **313-314**: 74-84.
- Anoop, A., S. Prasad, B. Plessen, N. Basavaiah, B. Gaye, R. Naumann, P. Menzel, S. Weise, and A. Brauer. 2013b. Palaeoenvironmental implications of evaporative gypsum crystals from Lonar Lake, central India. *Journal of Quaternary Science* **28**: 349-359.
- Azevedo, R. A., and P. J. Lea. 2001. Lysine metabolism in higher plants. *Amino Acids* **20**: 261-279.
- Badve, R. M., K. P. N. Kumaran, and C. Rajshekhar. 1993. Eutrophication of Lonar Lake, Maharashtra. *Current Science* **65**: 347-351.
- Bamzai, A. S., and J. Shukla. 1999. Relation between Eurasian Snow Cover, Snow Depth, and the Indian Summer Monsoon: An Observational Study. *Journal of Climate* **12**: 3117-3132.
- Bar-Matthews, M., A. Ayalon, and A. Kaufman. 1997. Late Quaternary paleoclimate in the eastern Mediterranean region from stable isotope analysis of speleothems at Soreq Cave, Israel. *Quaternary Research* **47**: 155-168.

- Barber, D. C., A. Dyke, C. Hillaire-Marcel, A. E. Jennings, J. T. Andrews, M. W. Kerwin, G. Bilodeau, R. McNeely, J. Southon, M. D. Morehead, and J. M. Gagnon. 1999. Forcing of the cold event of 8,200 years ago by catastrophic drainage of Laurentide lakes. *Nature* **400**: 344-348.
- Barnett, T. P., L. Dümenil, U. Schlese, E. Roeckner, and M. Latif. 1989. The effect of Eurasian snow cover on regional and global climate variations. *Journal of the Atmospheric Sciences* **46**: 661-685.
- Basavaiah, N., M. G. Wiesner, A. Anoop, P. Menzel, N. R. Nowaczyk, K. Deenadayalan, A. Brauer, B. Gaye, R. Naumann, N. Riedel, M. Stebich, and S. Prasad. 2014. Physicochemical analyses of surface sediments from the Lonar Lake, central India - implications for palaeoenvironmental reconstruction. *Fundamental and Applied Limnology* **184**: 51-68.
- Becker, E. W. 2007. Micro-algae as a source of protein. *Biotechnology advances* **25**: 207-210.
- Beer, J. 2000. Long-term indirect indices of solar variability. *Space Science Reviews* **94**: 53-66.
- Benner, R., and K. Kaiser. 2003. Abundance of amino sugars and peptidoglycan in marine particulate and dissolved organic matter. *Limnology and Oceanography* **48**: 118-128.
- Berger, A., and M. F. Loutre. 1991. Insolation values for the climate of the last 10 million years. *Quaternary Science Reviews* **10**: 297-317.
- Berglund, M., and M. E. Wieser. 2011. Isotopic compositions of the elements 2009 (IUPAC Technical Report). *Pure and Applied Chemistry* **83**: 397-410.
- Berkelhammer, M., A. Sinha, M. Mudelsee, H. Cheng, R. L. Edwards, and K. Cannariato. 2010. Persistent multidecadal power of the Indian Summer Monsoon. *Earth and Planetary Science Letters* **290**: 166-172.
- Bond, G., B. Kromer, J. Beer, R. Muscheler, M. N. Evans, W. Showers, S. Hoffmann, R. Lotti-Bond, I. Hajdas, and G. Bonani. 2001. Persistent solar influence on North Atlantic climate during the Holocene. *Science* **294**: 2130-2136.
- Bond, G., W. Showers, M. Cheseby, R. Lotti, P. Almasi, P. Demenocal, P. Priore, H. Cullen, I. Hajdas, and G. Bonani. 1997. A pervasive millennial-scale cycle in North Atlantic Holocene and glacial climates. *Science* **278**: 1257-1266.
- Bookhagen, B., and D. W. Burbank. 2010. Toward a complete Himalayan hydrological budget: Spatiotemporal distribution of snowmelt and rainfall and their impact on river discharge. *Journal of Geophysical Research: Earth Surface* **115**: F03019.
- Bookhagen, B., R. C. Thiede, and M. R. Strecker. 2005a. Abnormal monsoon years and their control on erosion and sediment flux in the high, arid northwest Himalaya. *Earth and Planetary Science Letters* **231**: 131-146.

- Bookhagen, B., R. C. Thiede, and M. R. Strecker. 2005b. Late Quaternary intensified monsoon phases control landscape evolution in the northwest Himalaya. *Geology* **33**: 149-152.
- Brandes, J. A., and A. H. Devol. 2002. A global marine-fixed nitrogen isotopic budget: Implications for Holocene nitrogen cycling. *Global Biogeochemical Cycles* **16**.
- Brandes, J. A., A. H. Devol, T. Yoshinari, D. A. Jayakumar, and S. W. A. Naqvi. 1998. Isotopic composition of nitrate in the central Arabian Sea and eastern tropical North Pacific: A tracer for mixing and nitrogen cycles. *Limnology and Oceanography* **43**: 1680-1689.
- Broccoli, A. J., K. A. Dahl, and R. J. Stouffer. 2006. Response of the ITCZ to Northern Hemisphere cooling. *Geophysical Research Letters* **33**: L01702.
- Bronk Ramsey, C. 2008. Deposition models for chronological records. *Quaternary Science Reviews* **27**: 42-60.
- Caner, L., D. Lo Seen, Y. Gunnell, B. R. Ramesh, and G. Bourgeon. 2007. Spatial heterogeneity of land cover response to climatic change in the Nilgiri highlands (Southern India) since the last glacial maximum. *The Holocene* **17**: 195-205.
- Carstens, D., K. E. Köllner, H. Bürgmann, B. Wehrli, and C. J. Schubert. 2012. Contribution of bacterial cells to lacustrine organic matter based on amino sugars and d-amino acids. *Geochimica Et Cosmochimica Acta* **89**: 159-172.
- Carstens, D., and C. J. Schubert. 2012. Amino acid and amino sugar transformation during sedimentation in lacustrine systems. *Organic Geochemistry* **50**: 26-35.
- Carter, P. W., and R. M. Mitterer. 1978. Amino acid composition of organic matter associated with carbonate and non-carbonate sediments. *Geochimica Et Cosmochimica Acta* **42**: 1231-1238.
- Casciotti, K. L. 2009. Inverse kinetic isotope fractionation during bacterial nitrite oxidation. *Geochimica Et Cosmochimica Acta* **73**: 2061-2076.
- Casciotti, K. L., C. Buchwald, A. E. Santoro, and C. Frame. 2011. Assessment of nitrogen and oxygen isotopic fractionation during nitrification and its expression in the marine environment, p. 253-280. In M. G. Klotz [ed.], *Methods in enzymology: research on nitrification and related processes*. Elsevier Academic Press Inc.
- Casciotti, K. L., D. M. Sigman, and B. B. Ward. 2003. Linking diversity and stable isotope fractionation in ammonia-oxidizing bacteria. *Geomicrobiology Journal* **20**: 335-353.
- Chandan, P., A. Chatterjee, and P. Gautam. 2008. Management planning of Himalayan high altitude wetlands. A case study of Tsomoriri and Tsokar wetlands in Ladakh, India, p. 1446-1452. In M. Sengupta and R. Dalwani [eds.], *The 12th World Lake Conference*.

- Chapin III, F. S., M. C. Chapin, P. A. Matson, and P. Vitousek. 2011. *Principles of terrestrial ecosystem ecology*. Springer.
- Clift, P. D., A. Carter, L. Giosan, J. Durcan, G. A. T. Duller, M. G. Macklin, A. Alizai, A. R. Tabrez, M. Danish, S. VanLaningham, and D. Q. Fuller. 2012. U-Pb zircon dating evidence for a Pleistocene Sarasvati River and capture of the Yamuna River. *Geology* **40**: 211-214.
- Clift, P. D., L. Giosan, J. Blusztajn, I. H. Campbell, C. Allen, M. Pringle, A. R. Tabrez, M. Danish, M. M. Rabbani, A. Alizai, A. Carter, and A. Lückge. 2008. Holocene erosion of the Lesser Himalaya triggered by intensified summer monsoon. *Geology* **36**: 79-82.
- Clift, P. D., and R. A. Plumb. 2008. *The Asian monsoon causes, history and effects*. Cambridge University Press.
- Collister, J. W., and J. Hayes. 1991. A preliminary study of the carbon and nitrogen isotopic biogeochemistry of lacustrine sedimentary rocks from the Green River Formation, Wyoming, Utah, and Colorado, p. C1 - C16. In M. Tuttle [ed.], *Geochemical, biogeochemical, and sedimentological studies of the Green River Formation, Wyoming, Utah and Colorado*. U.S. Geological Survey Bulletin 1973.
- Colombo, J. C., N. Silverberg, and J. N. Gearing. 1998. Amino acid biogeochemistry in the Laurentian Trough: vertical fluxes and individual reactivity during early diagenesis. *Organic Geochemistry* **29**: 933-945.
- Cowie, G. L., and J. I. Hedges. 1992. Sources and reactivities of amino acids in a coastal marine environment. *Limnology and Oceanography* **37**: 703-724.
- Cowie, G. L., and J. I. Hedges. 1994. Biochemical indicators of diagenetic alteration in natural organic matter mixtures. *Nature* **369**: 304-307.
- Cowie, G. L., J. I. Hedges, F. G. Prahl, and G. J. De Lange. 1995. Elemental and major biochemical changes across an oxidation front in a relict turbidite: An oxygen effect. *Geochimica Et Cosmochimica Acta* **59**: 33-46.
- Darling, W. G., A. H. Bath, J. J. Gibson, and K. Rozanski. 2006. Isotopes in water, p. 1-66. In M. J. Leng [ed.], *Developments in paleoenvironmental research*. Springer.
- Das, B. K. 2002. Biogeochemistry as an indicator of organic matter sources, paleolimnological and paleoenvironmental changes in lacustrine sediments—A study of two Himalayan lakes. *Environmental Geosciences* **9**: 115-126.
- Das, B. K., B. Gaye, and P. Kaur. 2008. Geochemistry of Renuka Lake and wetland sediments, Lesser Himalaya (India): Implications for source-area weathering, provenance, and tectonic setting. *Environmental Geology* **54**: 147-163.

- Das, B. K., B. Gaye, and M. A. Malik. 2010. Biogeochemistry and paleoclimate variability during the Holocene: A record from Mansar Lake, Lesser Himalaya. *Environmental Earth Sciences* **61**: 565-574.
- Dauwe, B., and J. J. Middelburg. 1998. Amino acids and hexosamines as indicators of organic matter degradation state in North Sea sediments. *Limnology and Oceanography* **43**: 782-798.
- Dauwe, B., J. J. Middelburg, P. M. J. Herman, and C. H. R. Heip. 1999. Linking diagenetic alteration of amino acids and bulk organic matter reactivity. *Limnology and Oceanography* **44**: 1809-1814.
- Davis, J., K. Kaiser, and R. Benner. 2009. Amino acid and amino sugar yields and compositions as indicators of dissolved organic matter diagenesis. *Organic Geochemistry* **40**: 343-352.
- Dean, W. E., and E. Gorham. 1998. Magnitude and significance of carbon burial in lakes, reservoirs, and peatlands. *Geology* **26**: 535-538.
- Degens, E. 1976. Molecular mechanisms on carbonate, phosphate, and silica deposition in the living cell, p. 1-112. In E. T. Degens, W. A. P. Luck and D. D. Perrin [eds.], *Topics in Current Chemistry*. Springer Berlin Heidelberg.
- Degens, E. T., and K. Mopper. 1975. Early diagenesis of organic matter in marine soils. *Soil Science* **119**: 65-72.
- Demske, D., P. E. Tarasov, B. Wünnemann, and F. Riedel. 2009. Late glacial and Holocene vegetation, Indian monsoon and westerly circulation in the Trans-Himalaya recorded in the lacustrine pollen sequence from Tso Kar, Ladakh, NW India. *Palaeogeography, Palaeoclimatology, Palaeoecology* **279**: 172-185.
- Denniston, R. F., L. A. González, Y. Asmerom, R. H. Sharma, and M. K. Reagan. 2000. Speleothem evidence for changes in Indian summer monsoon precipitation over the last ~2300 years. *Quaternary Research* **53**: 196-202.
- Dykoski, C. A., R. L. Edwards, H. Cheng, D. X. Yuan, Y. J. Cai, M. L. Zhang, Y. S. Lin, J. M. Qing, Z. S. An, and J. Revenaugh. 2005. A high-resolution, absolute-dated Holocene and deglacial Asian monsoon record from Dongge Cave, China. *Earth and Planetary Science Letters* **233**: 71-86.
- Emery, K. O., C. Stitt, and P. Saltman. 1964. Amino acids in basin sediments. *Journal of Sedimentary Research* **34**: 433-437.
- Enzel, Y., L. L. Ely, S. Mishra, R. Ramesh, R. Amit, B. Lazar, S. N. Rajaguru, V. R. Baker, and A. Sandler. 1999. High-resolution Holocene environmental changes in the Thar Desert, northwestern India. *Science* **284**: 125-128.

- Epard, J.-L., and A. Steck. 2008. Structural development of the Tso Morari ultra-high pressure nappe of the Ladakh Himalaya. *Tectonophysics* **451**: 242-264.
- Eugster, H. P., and L. A. Hardie. 1978. Saline lakes, p. 237-293. In A. Lerman [ed.], *Lakes: Chemistry, geology, physics*. Springer.
- Fleitmann, D., S. J. Burns, A. Mangini, M. Mudelsee, J. Kramers, I. Villa, U. Neff, A. A. Al-Subbary, A. Buettner, D. Hippler, and A. Matter. 2007. Holocene ITCZ and Indian monsoon dynamics recorded in stalagmites from Oman and Yemen (Socotra). *Quaternary Science Reviews* **26**: 170-188.
- Fleitmann, D., M. Mudelsee, S. J. Burns, R. S. Bradley, J. Kramers, and A. Matter. 2008. Evidence for a widespread climatic anomaly at around 9.2 ka before present. *Paleoceanography* **23**.
- Freudenthal, T., T. Wagner, F. Wenzhöfer, M. Zabel, and G. Wefer. 2001. Early diagenesis of organic matter from sediments of the eastern subtropical Atlantic: Evidence from stable nitrogen and carbon isotopes. *Geochimica Et Cosmochimica Acta* **65**: 1795-1808.
- Fuchs, G., and M. Linner. 1996. On the geology of the suture zone and Tso Morari dome in eastern Ladakh (Himalaya). *Jahrbuch der Geologischen Bundesanstalt* **139**: 191-207.
- Gadgil, S. 2003. The Indian monsoon and its variability. *Annual Review of Earth and Planetary Sciences* **31**: 429-467.
- Gasse, F. 2000. Hydrological changes in the African tropics since the Last Glacial Maximum. *Quaternary Science Reviews* **19**: 189-211.
- Gasse, F., M. Arnold, J.-C. Fontes, M. Fort, E. Gibert, A. Huc, B. Y. Li, Y. F. Li, Q. Liu, F. Mélières, E. Van Campo, F. B. Wang, and Q. S. Zhang. 1991. A 13.000-year climate record from western Tibet. *Nature* **353**: 742-745.
- Gasse, F., J.-C. Fontes, E. Van Campo, and K. Wei. 1996. Holocene environmental changes in Bangong Co basin (Western Tibet). Part 4: Discussion and conclusions. *Palaeogeography, Palaeoclimatology, Palaeoecology* **120**: 79-92.
- Gaye, B., K. Fahl, L. A. Kodina, N. Lahajnar, B. Nagel, D. Unger, and A. C. Gebhardt. 2007. Particulate matter fluxes in the southern and central Kara Sea compared to sediments: Bulk fluxes, amino acids, stable carbon and nitrogen isotopes, sterols and fatty acids. *Continental Shelf Research* **27**: 2570-2594.
- Giosan, L., P. D. Clift, M. G. Macklin, D. Q. Fuller, S. Constantinescu, J. A. Durcan, T. Stevens, G. A. T. Duller, A. R. Tabrez, K. Gangal, R. Adhikari, A. Alizai, F. Filip, S. VanLaningham, and J. P. M. Syvitski. 2012. Fluvial landscapes of the Harappan civilization. *Proceedings of the National Academy of Sciences* **109**: E1688-E1694.

- Goldman, J. C., D. A. Caron, and M. R. Dennett. 1987. Regulation of gross growth efficiency and ammonium regeneration in bacteria by substrate C:N ratio. *Limnology and Oceanography* **32**: 1239-1252.
- Granger, J., D. M. Sigman, J. A. Needoba, and P. J. Harrison. 2004. Coupled Nitrogen and Oxygen Isotope Fractionation of Nitrate during Assimilation by Cultures of Marine Phytoplankton. *Limnology and Oceanography* **49**: 1763-1773.
- Grasshoff, K., K. Kremling, and M. Ehrhardt. 1999. *Methods of seawater analysis*. Wiley-VCH.
- Gu, B. H., C. L. Schelske, and D. A. Hodell. 2004. Extreme ^{13}C enrichments in a shallow hypereutrophic lake: Implications for carbon cycling. *Limnology and Oceanography* **49**: 1152-1159.
- Gupta, A. K., D. M. Anderson, and J. T. Overpeck. 2003. Abrupt changes in the Asian southwest monsoon during the Holocene and their links to the North Atlantic Ocean. *Nature* **421**: 354-357.
- Gupta, A. K., D. M. Anderson, D. N. Pandey, and A. K. Singhvi. 2006. Adaptation and human migration, and evidence of agriculture coincident with changes in the Indian summer monsoon during the Holocene. *Current Science* **90**: 1082-1090.
- Gupta, A. K., M. Das, and D. M. Anderson. 2005. Solar influence on the Indian summer monsoon during the Holocene. *Geophysical Research Letters* **32**.
- Gupta, L., and H. Kawahata. 2007. ENSO related variations in biogeochemistry of AA and HA in settling particles along the equatorial Pacific Ocean. *Journal of Oceanography* **63**: 695-709.
- Gupta, L. P., V. Subramanian, and V. Ittekkot. 1997. Biogeochemistry of particulate organic matter transported by the Godavari river, India. *Biogeochemistry* **38**: 103-128.
- Haake, B., V. Ittekkot, S. Honjo, and S. Manganini. 1993. Amino acid, hexosamine and carbohydrate fluxes to the deep Subarctic Pacific (Station P). *Deep-Sea Research Part I-Oceanographic Research Papers* **40**: 547-560.
- Haake, B., V. Ittekkot, V. Ramaswamy, R. R. Nair, and S. Honjo. 1992. Fluxes of amino acids and hexosamines to the deep Arabian Sea. *Marine Chemistry* **40**: 291-314.
- Haug, G. H., K. A. Hughen, D. M. Sigman, L. C. Peterson, and U. Röhl. 2001. Southward migration of the intertropical convergence zone through the Holocene. *Science* **293**: 1304-1308.
- Heaton, T. H. E. 1986. Isotopic studies of nitrogen pollution in the hydrosphere and atmosphere: A review. *Chemical Geology* **59**: 87-102.

- Hecky, R. E., K. Mopper, P. Kilham, and E. T. Degens. 1973. The amino acid and sugar composition of diatom cell-walls. *Marine Biology* **19**: 323-331.
- Hedges, J. I., and P. E. Hare. 1987. Amino acid adsorption by clay minerals in distilled water. *Geochimica Et Cosmochimica Acta* **51**: 255-259.
- Henrichs, S. M., J. W. Farrington, and C. Lee. 1984. Peru upwelling region sediments near 15°S. 2. Dissolved free and total hydrolyzable amino acids. *Limnology and Oceanography* **29**: 20-34.
- Henrichs, S. M., and S. F. Sugai. 1993. Adsorption of amino acids and glucose by sediments of Resurrection Bay, Alaska, USA: Functional group effects. *Geochimica Et Cosmochimica Acta* **57**: 823-835.
- Hensen, C., M. Zabel, and H. N. Schulz. 2006. Benthic cycling of oxygen, nitrogen and phosphorus, p. 207-240. In H. D. Schulz and M. Zabel [eds.], *Marine geochemistry*. Springer.
- Hoch, M. P., M. L. Fogel, and D. L. Kirchman. 1992. Isotope Fractionation Associated with Ammonium Uptake by a Marine Bacterium. *Limnology and Oceanography* **37**: 1447-1459.
- Hodell, D. A., M. Brenner, S. L. Kanfoush, J. H. Curtis, J. S. Stoner, X. L. Song, Y. Wu, and T. J. Whitmore. 1999. Paleoclimate of Southwestern China for the past 50,000 yr inferred from lake sediment records. *Quaternary Research* **52**: 369-380.
- Hodell, D. A., and C. L. Schelske. 1998. Production, sedimentation, and isotopic composition of organic matter in Lake Ontario. *Limnology and Oceanography* **43**: 200-214.
- Hoefs, J. 2009. *Stable isotope geochemistry*. Springer.
- Hong, Y. T., B. Hong, Q. H. Lin, Y. X. Zhu, Y. Shibata, M. Hirota, M. Uchida, X. T. Leng, H. B. Jiang, H. Xu, H. Wang, and L. Yi. 2003. Correlation between Indian Ocean summer monsoon and North Atlantic climate during the Holocene. *Earth and Planetary Science Letters* **211**: 371-380.
- Hulthe, G., S. Hulth, and P. O. J. Hall. 1998. Effect of oxygen on degradation rate of refractory and labile organic matter in continental margin sediments. *Geochimica Et Cosmochimica Acta* **62**: 1319-1328.
- Hutchinson, G. E. 1937. Limnological studies in Indian Tibet. *Internationale Revue der gesamten Hydrobiologie und Hydrographie* **35**: 134-177.
- Ingalls, A. E., Z. F. Liu, and C. Lee. 2006. Seasonal trends in the pigment and amino acid compositions of sinking particles in biogenic CaCO₃ and SiO₂ dominated regions of the Pacific sector of the Southern Ocean along 170°W. *Deep-Sea Research Part I-Oceanographic Research Papers* **53**: 836-859.

- Ittekkot, V., E. T. Degens, and S. Honjo. 1984a. Seasonality in the fluxes of sugars, amino acids, and amino sugars to the deep ocean: Panama Basin. *Deep-Sea Research Part I-Oceanographic Research Papers* **31**: 1071-1083.
- Ittekkot, V., W. G. Deuser, and E. T. Degens. 1984b. Seasonality in the fluxes of sugars, amino acids, and amino sugars to the deep ocean: Sargasso Sea. *Deep-Sea Research Part I-Oceanographic Research Papers* **31**: 1057-1069.
- Jennerjahn, T. C., and V. Ittekkot. 1997. Organic matter in sediments in the mangrove areas and adjacent continental margins of Brazil: 1. Amino acids and hexosamines. *Oceanologica Acta* **20**: 359-369.
- Jennerjahn, T. C., V. Ittekkot, S. Klöpffer, S. Adi, S. P. Nugroho, N. Sudiana, A. Yusmal, Prihartanto, and B. Gaye-Haake. 2004. Biogeochemistry of a tropical river affected by human activities in its catchment: Brantas River estuary and coastal waters of Madura Strait, Java, Indonesia. *Estuarine Coastal and Shelf Science* **60**: 503-514.
- Johnsen, S. J., D. Dahl-Jensen, N. Gundestrup, J. P. Steffensen, H. B. Clausen, H. Miller, V. Masson-Delmotte, A. E. Sveinbjörnsdottir, and J. White. 2001. Oxygen isotope and palaeotemperature records from six Greenland ice-core stations: Camp Century, Dye-3, GRIP, GISP2, Renland and NorthGRIP. *Journal of Quaternary Science* **16**: 299-307.
- Joshi, A. A., P. P. Kanekar, A. S. Kelkar, Y. S. Shouche, A. A. Vani, S. B. Borgave, and S. S. Sarnaik. 2008. Cultivable bacterial diversity of alkaline Lonar Lake, India. *Microbial Ecology* **55**: 163-172.
- Jourdan, F., F. Moynier, C. Koeberl, and S. Eroglu. 2011. $^{40}\text{Ar}/^{39}\text{Ar}$ age of the Lonar crater and consequence for the geochronology of planetary impacts. *Geology* **39**: 671-674.
- Kandler, O. 1979. Zellwandstrukturen bei Methan-Bakterien. *Naturwissenschaften* **66**: 95-105.
- Kauppila, T., and V.-P. Salonen. 1997. The effect of Holocene treeline fluctuations on the sediment chemistry of Lake Kilpisjärvi, Finland. *Journal of Paleolimnology* **18**: 145-163.
- Keil, R. G., E. Tsamakis, and J. I. Hedges. 2000. Early diagenesis of particulate amino acids in marine systems, p. 69-82. In G. A. Goodfriend, M. J. Collins, M. L. Fogel, S. A. Macko and J. F. Wehmiller [eds.], *Perspectives in amino acid and protein geochemistry*. Oxford University Press.
- Kemp, A. L. W., and A. Mudrochova. 1973. The distribution and nature of amino acids and other nitrogen-containing compounds in Lake Ontario surface sediments. *Geochimica Et Cosmochimica Acta* **37**: 2191-2206.
- Kendall, R. A., J. X. Mitrovica, G. A. Milne, T. E. Törnqvist, and Y. X. Li. 2008. The sea-level fingerprint of the 8.2 ka climate event. *Geology* **36**: 423-426.

- Kennett, D. J., S. F. M. Breitenbach, V. V. Aquino, Y. Asmerom, J. Awe, J. U. L. Baldini, P. Bartlein, B. J. Culleton, C. Ebert, C. Jazwa, M. J. Macri, N. Marwan, V. Polyak, K. M. Prufer, H. E. Ridley, H. Sodemann, B. Winterhalder, and G. H. Haug. 2012. Development and Disintegration of Maya Political Systems in Response to Climate Change. *Science* **338**: 788-791.
- King, K. J. 1977. Amino acid survey of recent calcareous and siliceous deep- sea microfossils. *Micropaleontology* **23**: 180-193.
- Kinnersley, A. M., and F. J. Turano. 2000. Gamma aminobutyric acid (GABA) and plant responses to stress. *Critical Reviews in Plant Sciences* **19**: 479-509.
- Koinig, K., W. Shotyk, A. Lotter, C. Ohlendorf, and M. Sturm. 2003. 9000 years of geochemical evolution of lithogenic major and trace elements in the sediment of an alpine lake – the role of climate, vegetation, and land-use history. *Journal of Paleolimnology* **30**: 307-320.
- Koutavas, A., and J. P. Sachs. 2008. Northern timing of deglaciation in the eastern equatorial Pacific from alkenone paleothermometry. *Paleoceanography* **23**: PA4205.
- Kumar, V., S. Rai, and O. Singh. 2006. Water Quantity and Quality of Mansar Lake Located in the Himalayan Foothills, India. *Lake and Reservoir Management* **22**: 191-198.
- Lahajnar, N., M. G. Wiesner, and B. Gaye. 2007. Fluxes of amino acids and hexosamines to the deep South China Sea. *Deep-Sea Research Part I-Oceanographic Research Papers* **54**: 2120-2144.
- Lee, C. 1988. Amino acid and amine biogeochemistry in marine particulate material and sediments, p. 125-141. In T. H. Blackburn and J. Sorensen [eds.], *Nitrogen cycling in coastal marine environments*. Wiley.
- Lee, C., and J. L. Bada. 1977. Dissolved amino acids in the equatorial Pacific, the Sargasso Sea, and Biscayne Bay. *Limnology and Oceanography* **22**: 502-510.
- Lee, C., and C. Cronin. 1982. The vertical flux of particulate organic nitrogen in the sea: decomposition of amino acids in the Peru upwelling area and the equatorial Atlantic. *Journal of Marine Research* **40**.
- Lee, C., and C. Cronin. 1984. Particulate amino acids in the sea: Effects of primary productivity and biological decomposition. *Journal of Marine Research* **42**: 1075-1097.
- Lehmann, M. F., S. M. Bernasconi, A. Barbieri, and J. A. McKenzie. 2002. Preservation of organic matter and alteration of its carbon and nitrogen isotope composition during simulated and in situ early sedimentary diagenesis. *Geochimica Et Cosmochimica Acta* **66**: 3573-3584.

- Lehmann, M. F., S. M. Bernasconi, J. A. McKenzie, A. Barbieri, M. Simona, and M. Veronesi. 2004. Seasonal variation of the $\delta^{13}\text{C}$ and $\delta^{15}\text{N}$ of particulate and dissolved carbon and nitrogen in Lake Lugano: Constraints on biogeochemical cycling in a eutrophic lake. *Limnology and Oceanography* **49**: 415-429.
- Lei, Y. B., T. D. Yao, Y. W. Sheng, E. L. Zhang, W. C. Wang, and J. L. Li. 2012. Characteristics of $\delta^{13}\text{C}_{\text{DIC}}$ in lakes on the Tibetan Plateau and its implications for the carbon cycle. *Hydrological Processes* **26**: 535-543.
- Leipe, C., D. Demske, and P. E. Tarasov. in press. A Holocene pollen record from the north-western Himalayan lake Tso Moriri and its implication for palaeoclimatic and archaeological research. *Quaternary International*.
- Leng, M. J., A. L. Lamb, T. H. E. Heaton, J. D. Marshall, B. B. Wolfe, M. D. Jones, J. A. Holmes, and C. Arrowsmith. 2006. Isotopes in lake sediments, p. 147-184. In M. J. Leng [ed.], *Developments in paleoenvironmental research*. Springer.
- Liebezeit, G. 1993. Amino sugars in Bransfield Strait and Weddell Sea sediments. *Senckenbergiana maritima* **23**: 29-35.
- Liu, Y. H., G. M. Henderson, C. Y. Hu, A. J. Mason, N. Charnley, K. R. Johnson, and S. C. Xie. 2013. Links between the East Asian monsoon and North Atlantic climate during the 8,200 year event. *Nature Geoscience* **6**: 117-120.
- Lomstein, B. A., B. B. Jørgensen, C. J. Schubert, and J. Niggemann. 2006. Amino acid biogeo- and stereochemistry in coastal Chilean sediments. *Geochimica Et Cosmochimica Acta* **70**: 2970-2989.
- MacDonald, G. 2011. Potential influence of the Pacific Ocean on the Indian summer monsoon and Harappan decline. *Quaternary International* **229**: 140-148.
- Macko, S. A., and M. L. F. Estep. 1984. Microbial alteration of stable nitrogen and carbon isotopic compositions of organic matter. *Organic Geochemistry* **6**: 787-790.
- Madella, M., and D. Q. Fuller. 2006. Palaeoecology and the Harappan Civilisation of South Asia: A reconsideration. *Quaternary Science Reviews* **25**: 1283-1301.
- Magny, M., S. Joannin, D. Galop, B. Vanni re, J. N. Haas, M. Bassetti, P. Bellintani, R. Scandolari, and M. Desmet. 2012. Holocene palaeohydrological changes in the northern Mediterranean borderlands as reflected by the lake-level record of Lake Ledro, northeastern Italy. *Quaternary Research* **77**: 382-396.
- Mahajan, A. D. 2005. Preliminary survey of planktonic diversity in Lonar lake water, p. 58-62. In P. K. Banmeru, S. K. Banmeru and V. R. Mishra [eds.], *Biodiversity of Lonar crater*. Anamaya Publishers.

- Maksymowska, D., P. Richard, H. Piekarek-Jankowska, and P. Riera. 2000. Chemical and isotopic composition of the organic matter sources in the Gulf of Gdansk (Southern Baltic Sea). *Estuarine Coastal and Shelf Science* **51**: 585-598.
- Malu, R. A., K. M. Kulkarni, and M. S. Kodarkar. 2005. Conservation and management of biotic environment in Lonar crater lake: An ecological wonder of India, p. 39-46. In P. K. Banmeru, S. K. Banmeru and V. R. Mishra [eds.], *Biodiversity of Lonar crater*. Anamaya Publishers.
- Mariotti, A., and E. Peterschmitt. 1994. Forest savanna ecotone dynamics in India as revealed by carbon isotope ratios of soil organic matter. *Oecologia* **97**: 475-480.
- Martens, P. J. Biogeochemie holozäner und pleistozäner Sedimente aus dem Tso Moriri unter besonderer Berücksichtigung der Aminosäureverteilung. Submitted M.Sc. thesis, Universität Hamburg, Hamburg, pp. 68.
- MATLAB and Statistics Toolbox Release 2010. The MathWorks, Incorporated. Natick, Massachusetts, United States of America.
- Mayewski, P. A., E. E. Rohling, J. C. Stager, W. Karlén, K. A. Maasch, L. D. Meeker, E. A. Meyerson, F. Gasse, S. Van Kreveld, K. Holmgren, J. Lee-Thorp, G. Rosqvist, F. Rack, M. Staubwasser, R. R. Schneider, and E. J. Steig. 2004. Holocene climate variability. *Quaternary Research* **62**: 243-255.
- Mclaren, P., and D. Bowles. 1985. The effects of sediment transport on grain-size distributions. *Journal of Sedimentary Research* **55**: 457-470.
- Meckler, A. N., C. J. Schubert, G. L. Cowie, S. Peiffer, and M. Dittrich. 2004. New organic matter degradation proxies: Valid in lake systems? *Limnology and Oceanography* **49**: 2023-2033.
- Mengel, K. 1996. Turnover of organic nitrogen in soils and its availability to crops. *Plant and Soil* **181**: 83-93.
- Menzel, P., B. Gaye, M. G. Wiesner, S. Prasad, M. Stebich, B. K. Das, A. Anoop, N. Riedel, and N. Basavaiah. 2013. Influence of bottom water anoxia on nitrogen isotopic ratios and amino acid contributions of recent sediments from small eutrophic Lonar Lake, central India. *Limnology and Oceanography* **58**: 1061-1074.
- Meyers, P. A. 1994. Preservation of elemental and isotopic source identification of sedimentary organic matter. *Chemical Geology* **114**: 289-302.
- Meyers, P. A. 1997. Organic geochemical proxies of paleoceanographic, paleolimnologic, and paleoclimatic processes. *Organic Geochemistry* **27**: 213-250.
- Meyers, P. A., and R. Ishiwatari. 1993. Lacustrine organic geochemistry: An overview of indicators of organic matter sources and diagenesis in lake sediments. *Organic Geochemistry* **20**: 867-900.

- Meyers, P. A., and E. Lallier-Vergès. 1999. Lacustrine sedimentary organic matter records of Late Quaternary paleoclimates. *Journal of Paleolimnology* **21**: 345-372.
- Meyers, P. A., M. J. Leenheer, and R. A. Bourbonniere. 1995. Diagenesis of vascular plant organic matter components during burial in lake sediments. *Aquatic Geochemistry* **1**: 35-52.
- Meyers, P. A., and J. L. Teranes. 2002. Sediment organic matter p. 239-269. In W. M. Last and J. P. Smol [eds.], *Tracking environmental change using lake sediments. Volume 2: Physical and geochemical methods*. Kluwer Academic Publishers.
- Mishra, C., and B. Humbert-Droz. 1998. Avifaunal survey of Tsomoriri Lake and adjoining Nuro Sumdo wetland in Ladakh, Indian trans-Himalaya. *Forktail* **14**: 65-67.
- Misra, S., M. Arif, N. Basavaiah, P. K. Srivastava, and A. Dube. 2010. Structural and anisotropy of magnetic susceptibility (AMS) evidence for oblique impact on terrestrial basalt flows: Lonar crater, India. *Geological Society of America Bulletin* **122**: 563-574.
- Möbius, J., B. Gaye, N. Lahajnar, E. Bahlmann, and K. C. Emeis. 2011. Influence of diagenesis on sedimentary $\delta^{15}\text{N}$ in the Arabian Sea over the last 130 kyr. *Marine Geology* **284**: 127-138.
- Moodley, L., J. J. Middelburg, P. M. J. Herman, K. Soetaert, and G. J. De Lange. 2005. Oxygenation and organic-matter preservation in marine sediments: Direct experimental evidence from ancient organic carbon-rich deposits. *Geology* **33**: 889-892.
- Morrill, C., J. T. Overpeck, and J. E. Cole. 2003. A synthesis of abrupt changes in the Asian summer monsoon since the last deglaciation. *The Holocene* **13**: 465-476.
- Moy, C. M., G. O. Seltzer, D. T. Rodbell, and D. M. Anderson. 2002. Variability of El Niño/Southern Oscillation activity at millennial timescales during the Holocene epoch. *Nature* **420**: 162-165.
- Müller, P. J. 1977. C/N ratios in Pacific deep-sea sediments: Effect of inorganic ammonium and organic nitrogen compounds sorbed by clays. *Geochimica Et Cosmochimica Acta* **41**: 765-776.
- Müller, P. J., and E. Suess. 1977. Interaction of organic compounds with calcium carbonate—III. Amino acid composition of sorbed layers. *Geochimica Et Cosmochimica Acta* **41**: 941-949.
- Müller, P. J., E. Suess, and C. A. Ungerer. 1986. Amino acids and amino sugars of surface particulate and sediment trap material from waters of the Scotia Sea. *Deep-Sea Research Part I-Oceanographic Research Papers* **33**: 819-838.
- Nandy, N. C., and V. B. Deo. 1961. Origin of the Lonar Lake and its alkalinity. *Technical Journal of the Tata Iron and Steel Company* **8**: 144 - 155.

- New, M., D. Lister, M. Hulme, and I. Makin. 2002. A high-resolution data set of surface climate over global land areas. *Climate Research* **21**: 1-25.
- Nguyen, R. T., and H. R. Harvey. 1997. Protein and amino acid cycling during phytoplankton decomposition in oxic and anoxic waters. *Organic Geochemistry* **27**: 115-128.
- Niggemann, J., and C. J. Schubert. 2006. Sources and fate of amino sugars in coastal Peruvian sediments. *Geochimica Et Cosmochimica Acta* **70**: 2229-2237.
- Nirmala, E., K. N. Remani, and S. R. Nair. 1991. Limnological status of a freshwater lake ecosystem in a humid tropic region. *International Journal of Environmental Studies* **39**: 223-229.
- O'Leary, M. H. 1988. Carbon isotopes in photosynthesis. *Bioscience* **38**: 328-336.
- Overpeck, J. T., D. M. Anderson, S. Trumbore, and W. L. Prell. 1996. The southwest Indian Monsoon over the last 18000 years. *Climate Dynamics* **12**: 213-225.
- Parker, A. G., L. Eckersley, M. M. Smith, A. S. Goudie, S. Stokes, S. Ward, K. White, and M. J. Hodson. 2004. Holocene vegetation dynamics in the northeastern Rub' al-Khali desert, Arabian Peninsula: A phytolith, pollen and carbon isotope study. *Journal of Quaternary Science* **19**: 665-676.
- Pausata, F. S. R., D. S. Battisti, K. H. Nisancioglu, and C. M. Bitz. 2011. Chinese stalagmite $\delta^{18}\text{O}$ controlled by changes in the Indian monsoon during a simulated Heinrich event. *Nature Geoscience* **4**: 474-480.
- Peng, Y., J. Xiao, T. Nakamura, B. Liu, and Y. Inouchi. 2005. Holocene East Asian monsoonal precipitation pattern revealed by grain-size distribution of core sediments of Daihai Lake in Inner Mongolia of north-central China. *Earth and Planetary Science Letters* **233**: 467-479.
- Peterson, B. J., and B. Fry. 1987. Stable isotopes in ecosystem studies. *Annual Review of Ecology and Systematics* **18**: 293-320.
- Possehl, G. L. 1997. The transformation of the Indus Civilization. *Journal of World Prehistory* **11**: 425-472.
- Prasad, S., A. Anoop, N. Riedel, S. Sarkar, P. Menzel, N. Basavaiah, R. Krishnan, D. Q. Fuller, B. Plessen, B. Gaye, U. Röhl, H. Wilkes, D. Sachse, R. Sawant, M. G. Wiesner, and M. Stebich. 2014. Prolonged monsoon droughts and links to Indo-Pacific warm pool: A Holocene record from Lonar Lake, central India. *Earth and Planetary Science Letters* **391**: 171-182.
- Prasad, S., and Y. Enzel. 2006. Holocene paleoclimates of India. *Quaternary Research* **66**: 442-453.

- Prasad, V., A. Farooqui, A. Sharma, B. Phartiyal, S. Chakraborty, S. Bhandari, R. Raj, and A. Singh. 2014. Mid-late Holocene monsoonal variations from mainland Gujarat, India: A multi-proxy study for evaluating climate culture relationship. *Palaeogeography, Palaeoclimatology, Palaeoecology* **397**: 38-51.
- Prell, W. L., and J. E. Kutzbach. 1987. Monsoon variability over the past 150,000 years. *Journal of Geophysical Research-Atmospheres* **92**: 8411-8425.
- Rao, D. R., and H. Rai. 2002. Rb-Sr isotopic studies of Puga gneiss and Polokongka La granite from Tso-Morari region of Ladakh, J&K, India. *Current Science* **82**: 1077-1079.
- Rashid, M. A. 1985. *Geochemistry of marine humic compounds*. Springer.
- Rehfeld, K., N. Marwan, J. Heitzig, and J. Kurths. 2011. Comparison of correlation analysis techniques for irregularly sampled time series. *Nonlinear Processes in Geophysics* **18**: 389-404.
- Rein, B., A. Lückge, L. Reinhardt, F. Sirocko, A. Wolf, and W. C. Dullo. 2005. El Nino variability off Peru during the last 20,000 years. *Paleoceanography* **20**.
- Rosenfeld, J. K. 1979. Amino acid diagenesis and adsorption in nearshore anoxic sediments. *Limnology and Oceanography* **24**: 1014-1021.
- Roth, M., and A. Hampař. 1973. Column chromatography of amino acids with fluorescence detection. *Journal of Chromatography A* **83**: 353-356.
- Sabu, T., and B. Ambat. 2007. Floristic analysis of wetlands of Kerala, p. 91-105. 3rd Kerala Environmental Congress.
- Sandeep, K., A. Warriar, B. Harshavardhana, and R. Shankar. 2011. Rock Magnetic Investigations of Surface and sub-surface soil Samples from five Lake Catchments in Tropical Southern India. *International Journal of Environmental Research* **6**: 1-18.
- Schleifer, K. H., and O. Kandler. 1972. Peptidoglycan types of bacterial cell-walls and their taxonomic implications. *Bacteriological Reviews* **36**: 407-477.
- Schlesinger, W. 1997. *Biochemistry: An Analysis of Global Change*. Academic Press.
- Shackleton, N. J., and N. D. Opdyke. 1977. Oxygen isotope and paleomagnetic evidence for early northern hemisphere glaciation. *Nature* **270**: 216-219.
- Sharma, S., M. Joachimski, M. Sharma, H. J. Tobschall, I. B. Singh, C. Sharma, M. S. Chauhan, and G. Morgenroth. 2004. Lateglacial and Holocene environmental changes in Ganga plain, Northern India. *Quaternary Science Reviews* **23**: 145-159.

- Sigleo, A. C., and D. J. Shultz. 1993. Amino acid composition of suspended particles, sediment trap material, and benthic sediment in the Potomac estuary. *Estuaries* **16**: 405-415.
- Silfer, J. A., M. H. Engel, and S. A. Macko. 1992. Kinetic fractionation of stable carbon and nitrogen isotopes during peptide bond hydrolysis: Experimental evidence and geochemical implications. *Chemical Geology* **101**: 211-221.
- Singh, G. 1971. The Indus Valley culture: Seen in the context of post-glacial climatic and ecological studies in north-west India. *Archaeology & Physical Anthropology in Oceania* **6**: 177-189.
- Sinha, A., K. G. Cannariato, L. D. Stott, H. Cheng, R. L. Edwards, M. G. Yadava, R. Ramesh, and I. B. Singh. 2007. A 900-year (600 to 1500 A.D.) record of the Indian summer monsoon precipitation from the core monsoon zone of India. *Geophysical Research Letters* **34**.
- Sirocko, F., M. Sarnthein, H. Erlenkeuser, H. Lange, M. Arnold, and J. C. Duplessy. 1993. Century-scale events in monsoonal climate over the past 24,000 years. *Nature* **364**: 322-324.
- Sollins, P., G. Spycher, and C. A. Glassman. 1984. Net nitrogen mineralization from light- and heavy-fraction forest soil organic matter. *Soil Biology and Biochemistry* **16**: 31-37.
- Soltis, D. E., P. S. Soltis, D. R. Morgan, S. M. Swensen, B. C. Mullin, J. M. Dowd, and P. G. Martin. 1995. Chloroplast gene sequence data suggest a single origin of the predisposition for symbiotic nitrogen fixation in angiosperms. *Proceedings of the National Academy of Sciences of the United States of America* **92**: 2647-2651.
- Soon, W., V. M. Velasco Herrera, K. Selvaraj, R. Traversi, I. Usoskin, C.-T. A. Chen, J.-Y. Lou, S.-J. Kao, R. M. Carter, V. Pipin, M. Severi, and S. Becagli. 2014. A review of Holocene solar-linked climatic variation on centennial to millennial timescales: Physical processes, interpretative frameworks and a new multiple cross-wavelet transform algorithm. *Earth-Science Reviews* **134**: 1-15.
- Staubwasser, M., and H. Weiss. 2006. Holocene climate and cultural evolution in late prehistoric–early historic West Asia. *Quaternary Research* **66**: 372-387.
- Stuiver, M. 1975. Climate versus changes in ^{13}C content of the organic component of lake sediments during the Late Quaternary. *Quaternary Research* **5**: 251-262.
- Stuiver, M., and P. M. Grootes. 2000. GISP2 oxygen isotope ratios. *Quaternary Research* **53**: 277-284.
- Sun, D., J. Bloemendal, D. K. Rea, J. Vandenberghe, F. Jiang, Z. An, and R. Su. 2002. Grain-size distribution function of polymodal sediments in hydraulic and aeolian environments, and numerical partitioning of the sedimentary components. *Sedimentary Geology* **152**: 263-277.

- Surakasi, V. P., A. A. Wani, Y. S. Shouche, and D. R. Ranade. 2007. Phylogenetic analysis of methanogenic enrichment cultures obtained from Lonar Lake in India: Isolation of *Methanocalculus* sp. and *Methanoculleus* sp. *Microbial Ecology* **54**: 697-704.
- Talbot, M. R. 2001. Nitrogen isotopes in palaeolimnology, p. 401-439. In W. M. Last and J. P. Smol [eds.], *Tracking environmental change using lake sediments. Volume 2: Physical and geochemical methods*. Springer.
- Talbot, M. R., and T. Lærdal. 2000. The Late Pleistocene-Holocene palaeolimnology of Lake Victoria, East Africa, based upon elemental and isotopic analyses of sedimentary organic matter. *Journal of Paleolimnology* **23**: 141-164.
- Teller, J. T., D. W. Leverington, and J. D. Mann. 2002. Freshwater outbursts to the oceans from glacial Lake Agassiz and their role in climate change during the last deglaciation. *Quaternary Science Reviews* **21**: 879-887.
- Tempest, D. W., J. L. Meers, and C. M. Brown. 1970. Influence of environment on the content and composition of microbial free amino acid pools. *Journal of General Microbiology* **64**: 171-185.
- Thompson, L. G., T. Yao, E. Mosley-Thompson, M. E. Davis, K. A. Henderson, and P.-N. Lin. 2000. A high-resolution millennial record of the South Asian Monsoon from Himalayan ice cores. *Science* **289**: 1916-1919.
- Tieszen, L. L., M. M. Senyimba, S. K. Imbamba, and J. H. Troughton. 1979. The distribution of C₃ and C₄ grasses and carbon isotope discrimination along an altitudinal and moisture gradient in Kenya. *Oecologia* **37**: 337-350.
- Tripathi, J. K., B. Bock, V. Rajamani, and A. Eisenhauer. 2004. Is River Ghaggar, Saraswati? Geochemical constraints. *Current Science* **87**: 1141-1145.
- Trivedi, A., and M. S. Chauhan. 2009. Holocene vegetation and climate fluctuations in northwest Himalaya, based on pollen evidence from Surinsar Lake, Jammu region, India. *Journal of the Geological Society of India* **74**: 402-412.
- Unger, D., B. Gaye-Haake, K. Neumann, A. C. Gebhardt, and V. Ittekkot. 2005. Biogeochemistry of suspended and sedimentary material in the Ob and Yenisei rivers and Kara Sea: Amino acids and amino sugars. *Continental Shelf Research* **25**: 437-460.
- Unger, D., L. S. Herbeck, M. Li, H. Bao, Y. Wu, J. Zhang, and T. Jennerjahn. 2013. Sources, transformation and fate of particulate amino acids and hexosamines under varying hydrological regimes in the tropical Wenchang/Wenjiao Rivers and Estuary, Hainan, China. *Continental Shelf Research* **57**: 44-58.
- Veena, M. P., H. Achyuthan, C. Eastoe, and A. Farooqui. 2014. A multi-proxy reconstruction of monsoon variability in the late Holocene, South India. *Quaternary International* **325**: 63-73.

- Verma, A., and V. Subramanian. 2002. Organic matter and amino acid concentrations in surface sediments of Vembanad Lake - A tropical estuary, west coast of India. *Regional Environmental Change* **2**: 143-149.
- Voss, M., G. Nausch, and J. P. Montoya. 1997. Nitrogen stable isotope dynamics in the central Baltic Sea: influence of deep-water renewal on the N-cycle changes. *Marine Ecology Progress Series* **158**: 11-21.
- Wakeham, S. G., C. Lee, J. I. Hedges, P. J. Hernes, and M. L. Peterson. 1997. Molecular indicators of diagenetic status in marine organic matter. *Geochimica Et Cosmochimica Acta* **61**: 5363-5369.
- Wang, Y. J., H. Cheng, R. L. Edwards, Z. S. An, J. Y. Wu, C.-C. Shen, and J. A. Dorale. 2001. A high-resolution absolute-dated Late Pleistocene monsoon record from Hulu Cave, China. *Science* **294**: 2345-2348.
- Wang, Y. J., H. Cheng, R. L. Edwards, Y. Q. He, X. G. Kong, Z. S. An, J. Y. Wu, M. J. Kelly, C. A. Dykoski, and X. D. Li. 2005. The Holocene Asian monsoon: Links to solar changes and North Atlantic climate. *Science* **308**: 854-857.
- Wei, K., and F. Gasse. 1999. Oxygen isotopes in lacustrine carbonates of West China revisited: Implications for post glacial changes in summer monsoon circulation. *Quaternary Science Reviews* **18**: 1315-1334.
- Wetzel, R. G. 2001. *Limnology: Lake and river ecosystems*. Academic Press.
- Whelan, J. K. 1977. Amino acids in a surface sediment core of the Atlantic abyssal plain. *Geochimica Et Cosmochimica Acta* **41**: 803-810.
- Wilmshurst, J. M. 1997. The impact of human settlement on vegetation and soil stability in Hawke's Bay, New Zealand. *New Zealand Journal of Botany* **35**: 97-111.
- Wulf, H., B. Bookhagen, and D. Scherler. 2010. Seasonal precipitation gradients and their impact on fluvial sediment flux in the Northwest Himalaya. *Geomorphology* **118**: 13-21.
- Wünnemann, B., D. Damske, P. Tarasov, B. S. Kotlia, C. Reinhardt, J. Bloemendal, B. Diekmann, K. Hartmann, J. Krois, F. Riedel, and N. Arya. 2010. Hydrological evolution during the last 15 kyr in the Tso Kar lake basin (Ladakh, India), derived from geomorphological, sedimentological and palynological records. *Quaternary Science Reviews* **29**: 1138-1155.
- Yadava, M. G., and R. Ramesh. 2005. Monsoon reconstruction from radiocarbon dated tropical Indian speleothems. *The Holocene* **15**: 48-59.
- Zhang, J., P. D. Quay, and D. O. Wilbur. 1995. Carbon isotope fractionation during gas-water exchange and dissolution of CO₂. *Geochimica Et Cosmochimica Acta* **59**: 107-114.

Curriculum vitae

Philip Menzel

Born: 25.11.1980 in Hamburg
Nationality: German
Home address: An der Moorkuhle 9, 22145 Braak

Education

Since August 2010 Ph.D. student, Institute of Geology (formerly Institute of Biogeochemistry and Marine Chemistry), University of Hamburg
Thesis subject: *Reconstruction of the Holocene Indian monsoon climate variability based on biogeochemical analyses of lake sediments.*

December 2009 Graduation (Diploma)
Diploma-Thesis: *Grundwassermodellierung für den Bereich des Pinneberger Troges zwischen Elmshorn und Quickborn unter besonderer Berücksichtigung der Ellerbeker Rinne.*

2001 – 2009 Studies of Geology and Palaeontology (Diploma) at the University of Hamburg.
Emphasis on Quaternary geology, hydrogeology, and oceanography

2000 Abitur at Gymnasium Trittau

List of publications

Menzel, P., B. Gaye, M. G. Wiesner, S. Prasad, M. Stebich, B. K. Das, A. Anoop, N. Riedel, and N. Basavaiah. 2013. Influence of bottom water anoxia on nitrogen isotopic ratios and amino acid contributions of recent sediments from small eutrophic Lonar Lake, central India. *Limnology and Oceanography* **58**: 1061-1074.

Menzel, P., B. Gaye, P. K. Mishra, A. Anoop, N. Basavaiah, N. Marwan, B. Plessen, S. Prasad, N. Riedel, G. Schettler, M. Stebich, and M. G. Wiesner. In press. Linking Holocene drying trends from Lonar Lake in monsoonal central India to North Atlantic cooling events. *Palaeogeography Palaeoclimatology Palaeoecology*.

Menzel, P., K. Anupama, N. Basavaiah, B. K. Das, B. Gaye, N. Herrmann, and S. Prasad. The use of amino acid analyses in (palaeo-) limnological investigations: A comparative study of four Indian lakes in different climate regimes. Submitted to *Geochimica et Cosmochimica Acta*.

Anoop, A., S. Prasad, B. Plessen, N. Basavaiah, B. Gaye, R. Naumann, P. Menzel, S. Weise, and A. Brauer. 2013. Palaeoenvironmental implications of evaporative gaylussite crystals from Lonar Lake, central India. *Journal of Quaternary Science* **28**: 349-359.

Prasad, S., A. Anoop, N. Riedel, S. Sarkar, P. Menzel, N. Basavaiah, R. Krishnan, D. Q. Fuller, B. Plessen, B. Gaye, U. Röhl, H. Wilkes, D. Sachse, R. Sawant, M. G. Wiesner, and M. Stebich. 2014. Prolonged monsoon droughts and links to Indo-Pacific warm pool: A Holocene record from Lonar Lake, central India. *Earth and Planetary Science Letters* **391**: 171-182.

Basavaiah, N., M. G. Wiesner, A. Anoop, P. Menzel, N. R. Nowaczyk, K. Deenadayalan, A. Brauer, B. Gaye, R. Naumann, N. Riedel, M. Stebich, and S. Prasad. 2014. Physicochemical analyses of surface sediments from the Lonar Lake, central India - implications for palaeoenvironmental reconstruction. *Fundamental and Applied Limnology* **184**: 51-68.

Riedel, N., M. Stebich, A. Anoop, N. Basavaiah, P. Menzel, S. Prasad, D. Sachse, S. Sarkar, and M. G. Wiesner. Modern pollen vegetation relationships in a dry deciduous monsoon forest – a case study from Lonar Crater Lake, central India. Submitted to *Review of Palaeobotany and Palynology*.

Mishra, P. K., A. Anoop, G. Schettler, S. Prasad, A. Jehangir, P. Menzel, R. Naumann, E. A. R. Yousuf, N. Basavaiah, K. Deenadayalan, M. G. Wiesner, and B. Gaye. Reconstructed late Quaternary hydrological changes from Tso Moriri, NW Himalaya. Submitted to *Quaternary Research*.

Mishra, P. K., A. Anoop, A. Jehangir, S. Prasad, P. Menzel, R. Naumann, S. Weise, A. R. Yousuf, and B. Gaye. Limnology and modern sedimentation patterns in high altitude Tso Moriri, NW Himalaya – implications for proxy development. Submitted to *Fundamental and Applied Limnology*.

Declaration on oath

I hereby declare, on oath, that I have written the present dissertation by my own and have not used other than the acknowledged resources and aids.

City, date

Signature